A Comparison of a coupled and uncoupled numerical model of alluvial flows, COUPFLEX and HEC6. December 1996.

Author:
Saiedi, S.; Cox, R. J.

Publication details:
Commissioning Body: Unisearch Ltd.
Report No. UNSW Water Research Laboratory Report No. 186
0858240076 (ISBN)

Publication Date:
1996

DOI:
https://doi.org/10.4225/53/578d6fe3e0879

THE UNIVERSITY OF NEW SOUTH WALES
water research laboratory
Manly Vale N.S.W. Australia

A COMPARISON OF A COUPLED AND AN UNCOUPLED NUMERICAL MODEL OF ALLUVIAL FLOWS, COUPFLEX AND HEC6

by

Saied Saiedi and R J Cox

Research Report No. 186

December 1996

THE UNIVERSITY OF NEW SOUTH WALES
WATER RESEARCH LABORATORY

A Comparison of a Coupled and an Uncoupled Numerical Model of Alluvial Flows, COUPFLEX and HEC6

by

Saied Saiedi and R J Cox

Research Report No. 186
December 1996

---

https://doi.org/10.4225/53/578d6fe3e0879

BIBLIOGRAPHIC DATA SHEET

Report No. 186	Report Date: December 1996	ISBN: 0/85824/007/6

Title

A Comparison of a Coupled and an Uncoupled Numerical Model of Alluvial Flows, COUPFLEX and HEC6

Author(s)

Saied Saiedi and R J Cox

Sponsoring Organisation

Unisearch Ltd, Water Research Laboratory

Supplementary Notes

The work reported was carried out and published under the direction of the Director of the Water Research Laboratory.

Abstract

The Performance of an uncoupled numerical model of alluvial flow is compared with that of a coupled model. The uncoupled model is the well-known HEC6 sedimentation program and the coupled model is a newly developed non-dimensional model of riverine flow called COUPFLEX. The models are applied to the data obtained from some laboratory tests on river sedimentation carried out exclusively for this comparison. The experimental work and procedure are described and the models are reviewed. Application of the models to the experimental data, associated with fast flow and sedimentation processes, reveals the preferability of a coupled approach. The strong inter-relation between water and sediment components of alluvial flows is recognised in the coupled approach and this gives it advantages over the traditional uncoupled method in which the calculations of the water flow and bed level variations are separated to various degrees. Simulation of several carefully performed laboratory tests highlights three beneficial aspects of a coupled approach. The simulations show that a coupled model (i) gives more accurate results when rapid river processes are involved, (ii) obviates some computational difficulties such as production of false bed level oscillations, and (iii) allows more flexibility in the selection of the size of the computational time step.

Distribution Statement

For general distribution

Descriptors

Numerical model; Alluvial flows; COUPFLEX; HEC6

Identifiers

Number of Pages: 111	Price: On Application.

CONTENTS

LIST OF TABLES

LIST OF FIGURES

LIST OF SYMBOLS

Note. All variables with a superscript star * in the text such as Q^* denote the non-dimensional or normalised variables corresponding to primary variables such as Q. They are not listed here.

A = flow cross-sectional area
A_o = characteristic cross-sectional area used in non-dimensionalisation
A_1 to A_5= constants in Equation (5.3)
B = bottom width
C = Chezy's roughness coefficient
C_{fl} = a constant coefficient associated with the "backwater length"
C_o = characteristic concentration of suspended sediment used in non-dimensionalisation
C_s = volumetric suspended sediment concentration
D = sediment grain size
D_{50} = median sediment grain size
e1,e2,..= constants used to summarise algebraic operations for Q_s
Fr = Froude number
Fr_o = characteristic Froude number obtained by $\dfrac{V_o}{\sqrt{gh_o}}$
F_g = grain Froude number = $\dfrac{V}{\sqrt{g(s-1)D_{50}}}$
f = continuous differentiable function
f_i^j = value of variable (function) f at point (x,t)= $(i\Delta x, j\Delta t)$
Δf_i = change in the value of f_i from time level j to time level j+1; *ie* $\Delta f_i = f_i^{j+1} - f_i^j$
g = gravitational acceleration
H_w = weir height above the rigid bed in the flume (Equation 5.1)
h = flow depth
$\tilde{\tilde{h}}$ = distance from centroid of cross-sectional area of the flow to the water surface=$\alpha_1 \times h$
Δh = increment in flow depth
i = a subscript denoting the association of a variable or term with the point x= $(i-1)\Delta x$
j = a subscript denoting the association of a variable or term with the time t= $(j-1)\Delta t$
k_s = roughness height
L = length of the river reach
L_o = characteristic length used in non-dimensionalisation taken as "backwater length"
m1..m6 = constants used to summarise algebraic operations for S_f
n = Manning's roughness coefficient
n1,n2 = constants used to summarise algebraic operations for derivatives of Q_s
n_c = a constant
P = wetted perimeter
p = porosity of the sediment
Q = total flow rate
Q_w = water discharge
Q_s = sediment discharge
Q_{sb} = bed load discharge
Q_{ss} = suspended load discharge
Q_o = characteristic flow rate used in non-dimensionalisation
ΔQ = increment in flow rate
q = flow rate per unit width

q_L = lateral flow rate per unit length
q_{Ls} = lateral sediment discharge per unit length
R = hydraulic radius
R_o = characteristic hydraulic radius used in non-dimensionalisation
P_o = characteristic wetted perimeter used in non-dimensionalisation
Re_* = particle Reynolds number (Section 3.2.3)
S_o = characteristic bed slope used in non-dimensionalisation
S_f = friction slope
η = side slope of a channel
s = relative density of sediment
T = top width of the flow
= the width of channel over which the deposition or erosion can occur
u_D = a parameter used to normalise flow velocity
u1,..,u13= auxiliary parameters
V = mean flow velocity
V1 = an auxiliary parameter
V2 = an auxiliary parameter
w_s = fall velocity of sediment
x = longitudinal distance measured along the length of the stream from the upstream end
Y = water level above the rigid bed in the flume (Equation 5.1)
z = bed elevation
Δz = increment in bed elevation
α = damping factor in a numerical scheme
α_L = angle of lateral flow with the main stream at a junction
α_1 = a constant
α_s = a coefficient approximately equal to s-1
β = momentum correction factor
β_c = a constant
Δ = increment of a variable or term from time level j to time level j+1 *eg* in ΔQ
γ_s = weight density of sediment
ε_o = a constant associated with "backwater length"
ν = kinematic viscosity of water
ρ_w = mass density of water
ρ_s = mass density of sediment
τ_c, τ_e, τ_w= critical, effective, and wall shear stresses respectively
θ, φ = time and space weighting factors respectively
σ = geometric standard deviation of sediment size distribution

1. INTRODUCTION

Flow in alluvial channels consists of a simultaneous motion of water and sediment. Any change in either the water flow or sediment motion may cause a change in the other. Alluvial streams subjected to fast flows, such as peaky floods or strong tidal currents, involve a pronounced inter-connection of water flow and bed level variations. The logical way to account for this physical inter-relation in any competent numerical simulation of alluvial flow is a concurrent solution procedure for water-routing and sediment-routing components of the stream. Separating water flow and bed level computations, traditional uncoupled models ignore, to various degrees, the importance of the interaction of water and sediment movement.

In a recent work on simulation of riverine flow (Saiedi 1994a), it was shown that to reflect the physical interaction of water and sediment motion in alluvial streams, a coupled model should meet three basic requirements. First, its working equations must contain the relevant terms indicating the coupled nature of motion. This specifically means that equations describing the motion of water should include the effects of sediment motion and bed level variation. Secondly, the manner in which the equations are discretised for numerical solution should maintain a reasonable level of accuracy. Thirdly, the final system of equations must be solved simultaneously.

It was also shown that as in an uncoupled approach, the validity of the results from any coupled model depends on the accuracy of the relations used, particularly those for sediment transport capacity and hydraulic resistance.

Although attention to the coupled method of alluvial flow modelling dates back to early works such as that by Hsu and Chu (1964), one cannot find many workable coupled models in the literature. From more recent studies on the coupled simulation of riverine flows, a few are worthy of particular reference. Lyn (1987) and Lyn and Goodwin(1987) investigated the mathematical properties of alluvial flow equations and offered a valuable justification for the need for the coupled approach. Holly and his colleagues have dealt with the development of coupled alluvial flow models in several papers (see for instance Holly et al. 1987, Holly and Rahuel 1989, 1990a and b, Rahuel et al. 1989). Going beyond theoretical considerations, the investigations of Holly and his colleagues have led to implementation of some practical aspects in industrial applications such as allowance for sediment with multiple size classes , and inclusion of sorting equations and of advection-diffusion equations for suspension as a separate process from that of bed load movement. Lai (1991), in line with his previous investigations, presented a comprehensive study of the alluvial flow equations using an extended Method of Characteristics and reported successful field application of his model. A work on coupled modelling by Correia et al. (1992) contains a quick reference to early attempts in this area and indicates an improvement in considering alluvial bed roughness based on bed forms and an alternative solution procedure for the final system of equations.

More recently Saiedi (1994a) used the results of extensive numerical and experimental studies to compare the coupled approach with several existing uncoupled approaches. A major product of these studies, a numerical model of riverine flow called COUPFLEX, was employed to reveal some advantages of the coupled approach. COUPFLEX is a coupled and flexible numerical model of riverine flow developed with full recognition of the physical coupling of water and sediment phases of alluvial flows. The model is notable for its fully non-dimensional working equations, concurrent production of solutions from coupled and uncoupled approaches, presentation of the magnitudes of all terms in the working equations for all nodes at each time step, and its ability to operate as an alluvial or rigid-bed river model. A review of the mathematical formulation of the model is given in Saiedi (1994b). While several uncoupled approaches were incorporated into COUPFLEX and flume test results and many examples from the literature were simulated, no specific readily available computer program was used to make comparisons. Since the performance of a widely used uncoupled model compared with that of a coupled model would be of interest, it was decided to compare the performance of the sedimentation program HEC6 with that of COUPFLEX.

This study is an extension of the previous research work by Saiedi(1944a) in two ways:

(a) While in the previous study several uncoupled approaches (see Appendix III) were built into COUPFLEX to compare coupled and uncoupled methods, no readily available uncoupled computer program was employed for comparison with COUPFLEX. Here, HEC6 is chosen for this comparison.

(b) Compared to the limited number of laboratory tests on the sedimentation reported in the previous study, A completely new set of laboratory tests of sedimentation involving higher level of nonuniformity and unsteadiness have been achieved in the present study. Moreover, to derive the appropriate empirical sediment transport formula, non-equilibrium experiments are employed in the present study as opposed to the equilibrium tests used in the previous work. This would increase the reliability of the simulations.

2. MODEL DESCRIPTION

This section provides a review of both models HEC6 and COUPFLEX. HEC6 is introduced with less details as its full description is readily available in the literature.

2.1 HEC6

HEC6, dating back to 1965, has undergone several revisions and improvements in the last two decades and has been used extensively around the world (see HEC 1977, p.510 of Thomas 1982, Gee 1988, HEC 1993). HEC6 is a well-known one-dimensional movable boundary river flow numerical model to simulate and predict changes in river profiles resulting from erosion and/or deposition. A continuous flow record is segmented into a series of steady flow events. For each flow, a water surface profile is calculated using the "step backwater calculation" (Henderson 1966). In this sense, HEC6 employs the quasi-steady approximation in which the term associated with the temporal variation of the flow in the momentum equation is ignored.

The flow calculations provide hydraulic information such as energy slope, velocity and depth at each cross section. "Potential sediment transport rates are then computed at each cross section via user-selected functions. These rates, combined with the duration of the flow, permit a volumetric accounting of sediment within each subreach. The amount of scour or deposition at each cross section is then computed and the cross-section is adjusted accordingly. The computations then proceed to the next flow in the sequence and the cycle is repeated beginning with the updated geometry. The sediment calculations are performed by grain size fraction thereby allowing the simulation of hydraulic sorting and armouring. Features of HEC6 include: capability to analyze networks of stream, channel dredging, various levee and encroachment alternatives, and to use several methods for computation of sediment transport rates. ... The transport, deposition, and erosion of silts and clays may also be calculated. Effects of the creation and removal of an armour layer are also simulated." (p.1, HEC 1993)

Of main limitations of HEC6 is that there is no mechanism in the model for coupling the boundary roughness with the sediment characteristics and the sediment transport rate. Therefore, changes in the roughness created by the bed forms and the flow regime cannot be directly simulated. The hydraulic resistance of the river has to be incorporated using Manning's n roughness. However, the use of a roughness coefficient (n) variable with the flow rate is possible.

In the latest version of HEC6 (HEC 1993), a list of eleven formulae for the sediment transport capacity is adopted from the literature for selection by the user. Additionally, a particular form of user-specified formula is allowed. This is mentioned in more detail in Section 5.1.3 of this report.

2.2 COUPFLEX

2.2.1 General

COUPFLEX is a Coupled and Flexible riverine water and sediment model which is characterised by the following features:

1. Fully non-dimensional working equations;
2. Simultaneous production of the solutions from any of several uncoupled and simplified approaches together with the results from the complete and coupled approach;
3. Computation and presentation of the absolute and relative magnitudes of all terms in the working equations, for all nodes at each time step;
4. Ability to operate as either a hydraulic model simulating flow without bed level and sediment calculations, or as a sediment model simulating water flow and sediment movement in alluvial streams;
5. Experimental verification by laboratory tests carried out exclusively for verifying the model.

The first feature of COUPFLEX frees the model from any unit system and provides for systematic studies involving variation of key terms and variables. The second feature enables the user to compare the results of different approaches, to consider the possible need to renew an analysis performed in the past, and to observe the merits and disadvantages of various uncoupled approaches or the consequences of each simplification involved in an uncoupled or simplified model. The third feature makes it possible both to study the detailed behaviour of the model and the significance of terms and parameters, and to identify the causes of difficulties in the computation or programming which, as Cunge (1988, p.519) has pointed out, "is never free of bugs and errors". The fourth feature saves the user time and modelling resources, eliminating the need to shift between a rigid-bed flow model and an alluvial stream model in river engineering practice. The fifth feature distinguishes COUPFLEX from any previous attempt in this field, as far as it is known to the writer, as the experimental work including rapidly varied bed level and flow conditions, clearly demonstrates the merits of the coupled approach and limitations of the uncoupled approach. These features, plus the ability to select from several empirical relations for hydraulic resistance and from many empirical formulae for sediment transport, potentially make COUPFLEX a flexible tool for one-dimensional river flow modelling.

Details of derivation of non-dimensional forms, discretisation of the working equations, analysis of order of magnitude and physical significance of the terms, verification of the model by non-experimental tests mostly taken from the literature, and experimental verification of the model are presented by Saiedi (1994a).

2.2.2 *Dimensional Form of Working Equations*

In one-dimensional (1-D) motion of a water-sediment mixture in open channels (see Figure 2.1), the principles of conservation of mass and momentum lead to partial differential equations for continuity and momentum for the mixture which are respectively:

$$\underbrace{\frac{\partial Q}{\partial x}}_{1} + \underbrace{T\frac{\partial h}{\partial t}}_{2} + \underbrace{T\frac{\partial z}{\partial t}}_{3} \underbrace{- q_L}_{4} = 0 \tag{2.1}$$

$$\underbrace{\frac{\partial Q}{\partial t}}_{5} + \underbrace{\frac{\partial}{\partial x}\left(\frac{\beta Q^2}{A}\right)}_{6} + \underbrace{gA\frac{\partial h}{\partial x}}_{7} + \underbrace{gA\frac{\partial z}{\partial x}}_{8} + \underbrace{gASf}_{9} \underbrace{- q_L\left[V_L.Cos[\alpha_L] - \frac{Q}{A}\right]}_{10} +$$

$$\underbrace{gA\tilde{\bar{h}}\frac{s-1}{1+C_s(s-1)}\frac{\partial C_s}{\partial x}}_{11} + \underbrace{T\frac{Q}{A}\frac{\partial z}{\partial t}}_{12} = 0 \tag{2.2}$$

$$\underbrace{\frac{\partial Q_s}{\partial x}}_{13} + \underbrace{(1-p)T\frac{\partial z}{\partial t}}_{14} + \underbrace{TC_s\frac{\partial h}{\partial t}}_{15} + \underbrace{A\frac{\partial C_s}{\partial t}}_{16} \underbrace{- q_{Ls}}_{17} = 0 \tag{2.3}$$

where the terms are numbered for convenience of reference and:

Q is the flow rate of the sediment-water mixture consisting of both water discharge Q_W and total sediment discharge Q_S, so that $Q=Q_W+Q_S$, as a function of location x and time t ; A is the cross-sectional area of the stream with top width T and depth h; z is the bed elevation above a fixed horizontal datum; q_L is the lateral flow, positive for inflow and negative for outflow, in flow rate per unit length, consisting of both lateral contributions of water q_{Lw} and sediment q_{Ls}; β is the momentum correction factor to account for non-uniformity of velocity in the cross-section; S_f is friction slope; $V_L.\cos[\alpha_L]$ is the streamwise component of velocity of lateral flow with α_L being the angle with the main stream at the junction; $\tilde{\bar{h}}$ is the distance from the centroid of the area of cross-section to the water surface (this may be generally written as a coefficient α_1 times the depth h in which the coefficient depends on the geometry of the cross-section, being 1/2 for a rectangle); s is ρ_S/ρ_W the relative density of the sediment where ρ_S = density of the sediment grains and ρ_W = density of water; C_S is the average volumetric concentration of suspended sediment in the cross-section defined as Q_{SS}/Q in which Q_{SS} is the suspended sediment portion of the total sediment discharge, while the bed load portion is

$Q_{sb}= Q_s-Q_{ss}$; p is porosity such that the ratio of solid to bulk sediment volume at the bed is equal to 1- p.

Equations (2.1) and (2.3) without terms ***3***, ***11***, and ***12*** are 1-D equations of unsteady gradually varied flow in rigid bed rivers often used in flood routing through open channels. Addition of terms ***3***, ***11***, and ***12*** to these two unsteady flow equations, and of Equation (2.3) accounts for the mobile-bed aspect of the alluvial flow.

2.2.3 Non-Dimensionalisation of the Equations

Study of the behaviour of a model which, like the present model, contains many variables may be difficult when the equations are in dimensional form. The difficulty arises from the fact that there are numerous possible combinations in which the model variables and parameters can take different values. Examining model results corresponding to these sets of variables can be cumbersome and generalisation of the results may be erroneous. To avoid excessive computations in the study of water and sediment motion it is advantageous to use dimensionless equations. The use of dimensionless forms affords systematic change of key variables, allows for more general comparison, and frees the equations and the terms from numerical dependence on any specific dimensional system (Lai 1986). In a recent study, Lyn (1987) presented a non-dimensional form of the equations for unsteady sediment transport modelling. He examined them through mathematical analysis and showed some weaknesses in the usual uncoupled approaches. Here a different dimensionless form based on more complete equations is introduced. The starting point is the set of Equations (2.1) to (2.3).

(i) Basic Quantities for the Dimensionless Form

Following is the list of characteristic quantities used to obtain non-dimensional or normalised variables. A variable with a star (*) shows the dimensionless or normalised form of the corresponding variable defined previously.

- L_o "Backwater length" of the initial flow; dimensionless x is defined as $x^* = x / L_o$. The concept of backwater length is due to Samuels (1989). Using a simple perturbation analysis and with some practical simplifications he showed that a length scale equal to $L_o = C_{fl}(1 - Fr_o^2)h_o / S_o$ can be used to determine the extent of a river which is influenced by the backwater from a downstream control (h_o and Fr_o are defined later). Samuels (1989) found that for most practical cases C_{fl} is roughly equal to 0.7.
- Q_o Maximum flow discharge in the reach; in a flood event it is the peak of the inflow hydrograph; $Q^*=Q / Q_o$, $q_l^* = \dfrac{q_l \times L_o}{Q_o}$

- S_o A representative slope of the reach; it can be the initial mean bottom slope of the reach; $S_f^*=S_f / S_o$
- h_o Maximum normal depth in the reach corresponding to Q_o and S_o for a typical cross-section and a representative hydraulic resistance, obtained by a uniform flow formula such as Manning's. (In the case of a very flat bed slope for which $h_o \rightarrow \infty$, the critical depth corresponding to Q_o in a typical cross-section may be introduced); $h^*=h / h_o$. Also the dimensionless bed elevation can be defined as $z^*=z / h_o$.
- T_o Top width of flow corresponding to conditions producing h_o; $T^*=T / T_o$. Also the dimensionless bottom width can be defined as $B^*=B / T_o$.
- A_o A typical rectangular cross-sectional area corresponding to h_o and T_o; $A_o=T_o\, h_o$, $A^*=A/A_o$
- t_o A flow time scale defined as $t_o= L_o / (g\, h_o)^{1/2}$; $t^*=t / t_o$
- Fr_o Characteristic Froude number; $Fro = (Q_o/A_o) / (g\, h_o)^{1/2} = V_o / (g\, h_o)^{1/2}$, $V_L^*=V_L / V_o$
- Q_{so} Scale of total sediment transport corresponding to Q_o , h_o , S_o, ……. , for typical values of sediment and resistance variables; $Q_s^*=Q_s / Q_{so}$, $q_{Ls}^* = \dfrac{q_{Ls} \times L_o}{Q_{so}}$
- C_{so} Volumetric ratio of suspended sediment when the total sediment transport rate is Q_{so}; if the suspended portion of Q_{so} is Q_{sso} then $C_{so}= Q_{sso} / Q_o$, $C_s^* = C_s / C_{so}$.

C_o Volumetric ratio of total sediment to maximum water discharge corresponding to Q_{so}; if Q_{sso} and Q_{sbo} are respectively the suspended and bed load portions of the total Q_{so}, we have $Q_{so}=Q_{sso}+Q_{sbo}$ and then $C_o=Q_{so} / Q_o$.

(ii) Non-Dimensional Equations

Substitution of the above dimensionless or normalised variables into Equations (2.1) to (2.3) results in non-dimensional equations for flow continuity, flow momentum, and sediment continuity. The resulting dimensionless equations are respectively

$$[Fro]\frac{\partial Q^*}{\partial x^*}+T^*\frac{\partial h^*}{\partial t^*}+T^*\frac{\partial z^*}{\partial t^*}-[Fro]q_L^*=0 \tag{2.4}$$

$$[Fro]\frac{\partial Q^*}{\partial t^*}+[Fro^2]\frac{\partial}{\partial x^*}\left(\frac{\beta Q^{*2}}{A^*}\right)+A^*\frac{\partial h^*}{\partial x^*}+A^*\frac{\partial z^*}{\partial x^*}+[\varepsilon o]A^*Sf^*$$

$$-[Fro^2]q_L^*\left(V_L^*Cos[\alpha_L]-\frac{Q^*}{A^*}\right)+[Cso]\alpha 1\times\alpha s\times A^*h^*\frac{\partial Cs^*}{\partial x^*}+T^*\frac{Q^*}{A^*}\frac{\partial z^*}{\partial t^*}=0 \tag{2.5}$$

$$[C_oFr_o]\frac{\partial Q_s^*}{\partial x^*}+(1-p)T^*\frac{\partial z^*}{\partial t^*}+[C_{so}]T^*C_s^*\frac{\partial h^*}{\partial t^*}+[C_{so}]A^*\frac{\partial C_s^*}{\partial t^*}-[C_oFr_o]q_{Ls}^*=0 \tag{2.6}$$

with the dimensionless parameters

$Fr_o = (Q_o/A_o) / (g\, h_o)^{1/2} = V_o / (g\, h_o)^{1/2}$; $\varepsilon_o = C_{fl}(1-Fr_o^2)$; $C_o = Q_{so} / Q_o$; $C_{so} = Q_{sso} / Q_o$; and $\alpha_s = \dfrac{s-1}{1+C_s^*(s-1)}$.

At the maximum flow rate Q_o, these dimensionless parameters are indications of physical aspects of the water and sediment motion; Fro is an indication of the flow regime, ε_o is an indication of the physical extent of the backwater effect of a downstream control, C_o is an indication of capacity of the flow to carry sediment including both bed and suspended load, and C_{so} is an indication of the capacity of motion to carry sediment in suspension.

In these equations there are six unknowns, Q^*, h^*, z^*, S_f^*, C_s^*, and Q_s^*. Three auxiliary equations are required to relate friction, suspended sediment and total sediment to hydraulic and sediment characteristics. Through theoretical considerations and empirical formulae, S_f^*, C_s^* and Q_s^* can be written as functions of Q^*, h^* and sediment parameters. There is a large number of formulae available in the sediment transport literature, mostly empirical, giving different answers for given situations. They should be used with care regarding their limitations, approximations involved, and range of validity. Since there is no one universal relationship, it is a useful practice not to fix rigidly any specific formula to the model. The model should have room to accept any new relationship. In COUPFLEX it is essential to use formulae for S_f^*, C_s^* and Q_s^* in dimensionless forms. An example for each of the three relations is presented in Appendix I.

2.2.4 Discretisation of the Equations

In the working equations, each continuous function f and its derivatives are substituted by their difference form according to the familiar linear implicit four point scheme first proposed by Preissmann (Abbott and Basco, 1989) and slightly modified here as

$$
\begin{aligned}
f &\approx \theta\left[\phi \Delta f_{i+1} + (1-\phi)\Delta f_i\right] + \left[\phi f_{i+1} + (1-\phi) f_i\right] \\
\frac{\partial f}{\partial x} &\approx \frac{\theta}{\Delta x}\left[\Delta f_{i+1} - \Delta f_i\right] + \frac{1}{\Delta x}\left[f_{i+1} - f_i\right] \\
\frac{\partial f}{\partial t} &\approx \frac{1}{\Delta t}\left[\phi \Delta f_{i+1} + (1-\phi)\Delta f_i\right]
\end{aligned}
\tag{2.7}
$$

with $\Delta f_i = f_i^{j+1} - f_i^j$ and $\Delta f_{i+1} = f_{i+1}^{j+1} - f_{i+1}^j$, where f_i^j = the value of f at the point $(x,t) = (i\Delta x, j\Delta t)$, Δx and Δt being the mesh size of the distance and time steps respectively.

At each grid point, increments of S_f, C_s, and Q_s are written as functions of Q and h in the following forms:

$$\Delta Sf^* = \left[\frac{\partial Sf^*}{\partial Q^*}\right]\Delta Q^* + \left[\frac{\partial Sf^*}{\partial h^*}\right]\Delta h^*$$
$$\Delta Cs^* = \left[\frac{\partial Cs^*}{\partial Q^*}\right]\Delta Q^* + \left[\frac{\partial Cs^*}{\partial h^*}\right]\Delta h^* \qquad (2.8)$$
$$\Delta Qs^* = \left[\frac{\partial Qs^*}{\partial Q^*}\right]\Delta Q^* + \left[\frac{\partial Qs^*}{\partial h^*}\right]\Delta h^*$$

The derivatives in terms of Q and h depend on the type of empirical formulae used. It should be noted that Δf_i with the given definition denotes the change of f at point x=i.Δx from time t= j.Δt to t=(j+1).Δt. Therefore, each term with Δ contains an unknown value at j+1 minus the known value at j. Once Δf is found it must be added to f_i^j to obtain f_i^{j+1}.

The resulting linear system of algebraic equations, corresponding respectively to Equations (4),(5), and (6), is

$$C_1\Delta Q^*_{i+1} + C_2\Delta Q^*_i + C_3\Delta h^*_{i+1} + C_4\Delta h^*_i + C_5\Delta z^*_{i+1} + C_6\Delta z^*_i + D_1 = 0$$
$$C_{11}\Delta Q^*_{i+1} + C_{22}\Delta Q^*_i + C_{33}\Delta h^*_{i+1} + C_{44}\Delta h^*_i + C_{55}\Delta z^*_{i+1} + C_{66}\Delta z^*_i + D_{11} = 0 \qquad (2.9)$$
$$C_{111}\Delta Q^*_{i+1} + C_{222}\Delta Q^*_i + C_{333}\Delta h^*_{i+1} + C_{444}\Delta h^*_i + C_{555}\Delta z^*_{i+1} + C_{666}\Delta z^*_i + D_{111} = 0$$

Note that subscript 55, for example, should not be read as fifty five. It is a simple repeat of 5 indicating it is related to the fifth unknown (in the series of ΔQ^*_{i+1}, ΔQ^*_i, Δh^*_{i+1}, Δh^*_I, Δz^*_{i+1}, Δz^*_i) and belongs to the second equation. This notation removes some unnecessary complexities from the appearance of the equations. The coefficients are given in detail in Appendix II. All the coefficients contain known values at time level j, and all the unknowns are the changes in Q^* ,h^* and z^* from time j.Δt^* to (j+1).Δt^* at point i Δx^* or (i+1)Δx^* . For simplicity, superscript j is dropped in the coefficients.

In subcritical flow the system needs two upstream and one downstream boundary conditions (Cunge et al., 1980); at the upstream end, one for flow as a given function for Q or h or a relation between them, and another as an inflow sediment hydrograph or bed level variation; at the downstream end often water level (or flow depth) is defined but Q or a relation between Q and water level (or flow depth) can also be defined. To overcome a difficulty in relating the upstream sediment input to the bed level variation, Saiedi (1994c) conducted an experimental study. A preliminary analysis of the data resulted in simple empirical formula for the celerity of "frontal overloading sand waves".

To provide for comparative studies in numerical modelling of river flows, several uncoupled schemes in the discretisation of the sediment continuity equations are incorporated into COUPFLEX. When the model is utilised in its uncoupled mode, any of these schemes can be chosen. Appendix III reports these schemes.

3. EXPERIMENTAL WORK AND PROCEDURE

In what follows, a brief review of the experimental equipment and procedure is described. The design and features of the flume have previously been described in detail by Saiedi (1993).

3.1 General Description of the Flume

The conceptual picture of the flume is shown in Figure 3.1. In its present form, it is a non-recirculating 35 m long tiltable flume, 0.60 m deep, 0.61 m wide, with both sides glass-panelled.

The structural base of the flume consists of two parallel steel beams joined together, supported from the top by vertical hangers and from beneath by adjusting jacks. The length of the each beam is 6.1 m. Each pair of beams is connected to the next pair by means of two hinged arms. The hinge connection makes it possible to have different slopes along the flume.

Six steel U-frames made of hollow steel sections sit on each pair of beams. They support 24 mm thick Fibre Cement sheets (FC sheets) which form the actual flume bed, and vertical glass panels which form the side walls of the flume. Two parallel steel angles sit on the top of the U-frames to support the top sides of the glass panels. These capping angles are parallel to the flume bed and provide a base on which two trolleys run. The first trolley is used to mount an automatic Tactile Bed Profiler (Figure 3.2) and the second trolley is used to set the initial sediment level in the loose bed section of the flume. The sediment leveller (Figure 3.3) is operated manually. Both trolleys have six swivel type rubber tyred wheels rolling on the top capping angles and four similar but non-swivelling side wheels running on the glass sidewalls.

WRL uses water from a dam (Manly Dam) with average water level several metres above the laboratory floor. The average water level behind the dam provides sufficient head for a discharge of 125 litres per second without the pump and 230 litres per second with the pump operating. A calibrated electro-magnetic flowmeter is used to indicate the magnitude of the flow rate. Water enters the head tank through a 250 mm diameter pipe. Flow in the tank is quietened by screens and baffles. Between the flowmeter and the head tank there is an electrically actuated valve which responds to an analogue voltage computer signal to control the flow. The head tank sits on two steel angles bolted to the first two support beams and can be moved up and down with the beams when setting the slope of the flume. After the head tank, water passes a group of thin vertical galvanised metal sheets fixed to the flume bed and sides. These sheets are employed to straighten the flow before it enters the flume. The first few metres of the flume has a temporary false rough bed. A vibratory sediment supplier introduces sediment which is distributed uniformly by a chute spreader.

At the downstream end of the flume the bed load is collected in a suspended basket with a weighing device to record continuously the submerged weight of the basket and sediment. A removable sliding lid is used to cover the basket when the bed load is not to be weighed. The flume continues with the same cross-section a few metres beyond the basket and, after a steep slope, ends at a sluice gate which is used to regulate the downstream flow depth. The water enters a big tank which can be used to store sediment or as a recirculating tank.

The local water depths are measured using several capacitance wave probes which convert changes in water level to a corresponding voltage output. Some velocity measurement were performed using propeller type velocity probes but were discontinued for a reason to be explained later.

3.2 Temporary Rough Bed

The flowing water from the head tank requires several metres length of the flume to attain a fully developed velocity profile. In this entrance region the boundary layer is growing and the velocity profile is varying in the flow direction. This variation is not desirable for many open channel experiments including sediment studies. Generally the greater the mean velocity and the smoother the flume boundaries, the longer is this unusable entrance region.

In the experiments performed in this study a dense layer of sediment grains, with a thickness of 2 or 3 grain diameters, was glued to the faces of pieces of 24 mm thick FC sheets. When dried, it proved to be a durable and easy-to-handle false rough bed with a roughened surface which was not washed out by flowing water. Small pieces of galvanised metal box were used to raise the roughened sheets to the prescribed levels in the flume (see Figure 3.1, No. ⑧).

3.3 Bed Profiling System

The glass sides of a flume allow visual inspection of the flow and sediment transport and approximate tracing of the bed profile. Accurate measurement of bed topography requires provision of additional facilities. Here an automatic mechanical system of bed profiling , called Tactile Bed Profiler, is used and described.

Figure 3.2 shows a sketch of the system. It is composed of four major parts:

1. the computer and multi-function input/output interface;
2. the horizontal and vertical position motor drives and control logic unit;
3. the horizontal position motor and position feedback;
4. the vertical position motor and position feedback with tactile surface sensor.

The computer has overall supervision and control of the system and the multi-function input/output interface provides scaling for the analogue input and output voltages and currents and converts TTL (Transistor-Transistor-Logic) levels to RS232C (a standard to which signal levels conform) logic levels.

The horizontal and vertical position motor drivers and control unit convert the RS232C logic level command to high power drive signals for each motor. The control unit also provides excitation for the position feedback potentiometers and the tactile surface sensor.

The horizontal position motor is a single phase 240 volt AC reversible gear motor. The associated position feedback potentiometer is coupled via reduction gearing to the motor drive shaft. The horizontal motor, mounted at the end of the test section of the flume, drives the trolley through a multi-strand stainless steel wire and pulley system.

The vertical position motor is a 12 volt DC "print" motor coupled to the position feedback potentiometer and the tactile surface sensor via reduction gearing and a rack and pinion drive shaft. The tactile surface sensor activates an infra-red beam interrupt switch.

The tactile surface sensor is a light, thin wall, stainless steel tube with a small disc-shaped foot. The foot diameter is about 10 mm. When the foot touches the bed it becomes stationary relative to the infra-red switch's movement causing the switch to activate and stop the vertical motor. Horizontal and vertical movement of the system is controlled by three digital levels from the computer.

The bed profiler unit including the vertical motor and the surface sensor is mounted on a trolley similar to that of the bed leveller (Figure 3.3). This unit can move transversely on the top channels. When it is fixed in a position on the channels, the system will survey the profile in the respective longitudinal direction. For three-dimensional bed forms the transverse displacement of the unit allows the bed profile to be recorded for a series of parallel longitudinal lines.

3.4 Loose Bed Leveller

The initial level of the loose bed along the test section must be set to prescribed values. Figure 4.5 shows a simple manual arrangement for this purpose. The principle is to pour sediment into the flume, to set the levelling board (No. ⑩ in Figure 3.3) at the desired height above the flume's fixed bed, and to push the trolley along from one end to the other. The area in front of the levelling board should always have enough sediment to fill the gaps. The surplus sediment will be moved along with the board.

3.5 Spreading the Sediment Input

The sediment feeding system (No. ⑩ in Figure 3.1) consists of a commercially available vibratory feeder (OMNIMAT, model F-Tol-A, Vibra Flow Feeder) fed by a large hopper. The feeder is comprised of a funnel, vibrator unit, and a small chute. An adjusting knob changes the degree of vibration, varying the feed discharge.

A simple chute connects the small vibratory chute to the top width of the flume and is used to maintain the distribution of the sediment discharge across the flume width. Figure 5 shows a schematic sketch of this sediment spreader. As shown, the width of the chute at the top and near the bottom is divided into several equal divisions. Thin partitions, made out of 1 mm thick galvanised metal sheets, connect the division points. The partitions then join the outlet at right angles. The equal spacing at the top guarantees equal sediment intake into all compartments and the short end sections of the partitions cause the material to be distributed uniformly across the width of the flume.

The spreader has a clear Perspex cover to allow visual inspection and also to reduce dust emission. The cover is bent down to direct the material downward into the flume.

If the sediment is damp, the intake spacing should be large enough to let the material pass through. As an example, for wet material of fairly uniform quartz with $D_{50} \approx 2$ mm, dividing the 130 mm wide intake into six equal subdivisions resulted in compartments which were too small when sediment was damp but quite satisfactory when it was dry.

3.6 Water Discharge Control and Measurement

Water flow rate is controlled by a Bray Series 30 Wafer Pattern 250 mm Butterfly valve and an EL-o-Matic model EL350 electric actuator located in the supply pipe to the flume head box (No. ③ in Figure 3.1). The flow is proportional to valve position which is set by a 0-10 volt D.C. analogue signal received from the computer. The position of the valve(*ie* open, closed, or partially open) is transmitted to the computer as a 0-10 volt D.C. analogue signal from a position feedback potentiometer connected to the valve stem.

The flow rate is measured by a Danfoss Magflo Electromagnetic flowmeter comprising a type MAG DN 250 sensor and a MAG 3000 signal converter. The signal converter provides a visual display of flow rate and transmits a 0-20 mA analogue signal to the computer.

3.7 Water Level Measurement

Water level is measured using a Mark V Capacitance Wave probe designed by NSW Public Works Department, Australia. The capacitance wave probe has been designed to convert changes in water level to a corresponding voltage output. The sensing element or "probe" of the system is an insulted wire which forms a part of the capacitor, the other part being the water. As the capacitance is directly proportional to the length of immersion, changes in water level are sensed, processed electronically and an analogue D.C. voltage signal is output. The signal output was scaled for 25 mV per 1 mm immersion. The sensing element used is 400 mm in length.

The probe could not be installed inside the flume because it would obstruct the moving trolleys and would be susceptible to damaging impact or burial by the moving sediment. To overcome this difficulty the following provision was made:

Two holes were provided in each of the vertical clear Perspex pieces located in the front view side of the transition between the beams (see Figure 3.1). The probe was put in a vertical clear Perspex tube, 40 mm in diameter, installed outside the flume acting as a stilling well. A flexible hose, 20 mm in diameter, connected the bottom of the tube and one of the side holes of the flume. The water level in the stilling well was equal to that of the flume. There are some remarks which should be made:

1. Side holes were needed at different heights from the flume bed to prevent burial of the hose inlet by the sediment layer at the flume bed. If this was suspected to occur, the hose was connected to another hole above.

2. The water column in the tube and the connection provide a degree of damping for the water level fluctuations. Although generally beneficial, care should be taken about the possibility of slow response and excess damping. An analysis of the stilling well lag in unsteady flow was undertaken providing a basis for the design of the stilling wells (see Section 4.10.2, Saiedi 1994a).

3.8 Multifunction Computer Interface

All analogue and digital signals received and transmitted by the computer are passed through a multifunction interface. This interface is in two parts. The first part is a Metrabyte type DAS-16 multifunction input-output board, which is fitted to the backplane of the computer. It has 16 analogue inputs, 2 analogue outputs, 4 digital inputs, 4 digital outputs and a programmable timer. In this application 12 analogue inputs, 1 analogue output, 1 digital input and 3 digital outputs are used. The second part is a composite circuit board where each individual input or output is preconditioned on reception or transmission.

3.9 Sediment Properties

The sediment used was of fairly uniform size with the median grain size D_{50} = 2 mm, relative density = 2.60, and porosity at bed = 0.37. The porosity of the material under water in the flume was not the same as that in the sediment feeder. The reason is that in the former situation the void spaces between larger grains can be filled by the smaller grains in the movement processes. Also the formation of a deposition layer establishes a degree of grain inter-locking. These result in a fairly compact bed structure with a lesser porosity.

Table 3.1
Properties of the Sediment used in the Laboratory Experiments

Size(mm)	2.80	2.36	2.00	1.40	1.18	1.00	0.60	0.075
Percentage Finer (%)	100	86	46	5	3	1	0.2	0.05

D50$\approx$2 mm
Gradation Coefficient= $\dfrac{D_{84}/D_{50}+D_{50}/D_{16}}{2} = 1.2$
Grains Density= 2602 kg/m^3

Porosity in the Feeder =0.415
Porosity at the Bed =0.370

3.10 Attainment of Non-Uniformity

To highlight the significance of coupling of water and sediment motion a high degree of flow non-uniformity in the tests was required. This was achieved by adjusting the flume to the slope of 0.005 as well as provision of a downstream weir. The weir, of 170 mm height above the rigid bed, was installed at the downstream end of the test section. The height of this fixed weir, given the flume bed slope of 0.005, was considerably greater than the uniform flow depths associated with the flow rates in the experiments. This caused a significant longitudinal flow depth variation in all tests which in turn gave rise to significant variation of the sediment transport capacity along the test section. The weir also prevented the bed load from leaving the test section (see Figure 3.5).

3.11 Preliminary Water Surface Profile Examination

To examine preliminary the general pattern of water surface profiles in the flume, several preparatory tests were performed with and without a sediment layer at the bed. Figures 3.5 and 3.6 show typical examples of these tests in case of rigid and loose bed respectively. The height of the weir for the respective tests was 200 mm above the rigid bed.

The figures indicate that the presence of the weir causes the water surface to be nearly horizontal regardless of the flow rate and the presence of the sediment layer.

To investigate the sensitivity of the water surface calculations to the value of the roughness coefficient, a few water surface profile calculations were performed using various Manning's n values. The actual cross section consisted of the bed, covered by sediment grains of 2 mm in diameter, and two glass sides. In the calculations values of 0.011, 0.013, and 0.015, adopted for the overall cross section, were tried. Figure 3.7 shows the results of an example of these calculations assuming a weir height of 200 mm above the rigid bed. The figure implies that the water surface profiles are not significantly sensitive to values of n. This can be justified noting that a constant flow rate is associated with a given downstream water level corresponding to the free weir overflow. This water level is considerably greater than the respective uniform flow depth, thereby affecting the water depth all along the test section. In other words, the flow in the reservoir created by the presence of the weir, would not be significantly sensitive to the value of the roughness coefficient.

3.12 Experimental Procedure

The flume was filled with sediment to a desired depth. The upstream roughened bed section was set level with the surface of the sediment layer to provide an initial continuous bed for the whole flume length. Using a personal computer and developing the required data acquisition, feedback and control programs, the flow rate was regulated to follow any prescribed flow hydrograph. The height of the downstream weir was kept constant and equal to 170 mm for all tests reported hereafter. Figure 3.8 presents a conceptual view of the test components.

In all experiments, regulation and recording of the flow rate, operation of the bed profiler and recording the bed levels and water levels at five equal intervals along the test section were all accomplished automatically using the computer and the programs developed in the course of the studies at WRL. The vibratory sediment feeder was regulated manually to feed the flow a prescribed rate of sediment input where required. The computer record of the flow and bed level variations was supplemented by visual observation including both eye and the systematic use of a video camera.

To end the test at the due time, the sediment feed was stopped, the downstream gate (no. 20 in Figure 3.1) was lowered to raise the water level and reduce the velocity resulting in termination of sand wave movement, and simultaneously the water flow was stopped. Then the flume was carefully and slowly drained in order not to disturb the final bed profile which was sometimes used for a final check on the video film and still photo data.

The bed profile along the flume was finally surveyed and recorded by the bed profiler along three parallel longitudinal lines; one in the middle of the flume and the other two 100 mm from the side walls. The average value was considered to be the representative depth of the sediment layer. However, in most of the tests the resulting profiles were fairly two-dimensional.

In some tests, the survey of the bed profile was to be performed before the end of the whole experiment. While the simultaneous operation of the bed profiler during a run was possible, it was not practised. The reason was that it took several minutes, depending on the size of the longitudinal intervals, for the bed profiler to cover the length of the test section obstructing instantaneous record of the bed levels.

To resolve this difficulty, the flow was carefully stopped and the flume was gradually drained before the bed is surveyed. To resume the run, the flow was gradually increased to the prescribed value at which the experiment had been discontinued. Starting from a low flow rate and using the downstream regulatory gate, the flow depth was held at considerably greater values (while the weir was submerged lacking any free overflow), to prevent premature movement of the sediment. As soon as the flow rate was established, the downstream gate was fully open allowing the flow to pass freely over the weir.

4. EXPERIMENTAL TESTS AND RESULTS

4.1 A Summary of the Tests

Table 4.1 lists a summary of 14 detailed experiments performed in this study. Some similarities among the tests should be noted. Test 10 is similar to Test 9 except for a longer duration of the second largest flow rate in Test 10. The hydrographs of Tests 5 and 8 are similar except for a longer duration of the peak flow in Test 8. Regardless of the existence or the magnitude of the upstream sediment supply, Tests 4 and 8, 6 and 7, 7 and 13, 10 and 14 are effectively the same. For a quick comparison, the input flow hydrographs of all tests are replotted in Appendix IV.

Table 4.1. Details of the Experimental Tests

(1)	(2)	(3)	(4)	(5)	(6)	(7)	(8)
Test No.	Initial Depth of Sediment Layer (mm)	Total Duration (min)	Peak Flow Rate (m3/s)	Input Hydrograph	No. of Stages	Upstream Sediment Input (kg/min)	Results
1	47	217	-	Figure 4.1	5	-	Figures 4.2 to 4.7
2	59	80	0.076	Figure 4.8	1	-	Figures 4.9, 4.10
3	62	50	0.088	Figure 4.11	1	-	Figures 4.12, 4.13
4	62	40	0.088	Figure 4.14	1	-	Figures 4.15, 4.16
5	62	40	0.087	Figure 4.17	1	-	Figures 4.18, 4.19
6	65	23	0.092	Figure 4.20	1	-	Figures 4.21, 4.22
7	65	23	0.092	Figure 4.23	1	1.5 (for 23 min)	Figures 4.24, 4.25
8	65	40	0.087	Figure 4.26	1	1.5 (for 40 min)	Figures 4.27, 4.28
9	68	18	0.098	Figure 4.29	1	-	Figures 4.30, 4.31
10	68	18	0.098	Figure 4.32	1	-	Figures 4.33, 4.34
11	65	47	0.097	Figure 4.35	3	-	Figures 4.36-4.39
12	64	30	0.095	Figure 4.40	1	1.5 (from t=6 to t=18 min)	Figures 4.41, 4.42
13	65	23	0.092	Figure 4.43	1	4.5 (for 23 min)	Figure 4.44
14	68	18	0.098	Figure 4.45	1	6.15 (for 18 min)	Figure 4.46

Note: In all tests the sediment size was D_{50}=2 mm, the bed slope= 0.005, and the weir height above the rigid bed=170 mm.

4.2 Results

This section contains figures presenting the input hydrographs and the resulting bed profiles and water surface levels of the tests. Regarding these figures some remarks should be made:

2. In the 3rd, 4th, and 5th stages of Test 1, the erosion at the upstream area reached the rigid bed. In the respective figures, this is represented by a solid line showing a zero depth of sediment layer.

3. The water level records of Tests 13 and 14 were not available.

4. The cut-off of the flow hydrographs, represented by a sharp decrease in the respective figures, caused a highly nonuniform decrease in the actual flow rate to follow the nonlinear process of the valve shut-off. The linear representation of this decrease in the hydrographs is only an approximation of this process with negligible effect on the results of all simulations in the context on this study. The same explanation applies to the linear assumption for the flow rate variations between two successive readings in all the hydrographs.

5. MODEL APPLICATIONS

5.1 Empirical Relations Used in the Simulations

Empirical relations to be used in the simulation of the flume tests were those of the downstream boundary condition for water flow, the hydraulic friction, and the sediment transport capacity.

5.1.1 The Downstream Rating Curve

All data obtained from the first 12 tests, for which the water surface information was available, were used to establish an empirical rating curve for the downstream boundary condition shown schematically in Figure 5.1. The data is listed in Table 5.1.

Table 5.1. Details of the Tests Used to Establish the Downstream Rating Curve

Test No.	Sediment Layer(mm)	Q (L/s)	Y (mm)	[Y- H_W] (mm)
1	47	49	270	100
1	47	49	270	100
2	59	49	268	98
2	59	49	268	98
2	59	54.1	273	103
2	59	63	287	117
2	59	70.1	293	123
2	59	75.4	304	134
3	62	49	270	100
3	62	54	274	104
3	62	65	290	120
3	62	70	294	124
3	62	88.5	317	147
4	62	49.3	268	98
4	62	53.9	275	105
4	62	64.4	288	118
4	62	88.3	316	146
4	62	88.3	316	146
5	62	49.3	268	98
5	62	54.5	274	104
5	62	64.6	291	121
5	62	75.3	302	132
6	65	55.8	276	106
6	65	70.4	295	125
6	65	88.3	316	146
7	65	55.8	280	110
7	65	76.9	305	135
7	65	86.5	315	145
7	65	88.4	316	146
8	65	48.3	267	97
8	65	63.9	287	117
8	65	68.8	292	122
8	65	87	316	146
8	65	87	316	146
9	68	54.7	275	105

Test No.	Sediment Layer(mm)	Q (L/s)	Y (mm)	[Y- H_W] (mm)
9	68	64	287	117
9	68	82.3	310	140
9	68	88.5	320	150
10	68	54	276	106
10	68	75.5	300	130
10	68	86.6	316	146
10	68	86.6	316	146
10	68	86.6	316	146
10	68	97.3	325	155
11	65	48	266	96
11	65	48.3	267	97
11	65	65	289	119
11	65	69.5	295	125
11	65	92	321	151
12	64	63.9	288	118
12	64	69.1	294	124
12	64	86.8	315	145
12	64	89.7	317	147
12	64	95.7	325	155

The graphical representation in Figure 5.2, allows an empirical relation to be fitted to the data. The set of 49 tests, all involving bottom sediment layer, resulted in the following relation for flow over the downstream weir:

$$Q = 1.470(Y - H_w)^{1.465} \tag{5.1}$$

where Q in m^3/s is the water flow rate, Y in m is the water level above the rigid bed at 50 mm upstream from the weir (where the water level measuring probe was located), and H_W in m is the weir height above the rigid bed. For all tests, a constant H_W=0.170 m was used. Equation (5.1) was valid for flow rates in the range 0.045 to 0.098 m^3/s in the flume with the bed slope 0.005.

5.1.2 Friction Formula

The only form of the friction relation permitted by HEC6 is through the use of Manning's n. For the hydraulic friction a constant Manning's roughness coefficient n=0.013 was obtained from several water surface profile calculations in the flume. The flume cross section consisted of the bed, covered by the sediment grains of 2 mm, and two glass sides. In a large proportion of the tests leading to this roughness coefficient, the sediment was moving as bed load showing pronounced bed forms along the test section.

Some remarks should be made here. (1) As previously mentioned, several water surface profile calculations indicated that under the laboratory conditions of this study, the water surface is not significantly sensitive to the value of n (see Section 3.11). (2) Given the low sensitivity of the flow to the value of n, it should also be noted that calibration of the sediment sensitivity of the flow to the value of n, it should also be noted that calibration of the sediment transport relation using the actual data is another adjusting factor which would make up for any possible unsuitability of a constant n value. (3) Later computer simulation of the tests revealed that selection of a Manning's roughness value variable with flow rate did not show any significant improvement over the use of the chosen constant value for the tests.

5.1.3 Sediment Transport Formula

To obtain the empirical sediment function special care was practised. From previous experience in the same laboratory conditions, it was known that a transport formula obtained from equilibrium transport tests might result in gross approximation when used in highly nonuniform and unsteady conditions (see Section 7.4.2 of Saiedi 1994a). While COUPFLEX provides for a considerable flexibility in choosing the form of the sediment transport relation, to allow comparison with HEC6, the selection of the user-specified function had to be in accordance with the following limited form prescribed by HEC6:

$$Q_s = \left(\frac{h.S_f - A_3}{A_1}\right)^{A_2}.B.(10^{-6}.A_4.n^{A_5}) \tag{5.2}$$

where Q_s in ton/day is the sediment discharge, h in ft is the effective depth, S_f is the energy slope, coefficients A_1, A_2, A_3, A_4, and A_5 are constant, B in ft is the effective width, and n is the Manning's roughness coefficient (for details see pp. 41-42 and A-35 of HEC 1993).

The first three sedimentation tests, listed in Table 4.1, were used to calibrate the user-specified transport function of the flume. In Test 1, only the first two stages of the process, in which the upstream erosion did not reach the rigid bed, were used. Figures 4.1, 4.8, and 4.11 show the input hydrographs and the solid lines in Figures 4.3, 4.9, and 4.12 show the actual bed profiles along the test section at the end of the hydrographs as measured by the bed profiler. The dotted lines in the latter figures represent the initial levelled bed. The calibration of Equation (5.2) led to the following values for the coefficients:

$$A_1=0.006, \quad A_2=1.35, \quad A_3=18 \times 10^5, \quad A_4= 75 \times 10^6, \quad A_5=0 \tag{5.3}$$

The same relation was used in COUPFLEX. Both COUPFLEX and HEC6 were employed to predict the sedimentation pattern of the calibration tests using computational distance and time steps $\Delta x = 1$ m and $\Delta t = 1$ min respectively. The predicted values are shown in Figures 5.3, 5.4, and 5.5. It is observed that both models fit the actual profiles with effectively the same level of accuracy. The fact that both models give effectively the same answers for these nonequilibrium calibration tests, indicates the overall suitability of the selected friction coefficient and the sediment transport function for the respective experimental conditions.

It should be noted that both COUPFLEX and HEC6, like all other one-dimensional alluvial flow models, give the general sedimentation pattern rather than microscale geometry of the bottom topography. Prediction of microscale bed forms (ripple/dune) requires provision of detailed equations describing small scale motion of sediment and water in at least two dimensions. The present knowledge of rules of small scale motion of sediment transport is insufficient to allow such prediction. Therefore, in evaluation of the accuracy of the predicted results in these and all other figures in this paper, the imaginary smooth bed profiles passing through the actual bed forms along the test section should be considered.

5.2 Modelling Results

Tests 1 to 3 were used to obtained calibrated roughness and sediment transport function as described in the previous section. Tests 4 to 14 were employed to compare the performance of COUPFLEX and HEC6. Both models were applied to these tests to predict the bed level evolution. The results are plotted in Figures 5.6 to 5.20. A few remarks are worth mentioning:

1. Unless otherwise stated, in all model runs, the computational distance and time steps $\Delta x = 1$ m and $\Delta t = 1$ min respectively were used.

2. To examine the sensitivity of the models to Δt, Tests 13 and 14 were reworked using $\Delta x = 1$ m and $\Delta t = 2$ min. The results are shown in Figures 5.19 and 5.20 for HEC6. There was no significant difference for COUPFLEX.

3. As the erosion did not reach the rigid bottom in Test 11, all three stages of the test were modelled. This could not be done for Test 1 for the same reason. As soon as the erosion depth reaches the rigid bottom, the calibrated sediment transport formula becomes invalid rendering the simulation unreliable.

4. Given the height of the downstream weir and the fact that the sediment moved entirely as bed load, no sediment left the test section. Moreover, the large flow depth in the vicinity of the weir caused the respective bed section to be fairly inactive.

5. Sample input and output computer files for HEC6 runs are contained in Appendix V.

5.3 Discussion

The results of the model applications are interpreted and the relevant conclusions are drawn under three different categories namely accuracy, regularity, and sensitivity.

5.3.1 Accuracy

While Tests 1, 2, and 3 involve a significant level of nonuniformity and/or unsteadiness, the extent of nonuniformity and unsteadiness in most of the other tests is much greater. For the latter tests, the predicted bed profiles from COUPFLEX show a superior accuracy compared to those from HEC6. Given the fact that both models employed the same calibrated boundary conditions, roughness coefficient, and sediment transport function, this greater accuracy is attributed only to the coupling of the water and sediment phases of the motion. In HEC6, like any other traditional uncoupled model, first the flow equations are solved to obtain hydraulic information, then the resulting flow depths and velocities (or discharges) and the sediment information are input to the sediment component of the model to predict sediment transport and bed level variations. In this approach the main drawback is the assumption of a "fixed-bed" channel when solving the flow equations. In short term prediction of situations involving slow flow and bed level changes, this assumption may be justified. However, in dealing with fast variations, this assumption brings about an error in the calculation of bed level and flow conditions. This error, however small in a time step, may lead to unacceptable inaccuracy in subsequent time steps through error accumulation and increasing deviation of the predicted bed profiles and sediment transport from the actual ones. The faster the rate of variations in the flow and sediment conditions, the greater deviation that can be caused by the uncoupled procedure.

As far as the water flow component is concerned, HEC6 is a quasi-steady model. This means it does not include the term associated with temporal variation of flow rate or velocity. A remark should be made here. The quasi-steady assumption, under laboratory conditions, cannot contribute significantly to the inaccuracy in question. In laboratory flumes, where any new flow rate will soon dominate the entire flume length within usual computational time steps, the application of the quasi-steady approximation is reasonable. This reasoning was substantiated through application of COUPFLEX to the tests employing the model in its quasi-steady mode. The results did not differ significantly from those using the full dynamic flow equations. This indicates that the significant difference between the results of COUPFLEX and HEC6 can only be explained by coupling and decoupling concepts.

5.3.2 Regularity

It was previously mentioned in Section 5.1.3 that the present alluvial flow models are not expected to go beyond the prediction of general sedimentation pattern and give the detailed bed topography consisting of micro bed forms. Such possible ripple/dune like bed profiles obtained from a numerical model of one-dimensional flow, in which the required predictive mechanisms are not provided, are indications of computational anomalies. Numerically induced bed level oscillations, encountered in many numerical models of alluvial flows, are clear examples of such computational irregularities. Saiedi (1994a) dealt with these oscillations and showed how some numerical discretisation schemes used in uncoupled models could cause artificial bed level oscillations.

While the predicted bed profiles from COUPFLEX do not show bed profile irregularities in any of the present tests, evidence of bed level oscillations, numerically generated by HEC6, can be found in Figures 5.10, 5.16, and 5.17 to 5.20 associated with Tests 8, 12, 13 to 14 respectively. These latter two tests , for example, involve not only the same rapid flow hydrographs as in their corresponding Tests 7 and 10, but also rapid upstream boundary condition changes caused by substantial upstream sediment supply.

Among major sources of these false oscillations are inappropriate discretisation schemes for the situation under study, incompatibility of the chosen computational distance and time steps with the actual extent and rate of the physical processes involved, and inappropriate representation of the physical phenomenon by insufficient mathematical formulation. These false oscillations, if significant, give rise to simultaneous sudden changes in flow characteristics, such as in the flow depths and energy slope, leading possibly to the failure of the numerical model to proceed with any solution. This is because any numerical model, regardless of its solution procedure, is confined to specific limitations imposed by the validity range of its underlying equations.

A disadvantage of the uncoupled approach to numerical modelling of alluvial flows is that false bed level oscillations can grow freely in a time step without the interference of the flow conditions. In the coupled method, part of the oscillations may be dampened due to concurrent influence of the water depth and velocity, reducing the risk of generating bed irregularity incompatible with the corresponding flow characteristics.

5.3.3 Sensitivity

In selecting the size of the computational distance and time steps, Δx and Δt, the physical extent and speed of water and bed level changes in the situation being modelled should be taken into account. A typical example of this is the significance of the celerity of water surface disturbances used to impose some limitations on the selection of Δx and Δt in water flow models. Referring to a simple physical argument on the importance of the upstream boundary condition for sediment in a numerical model of river sedimentation, Saiedi (1994c) presented a conceptual formulation for the propagation velocity of overloading sand waves to be used in numerical models.

While the necessity of this physical consideration for selection of Δx and Δt is straightforward, its practical implementation is much less so. For instance, the main difficulty in the inclusion of the propagation speed of sand waves in numerical models of mobile bed rivers is the lack of sufficient information on this speed for most situations.

From the above argument, implying that it is not always possible to specify the most realistic choice of Δx and Δt, it can be concluded that it would be advantageous if a numerical model allowed flexibility in this choice without causing serious errors in the results.

To examine the sensitivity of COUPFLEX and HEC6 to the size of Δt, Tests 13 and 14 were reworked using the same computational elements except that $\Delta t = 2$ min was used rather than the previous value of $\Delta t = 1$ min. The results from COUPFLEX did not show any distinguishable difference but the results from HEC6 were different. These are shown in Figures 5.19 and 5.20. A comparison with the case of $\Delta t = 1$ min reveals that HEC6 is much more sensitive to the size of the computational time step for the tests in question.

The following gives a brief explanation why the solutions for a given sedimentation problem sometimes converge to effectively the same answers while using different computational time and distance steps.

Let us consider a case of a degradation situation due to cessation of the upstream sediment input in a steady and initially uniform flow. Given a fixed Δx, the computations associated with Δt_2 greater than Δt_1 would lead to the corresponding erosion depths Δz_2 less than Δz_1. This is because these two different time steps lead to different values for sediment transport deficit to be distributed over the same Δx for the first upstream subreach. Let us also assume that the actual time required for the extent of the erosion to cover a distance Δx is Δt_1 so that the selection of Δt_2 greater than Δt_1 causes an overestimation of the erosion depth. This overestimated erosion, in a subcritical flow for instance, leads to a corresponding overestimation of the respective flow depths and underestimation of the respective flow velocities. These in turn give rise to underestimating sediment transport capacity causing a reduction in the erosion depth in the subsequent time steps. The interference of the flow characteristics through adjustment of the sediment transport capacity may compensate for some previous deviations from the actual bed level variations. In a coupled model this interference is simultaneously present providing for a faster convergence of the solutions as well as for a faster suppression of the deviation from the actual bed levels.

6. CONCLUDING REMARKS

Several detailed flume tests on river sedimentation were undertaken exclusively to compare the performance of a well known uncoupled computer program of sedimentation, HEC6, to that of a newly developed coupled numerical model of riverine flow, COUPFLEX. The tests were designed to achieve a high level of nonuniformity and unsteadiness in the water and sediment motion to highlight the importance of interconnection between the water flow and bed level variations. The results showed that the coupled model COUPFLEX provided a better prediction of sediment motion than did the uncoupled model HEC6 when flow and sediment conditions were changing rapidly. From the simulations it can be concluded that a coupled approach is preferable to the traditional uncoupled model because:

(a) A coupled model calls for little extra computational effort to develop but provides for a better mathematical formulation of the reality of alluvial flows by concurrent solution of the equations for two concurrent phases of the motion, *ie* water and sediment phases.

(b) Separation of water and sediment calculations, as practised in uncoupled modelling, in cases where fast flow and bed level changes are involved, gives rise to small deviations from corresponding experimental results and those from a coupled model. These deviations may grow with time leading possibly to gross errors.

(c) A coupled model prevents some computational difficulties arising from decoupling of the equations of water and sediment. These difficulties, such as numerically induced bed level oscillations, are often encountered in modelling rapidly changing flow and boundary conditions.

(d) A coupled model shows less sensitivity to the sizes of computational time and distance steps.

While computer programs such as HEC6 are useful tools in dealing with most laboratory and field applications, for the development of new commercial computer programs of alluvial flows consideration of the coupled method as opposed to the traditional uncoupled methods seems inevitable.

7. REFERENCES

Abbott M.B., Basco D.R. (1989), *Computational Fluid Dynamics, an Introduction for Engineers,* Longman Scientific & Technical, John Wiley & Sons.

Ashida K., Michiue M. (1972), "Study on Hydraulic Resistance and Bed Load Transport Rate in Alluvial Streams", *Proceeding of Jap. Soc. Civ. Engrs.* No. 206 (in Japanese).

Brownlie W.R. (1981), "Prediction of Flow Depth and Sediment Discharge in Open Channels", *W M Keck Laboratory of Hydraulics and Water Resources,* California Institute of Technology, Pasadena, Calif., USA, *Report* kh-R-43A.

Celik I., Rodi W. (1991), "Suspended Sediment Transport Capacity for Open Channel Flow", *Journal of Hydraulic Engineering,* ASCE, Vol. 117, No. 2, pp. 191-204.

Chang H.H. (1982), "Mathematical Model for Erodible Channels", *Journal of Hydraulic Engineering,* ASCE, Vol. 108.

Correia L., Krishnappan B.G., Graf W.H. (1992), "Fully Coupled Unsteady Mobile Boundary Flow Model", *Journal of Hydraulic Engineering,* ASCE, Vol. 118, No. 3, March.

Correia L., Krishnappan B.G., Graf W.H. (1992), "Fully Coupled Unsteady Mobile Boundary Flow Model", *Journal of Hydraulic Engineering,* ASCE, Vol. 118, No. 3, March.

Cunge J.A., Predreau N. (1973), "Mobile Bed Fluvial Mathematical Models ", *La Houille Blanche*, no. 7, 1973, pp.562-580.

Cunge J.A., Holly F.M., Verwey A.S. (1980), *Practical Aspects of Computational River Hydraulics*, Pitman Publishing Ltd.

Cunge J.A. (1988), "Wrap Up Discussion in the Second Seminar on Stream Sedimentation Models", in Fan S.S. (ed) *Twelve Selected Computer Stream Sedimentation Models Developed in the United States*, Interagency Ad Hoc Sedimentation Work Group, Published by Federal Energy Regulatory Commission.

Engelund F., Hansen E. (1967), *A Monograph on Sediment Transport in Alluvial Streams,* Teknisk Vorlag, Copenhagen, Denmark.

Gee D.M. (1988), "Status of HEC6, Scour and Deposition in Rivers and Reservoirs", in Fan S.S. (ed) *Twelve Selected Computer Stream Sedimentation Models Developed in the United*

States, Interagency Ad Hoc Sedimentation Work Group, Published by Federal Energy Regulatory Commission.

Gessler J. (1971), "Aggradation and Degradation" in Shen H.W. (ed) *River Mechanics*, Vol. 1.

Graf W.H. (1971), *Hydraulics of Sediment Transport*, McGraw-Hill Book Company.

Gysel A.V., Huggens M., Verhoeven R. (1992), "Mathematical Simulation of Non-Permanent River Flow with Movable Bed", *Proceeding of Hydrosoft 1992* Fluid Flow Modelling.

HEC (Hydrologic Research Center) (1977), *HEC6, Scour and Deposition in Rivers and Reservoirs, User Manual*, U.S. Army Corps of Engineers

HEC (Hydrologic Research Center) (1993), *HEC6, Scour and Deposition in Rivers and Reservoirs, User Manual*, U.S. Army Corps of Engineers, August.

Henderson F.M. (1966), *Open Channel Flow*, Macmillan Company.

Holly F.M. Jr. , Cunge J.A. , Wignyosukarto B., Einhelling R. (1987), "Coupled Implicit Simulation of Mobile-Bed Rivers", National Conference on Hydraulic Engineering, ASCE, Williamsburg, VA, USA, 3-7 August.

Holly F.M. Jr. , Rahuel J.L. (1989), "Advances in Computational Mobile-Bed Hydraulics", in Wang S.S.Y (ed) "Sediment Transport Modeling", *Proceeding of the International Symposium*, ASCE, New Orleans, Louisiana, 14-18 August.

Holly F.M. Jr. , Rahuel J.L. (1990a), "New Numerical/Physical Framework for Mobile-Bed Modeling, part 1. Test Applications", *Journal of Hydraulic Research*, IAHR, No. 5, Vol. 28, pp. 545-563

Holly F.M. Jr., Rahuel J.L. (1990b), "New Numerical/Physical Framework for Mobile-Bed Modeling, part 1. Numerical and Physical Principles", *Journal of Hydraulic Research*, IAHR, No. 4, Vol. 28, pp. 401-416.

Hosseinipour Z. (1989), "Development and Application of a Fluvial Hydrodynamic and Sediment Transport Model" in Falconer, R.A. et al (eds) "Hydraulic and Environmental Modelling of Coastal, Estuarine and River Waters", *Proceeding of International Conference* at University of Bradford, USA

Hsu H-C, Chu P-C, (1964), "Study of River Bed Degradation and Aggradation by the Method of Characteristics", *Chinese J of Hydraulic Engineering,* No. 5, pp.1-20, also in Scientia Sinica , Vol. XIV. No. 11, 1965, pp. 1673-1690.

Lai C. (1986), "Numerical Modeling of Unsteady Open-Channel Flow", in *Advances in Hydroscience,* Vol. 14, Academic Press.

Lai C. (1991), "Modeling Alluvial Channel Flow by Multimode Characteristics Method", *Journal of Hydraulic Engineering,* ASCE, Vol. 117, No. 1

Lyn D.A., Goodwin S.M. (1987), "Stability of a General Preissmann Scheme", *Journal of Hydraulic Engineering,* ASCE, Vol. 113, No. 1, Jan, 16-28.

Lyn D.A. (1987), "Unsteady Sediment Transport Modeling", *Journal of Hydraulic Engineering,* ASCE, Vol. 113, No. 1, January, 1-15.

Meyer-Peter E., Muller R. (1948), "Formula for Bed Load Transport", *Proceeding 2nd Meeting IAHR,* Vol. 6.

Michiue M., Suzuki K. (1982), "A Computation Method on River Bed Variations of Large Scale", *3rd Congress of the Asian and Pacific Region Division, IAHR,* Indonesia.

Morse B., Townsend R.D. (1990), "Modelling Channel Bed Transients using Explicit F-D Schemes", *Journal of Hydraulic Engineering,* ASCE, Vol. 116, No.11.

Rahuel J.L., Holly F.M. Jr. , Chollet J.P., Belleudy P.J., Yang G. (1989), "Modeling of Riverbed Evolution for Bedload Sediment Mixtures", *Journal of Hydraulic Engineering,* ASCE, Vol. 115, No. 11, pp. 1521-1541

Saiedi S. (1993), "Experience in Design of a Laboratory Flume for Sediment Studies", *International Journal of Sediment Research,* Vol. 8, No. 3, pp.89-101, IRTCES (International Research and Training Centre on Erosion and Sedimentation), Beijing, China.

Saiedi S. (1994a), "Numerical and Experimental Studies of Unsteady Water and Sediment Flow in Open Channels", *Ph.D. Thesis* , School of Civil Engineering, University of New South Wales, Australia

Saiedi S. (1994b), "A Non-dimensional Coupled Numerical Model of Alluvial Flow", *International Journal of Sediment Research*, Vol. 9, No. 2, pp. 59-79, IRTCES (International Research and Training Centre on Erosion and Sedimentation), Beijing, China.

Saiedi S. (1994c), "Experimental Study on Sand Waves in Open Channels with Oversupply of Sediment", *Proc. of Conference on Hydraulics in Civil Engineering*, The Institution of Engineers, Australia, 15-17 Feb., Brisbane, Australia, pp. 309-314.

Samuels P.G. (1989), "Backwater Lengths in Rivers", *Proceeding of Institution of Civil Engineers*, Part 2, Vol. 87, 571-582.

Thomas W.A., Prasuhn A.L. (1977), "Mathematical Modelling of Scour and Deposition", *Journal of Hydraulic Engineering*, ASCE, Vol. 103, No. HY8.

Thomas W.A. (1982), "Mathematical Modelling of Sediment Movement", Chapter 18 in Hey R.D. et al (eds) *Gravel-Bed Rivers*, John Wiley & Sons Ltd.

Tingsanchali T., Panvanich S. (1981), "Morphological Computation of River Bed Degradation Due to Sand Dredging in Chao Phraya River", *Proceeding of South-East Asian Reg Symposium on Problems of Soil Erosion and Sedimentation*, Bangkok, Thailand.

Vries M. de (1981), "Morphological Computations", Lecture Notes, F10a.I, Technische Hogeschool, Afdelingder Civiele Techniek, Delft, The Netherlands.

Yang C.T., (1973), "Incipient Motion and Sediment Transport", *Journal of Hydraulic Engineering*, ASCE, Vol. 99 No.10.

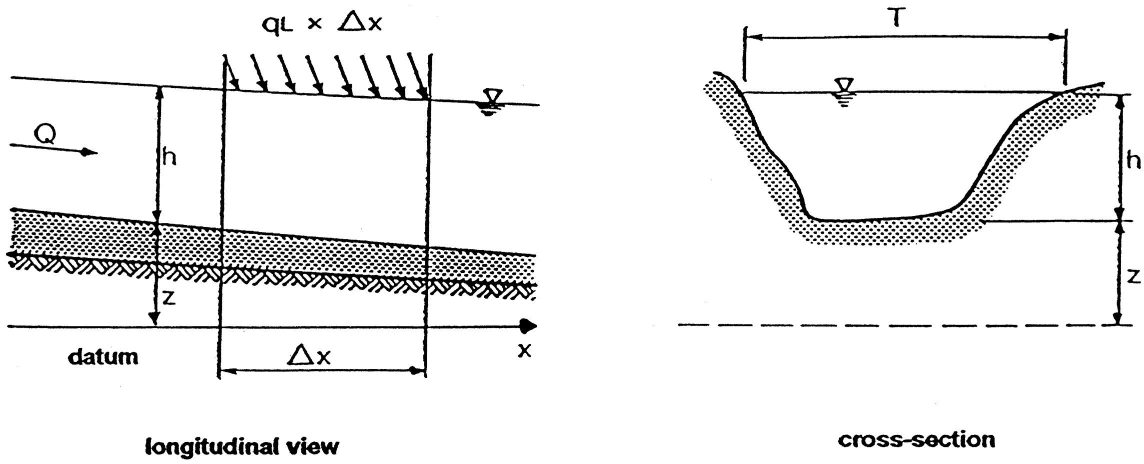

Figure 1 Definition Sketch of Flow in Alluvial Channels

Legend

1. Pump
2. Electro-Magnetic Flowmeter
3. Valve, Electrical Actuator
4. Head Tank
5. Screens & Steel Balls
6. Main Support
7. Flow Straightener
8. Raised Roughened Bed
9. Jacks
10. Sediment Feeder System
11. Bed Profiler
12. Sediment Leveller
13. Load Cell & Pulley System
14. Digital Scale Indicator
15. Sediment Collecting Basket
16. Guide Rollers
17. Sliding Lid
18. Rubber Sheet
19. Hinged Lever
20. Sluice Gate

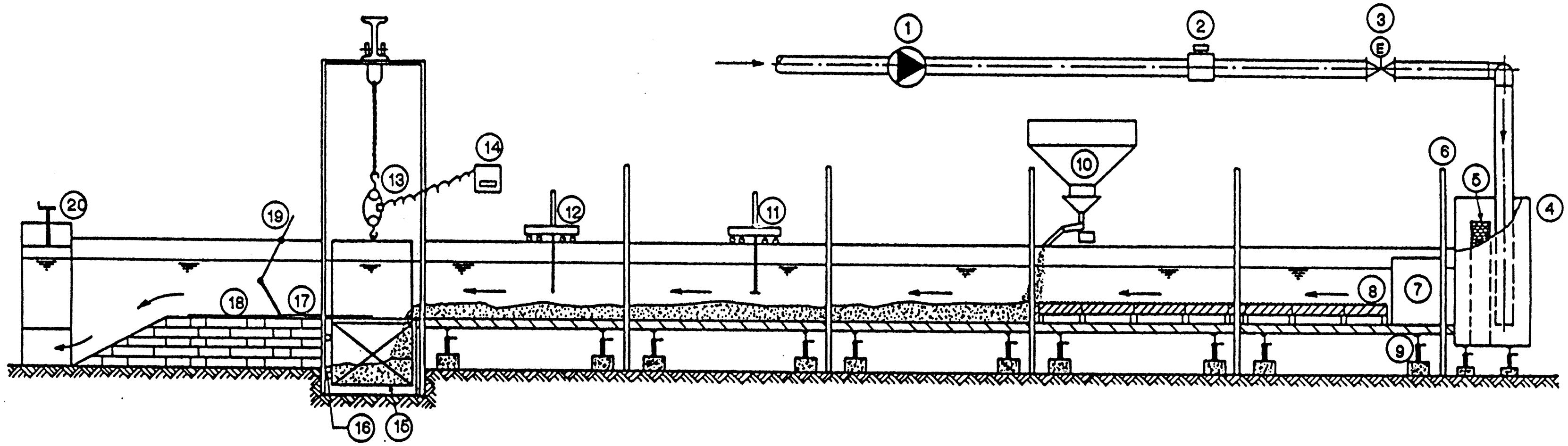

Figure 2 General View of Experimental Setup
(not to scale)

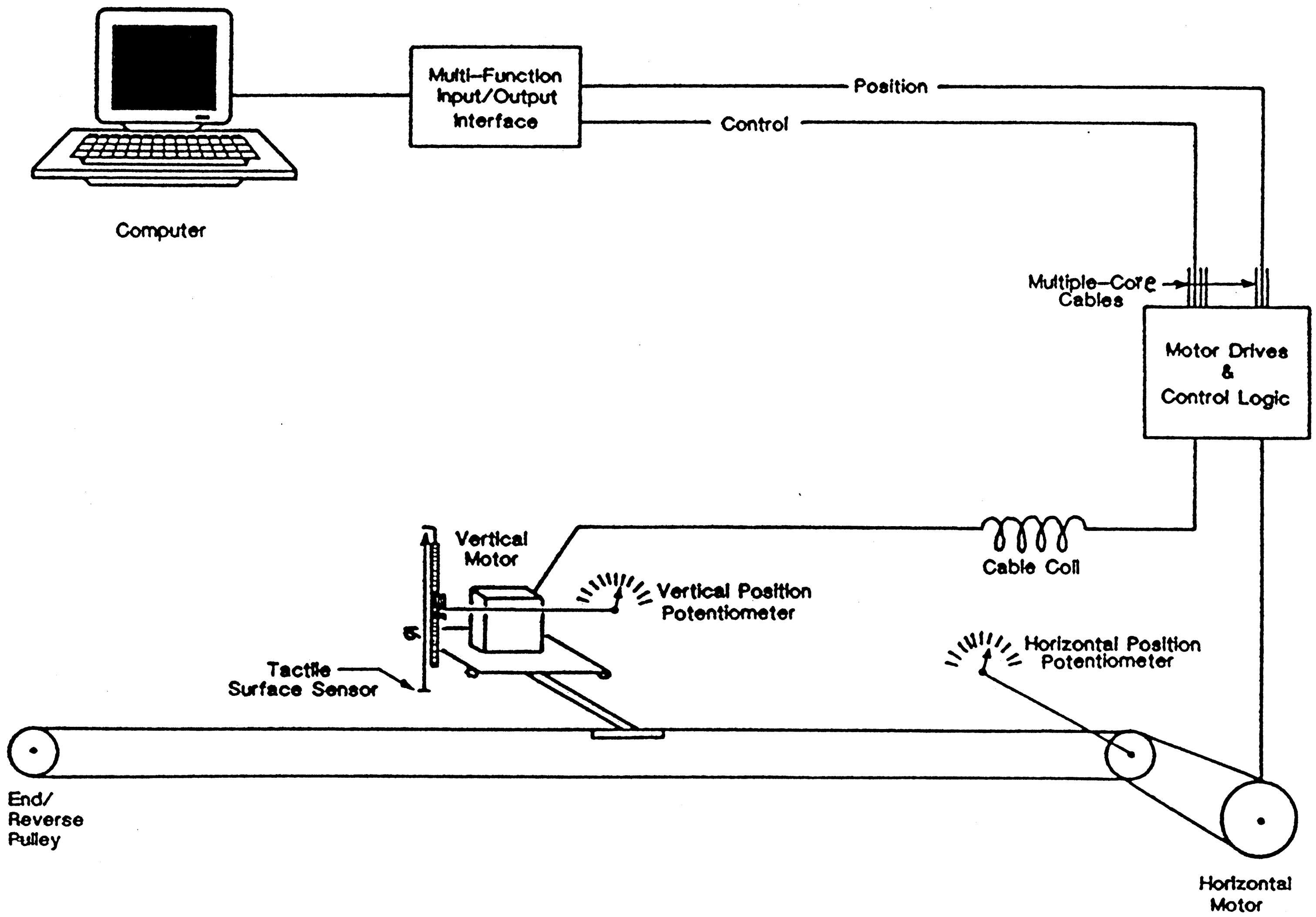

Figure 3 Conceptual Sketch of the Bed Profiling System
(not to scale)

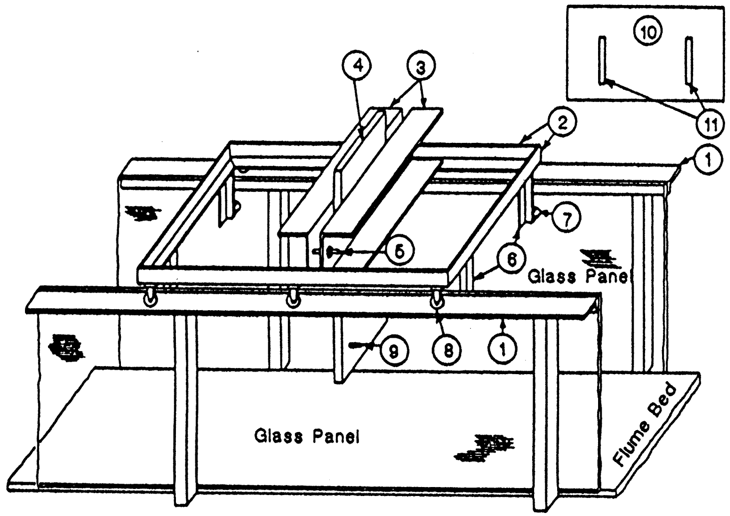

Legend

1. Capping Angle, Top of the Flume
2. Trolley Main Frame, Aluminium Angles
3. Aluminium Channels
4. Plywood Board
5. Clamping Screws
6. Side Wheel Base, Aluminium Angle
7. Side Rubber Wheels
8. Main (Rubber) Wheels
9. Fixed Screws
10. Levelling Board, Plywood
11. Slots

Figure 4 (a) Trolley and Sediment Leveller (not to scale)

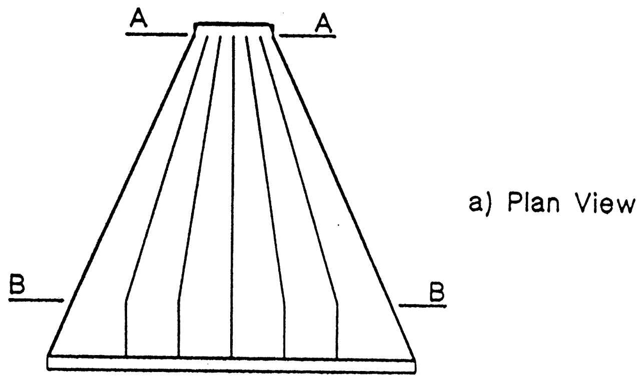

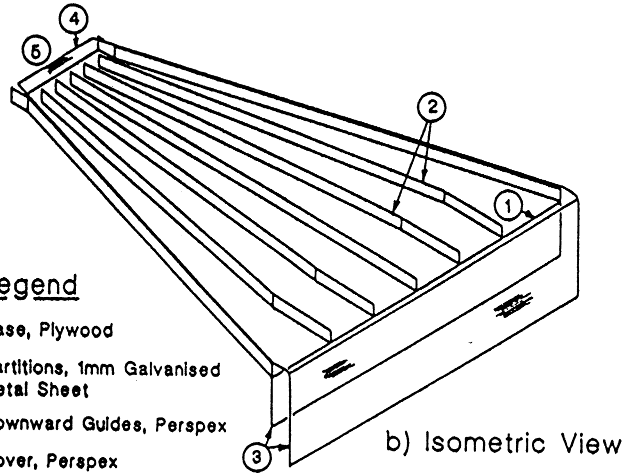

Legend

1. Base, Plywood
2. Partitions, 1mm Galvanised Metal Sheet
3. Downward Guides, Perspex
4. Cover, Perspex
5. Entrance

Figure 4 (b) Schematic Sketch of the Sediment Spreader (not to scale)

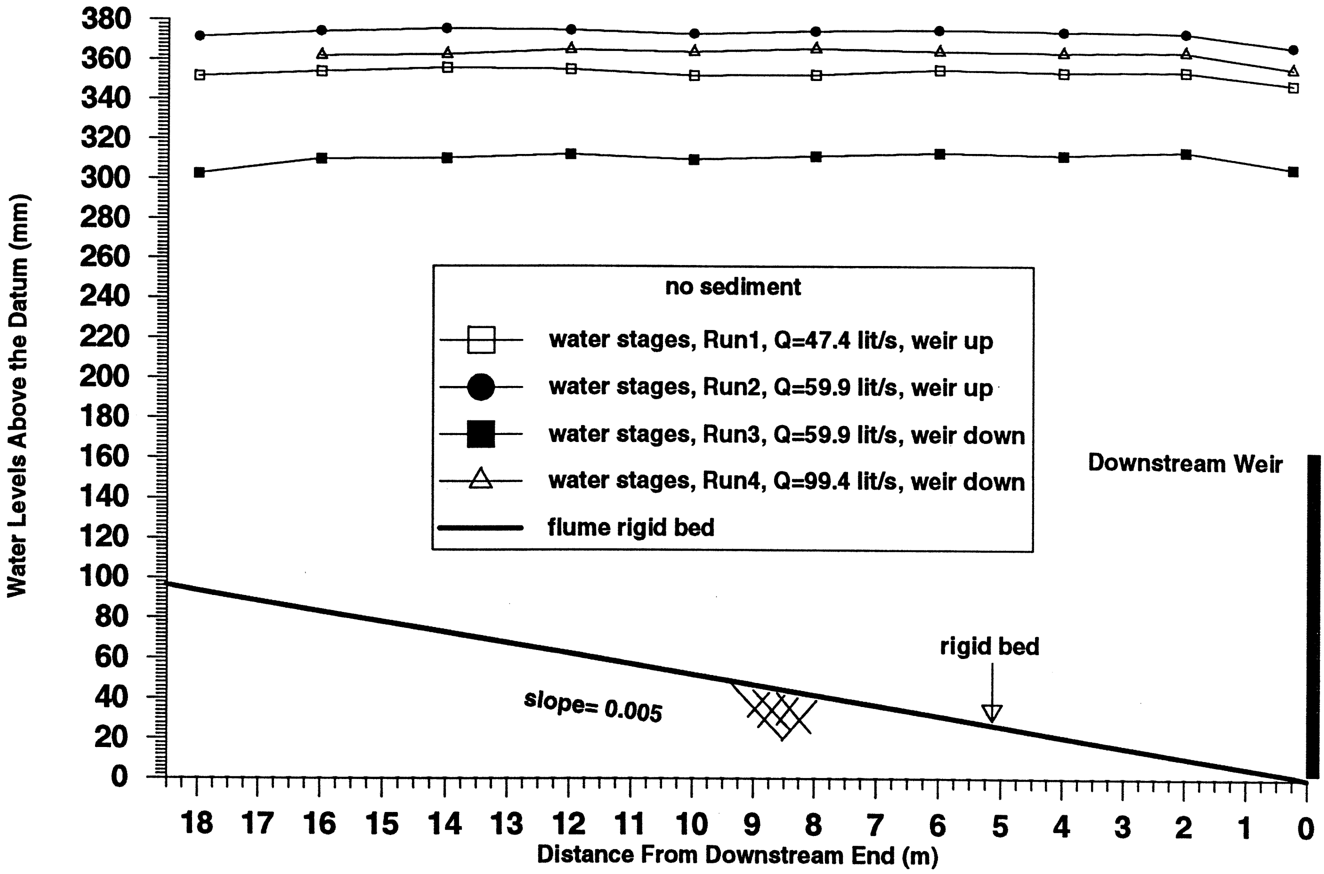

Figure 5(a) Preliminary Tests for Water Profiles in the Flume without Sediment Layer

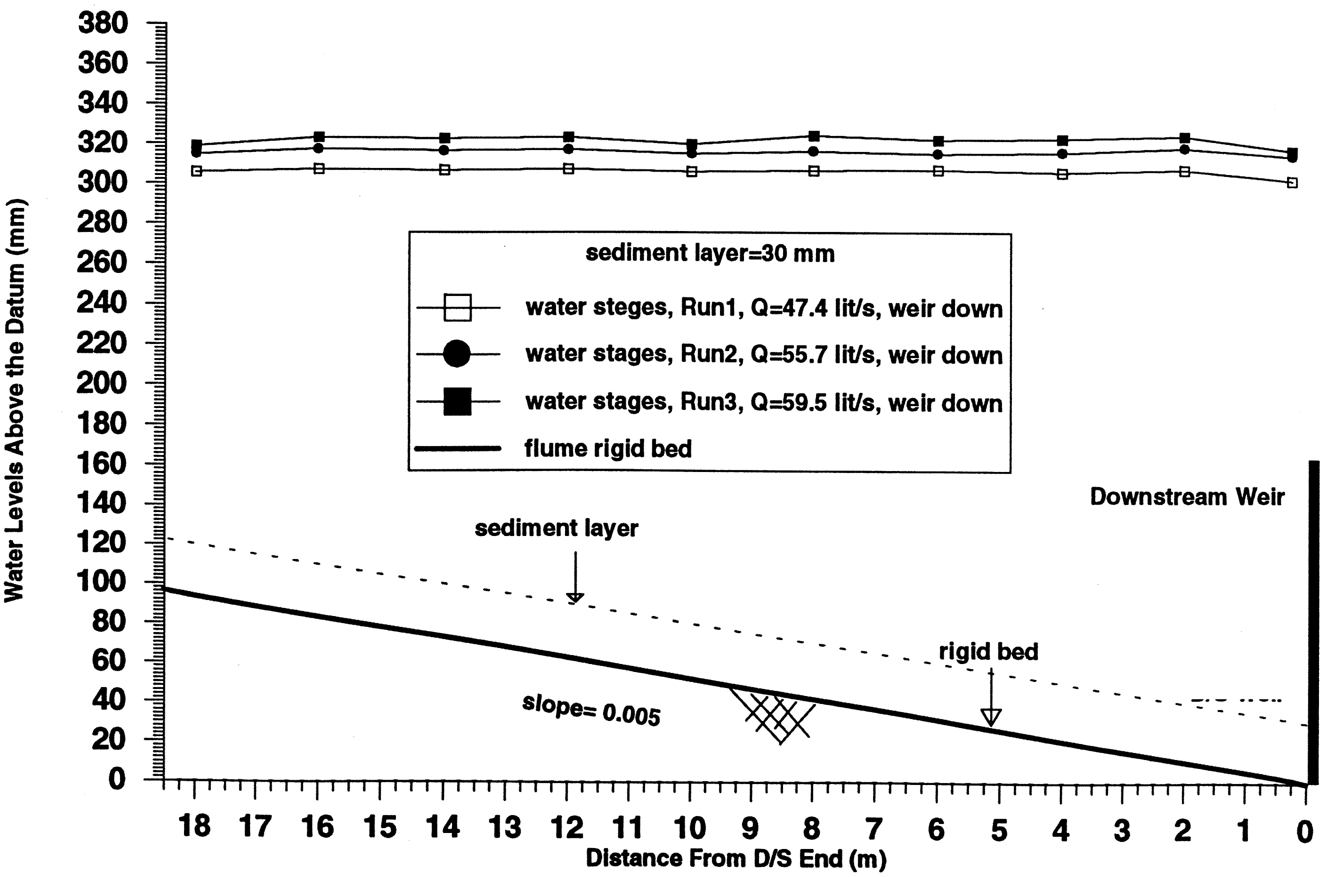

Figure 5(b) Preliminary Tests for Water Profiles in the Flume with Sediment Layer

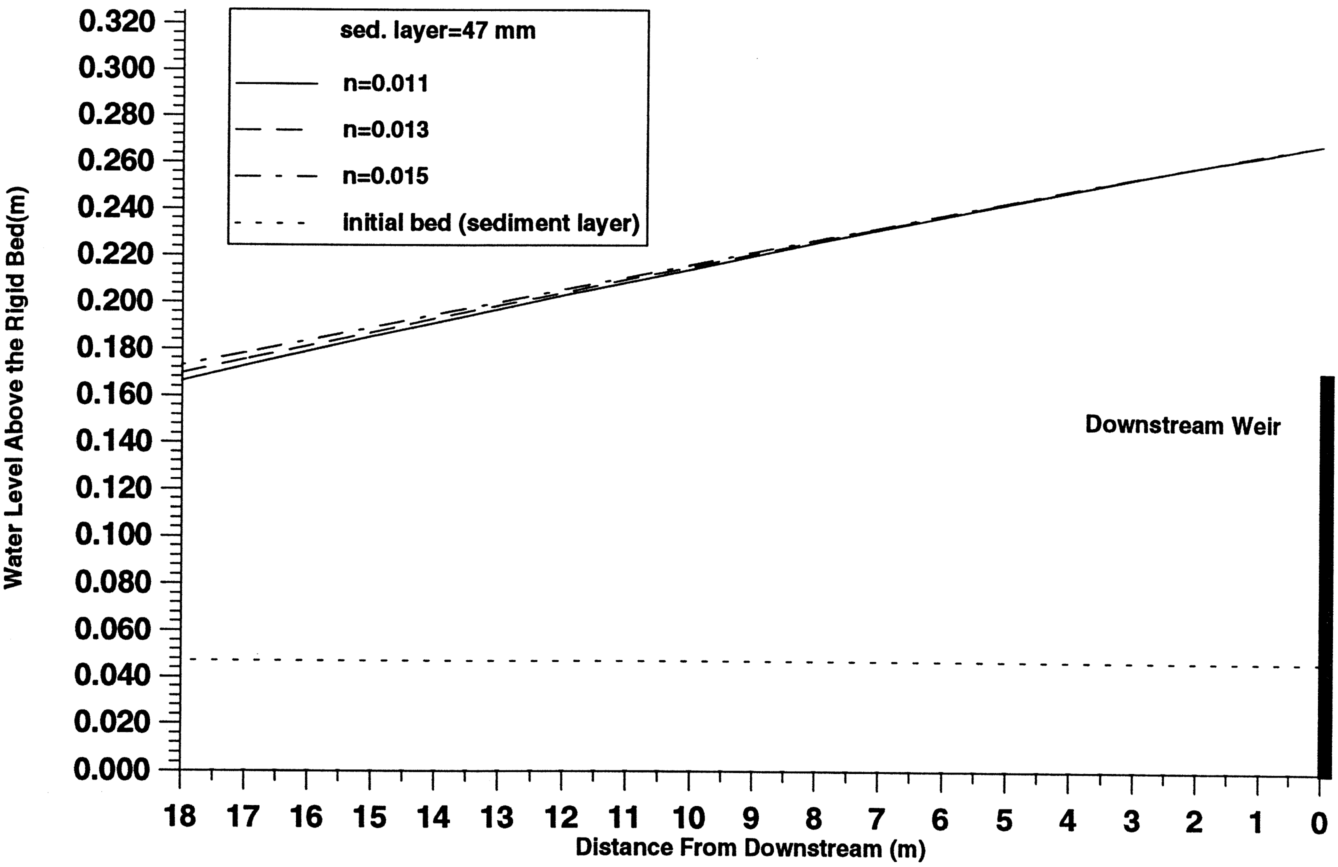

Figure 6(a) Water Surface Profiles with Various Manning's n

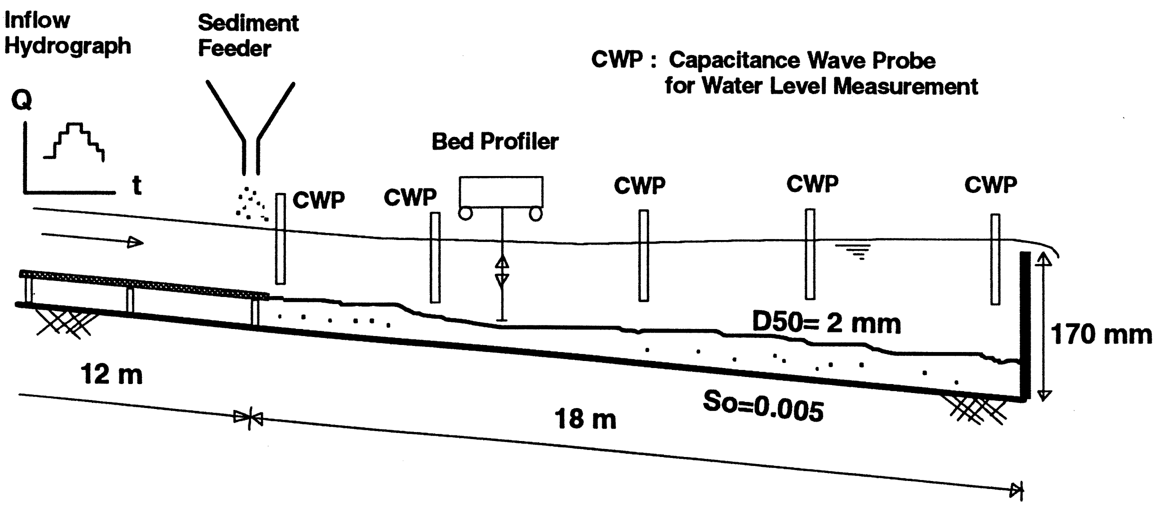

Figure 6(b) Schematic View of the Flume
(not to scale)

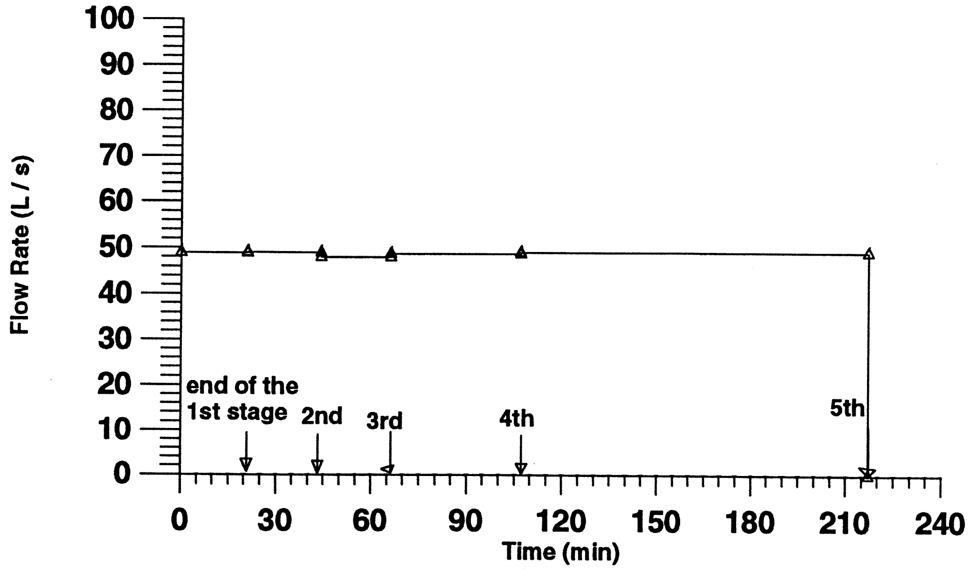

Figure 7(a) Flow Hydrograph in Test 1

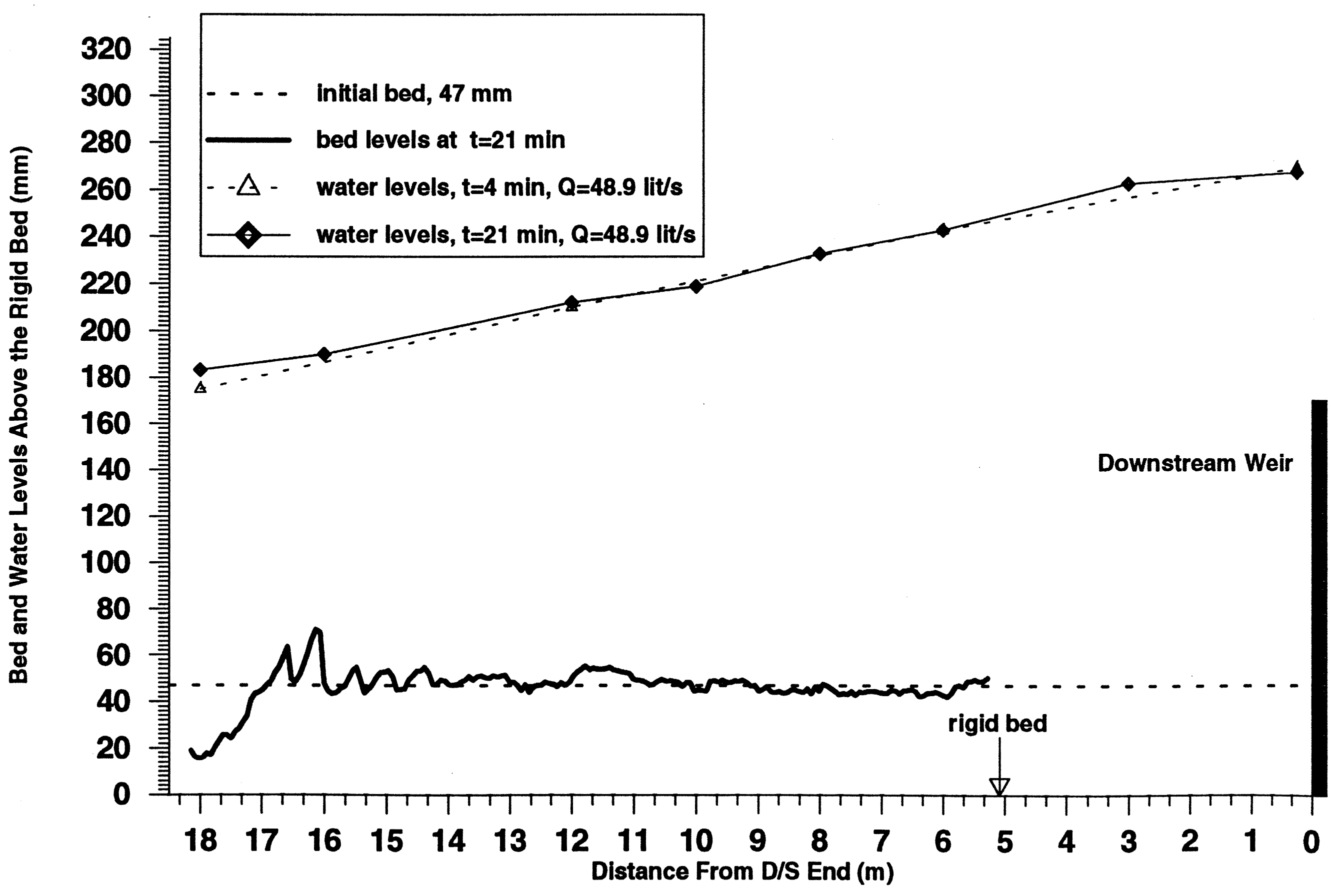

Figure 7(b) Bed and Water Levels in Test 1 (1st stage)

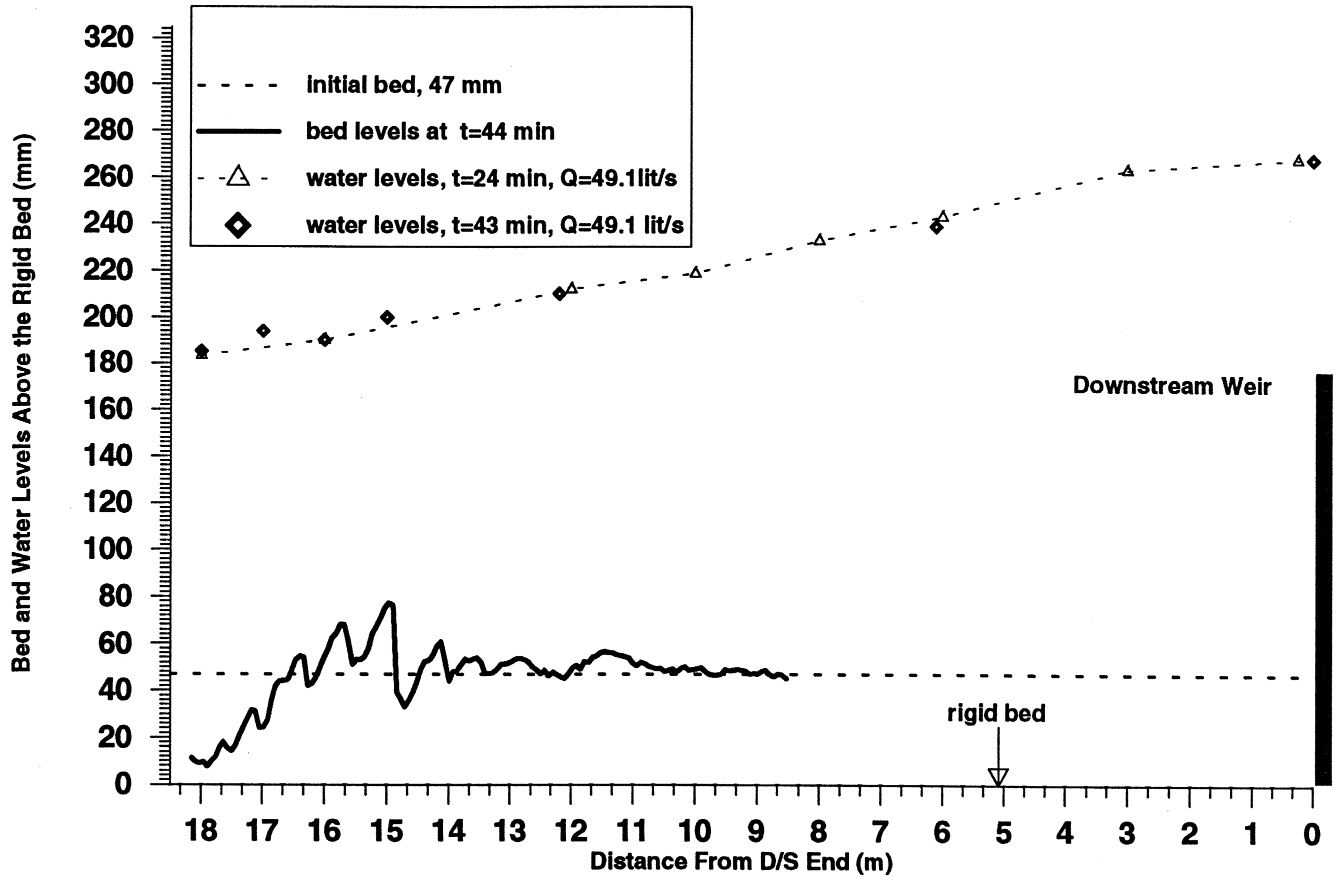

Figure 8(a) Bed and Water Levels in Test 1 (2nd stage)

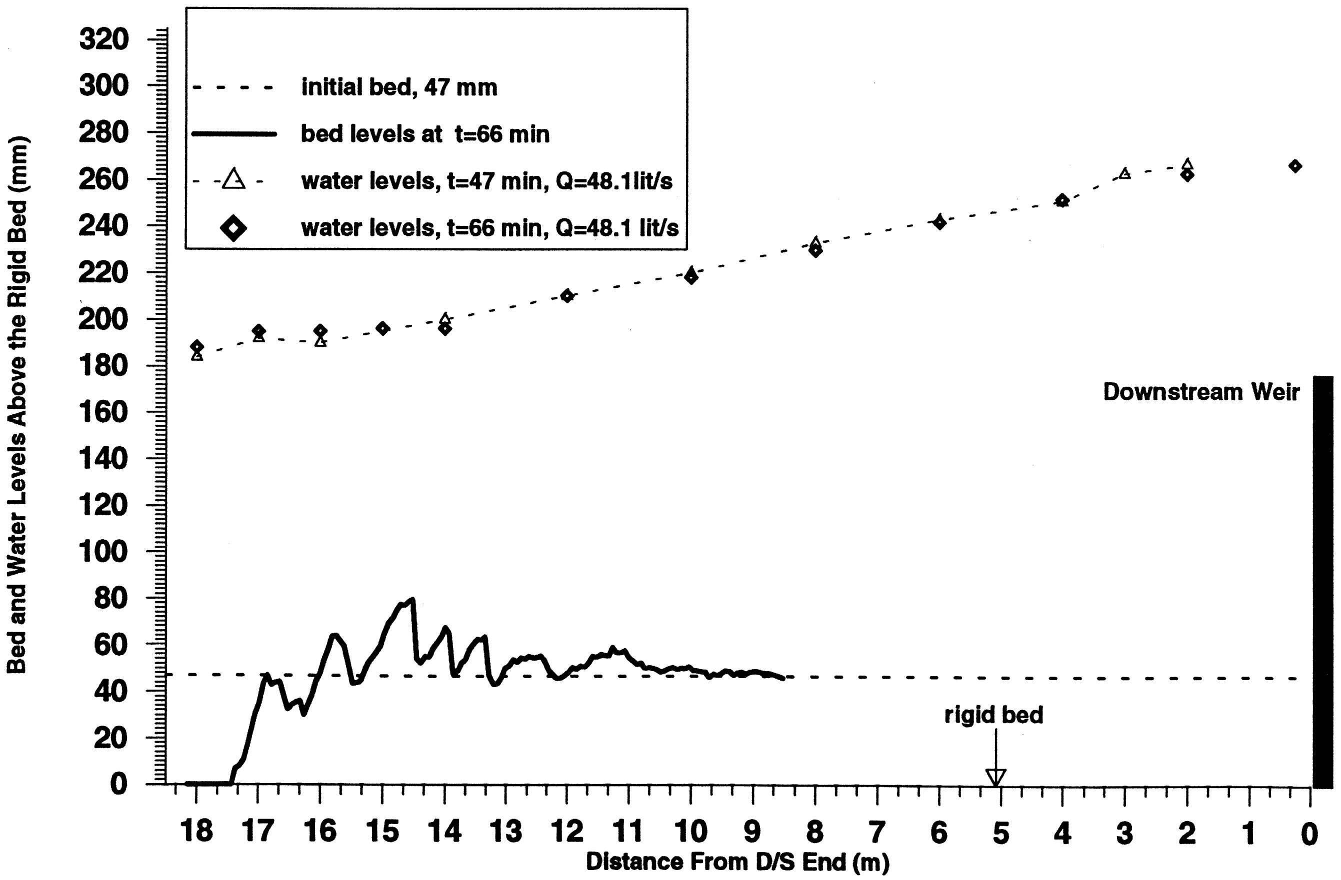

Figure 8(b) Bed and Water Levels in Test 1 (3rd stage)

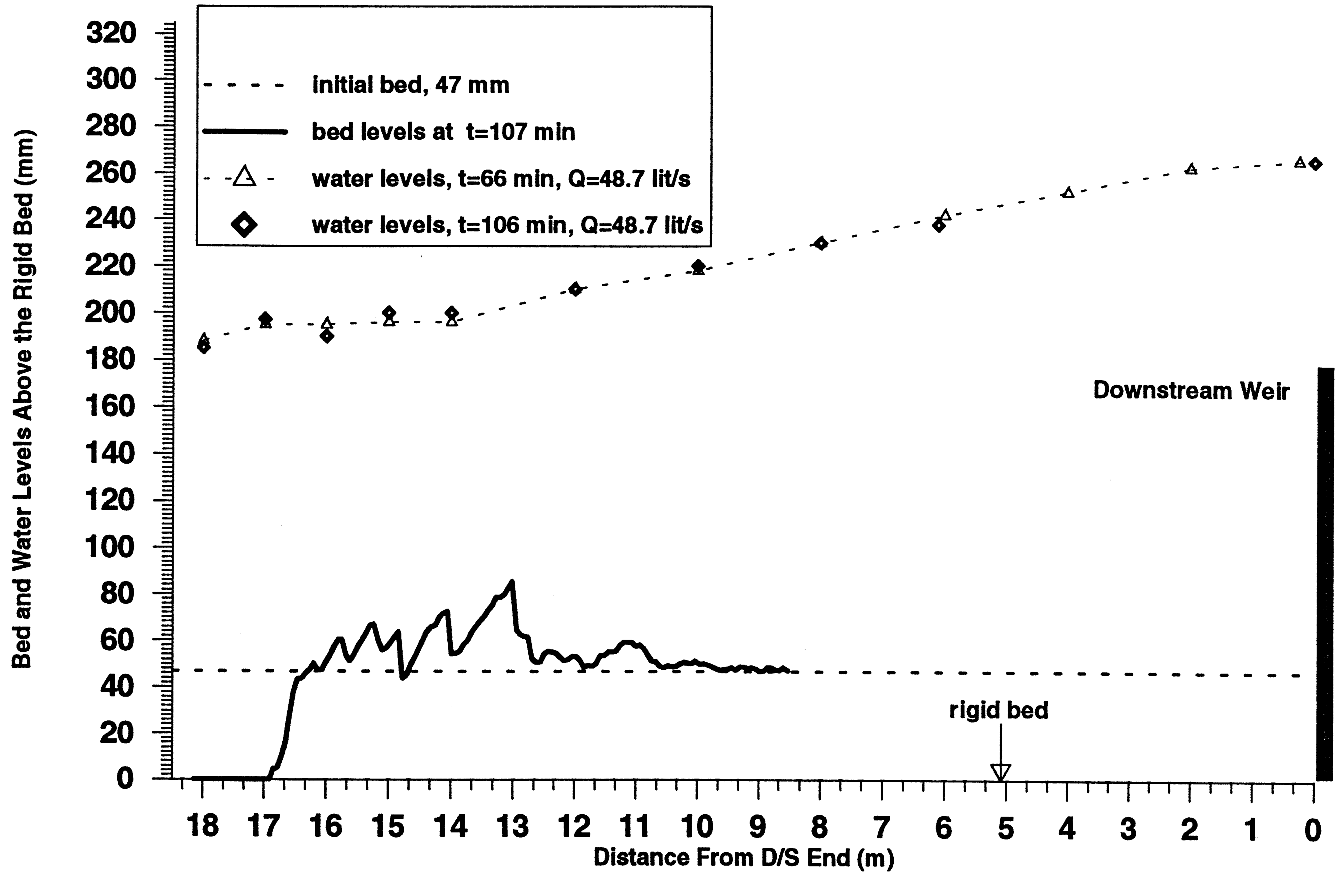

Figure 9(a) Bed and Water Levels in Test 1 (4th stage)

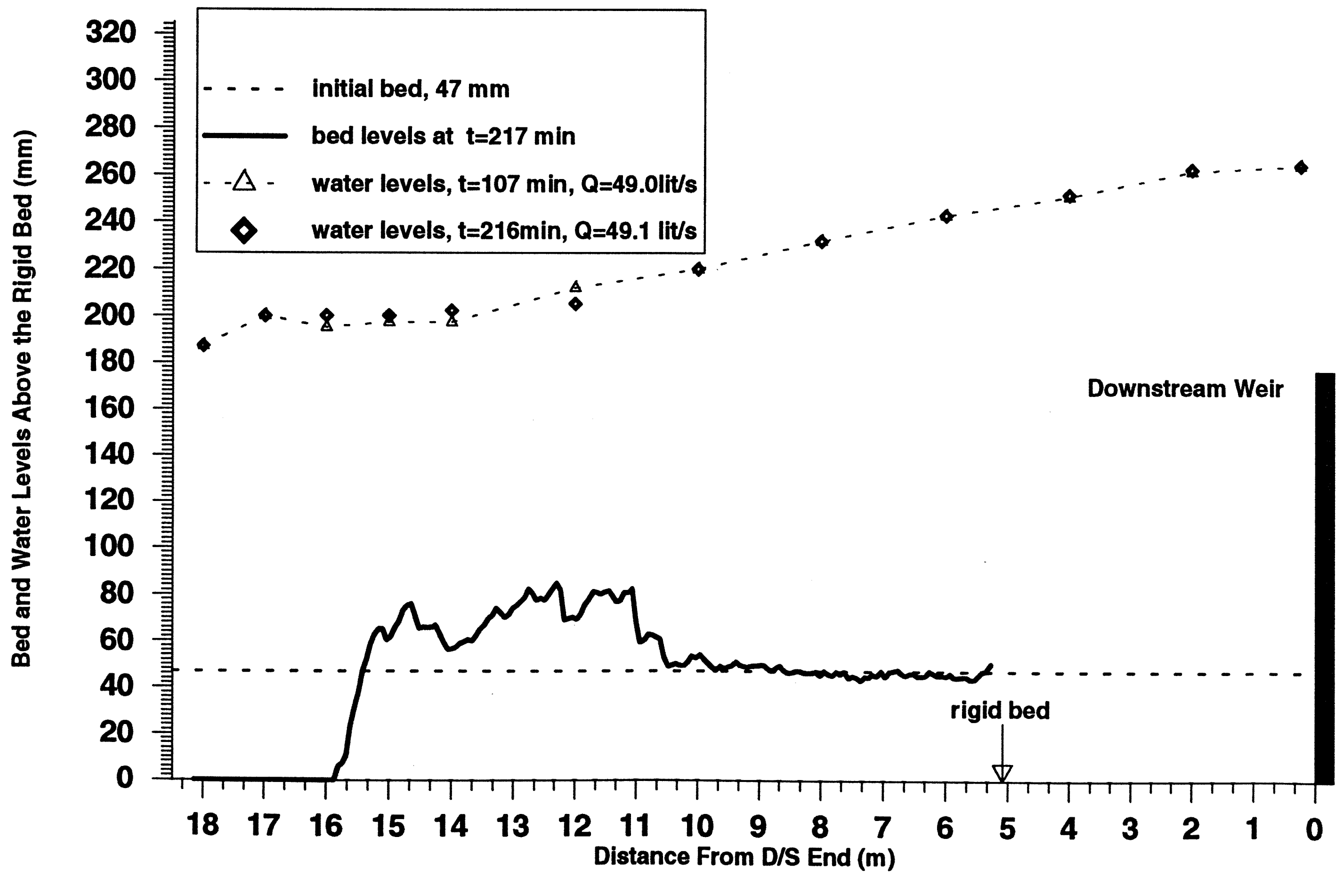

Figure 9(b) Bed and Water Levels in Test 1 (5th stage)

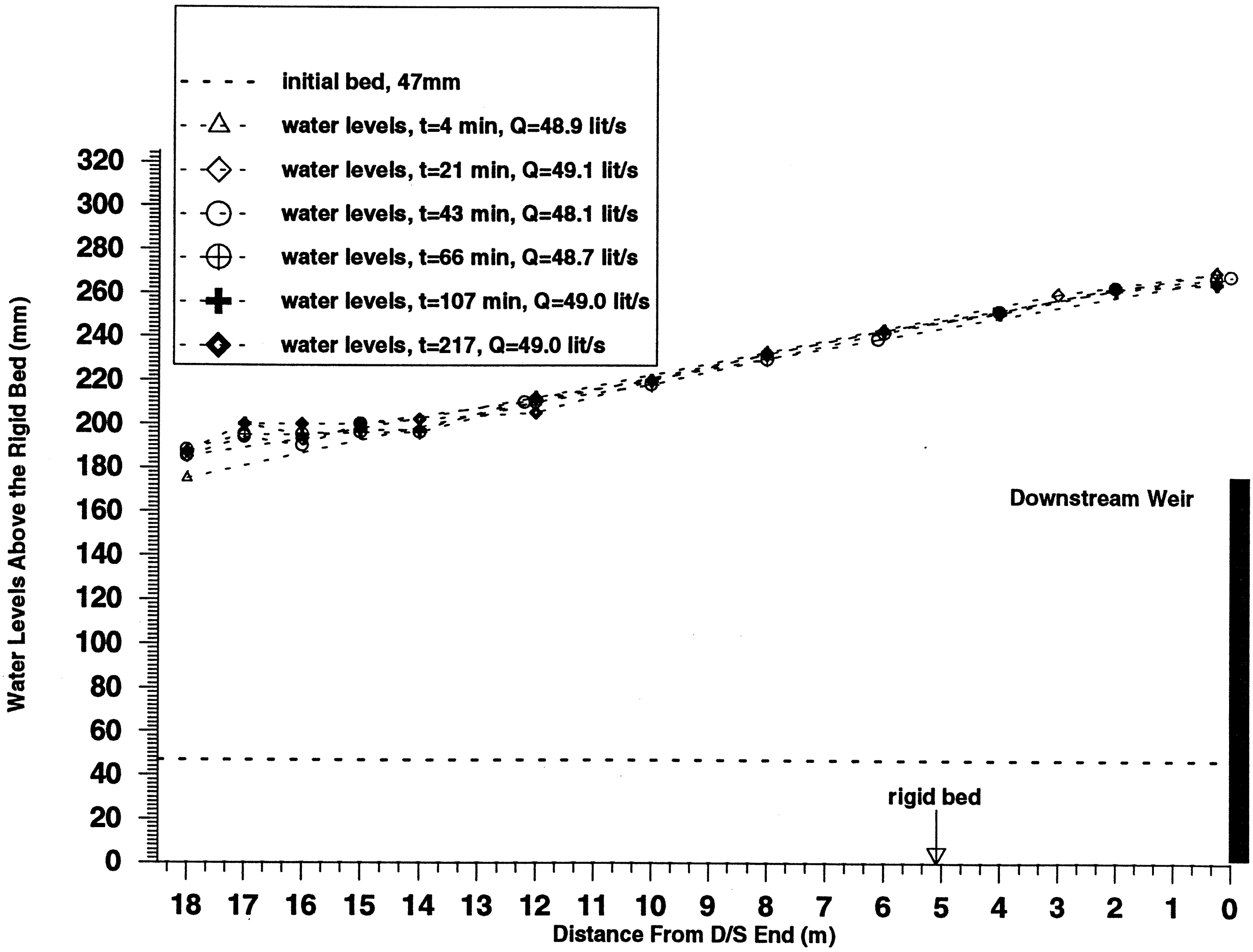

Figure 10 Water Levels in Test 1

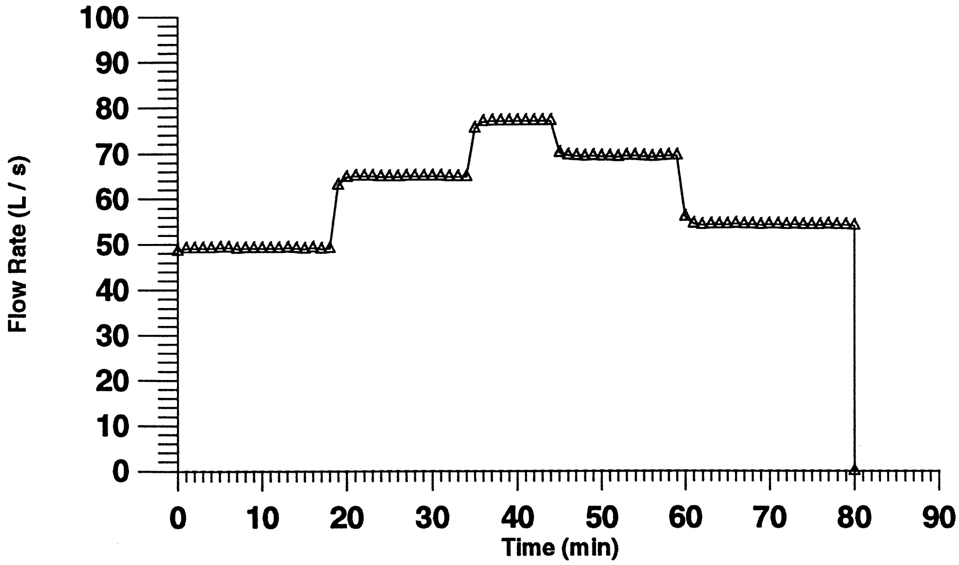

Figure 11(a) Flow Hydrograph in Test 2

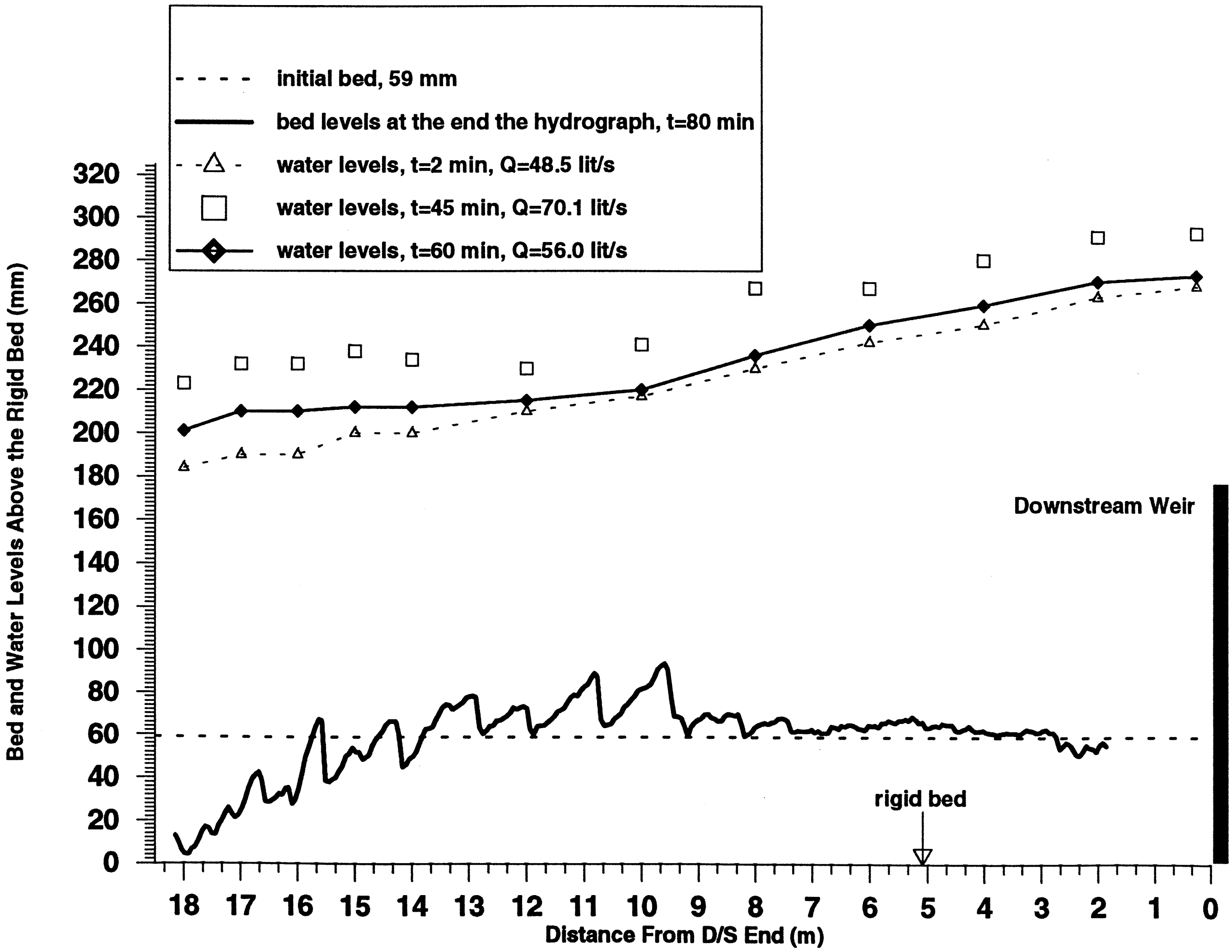

Figure 11(b) Bed and Water Levels in Test 2

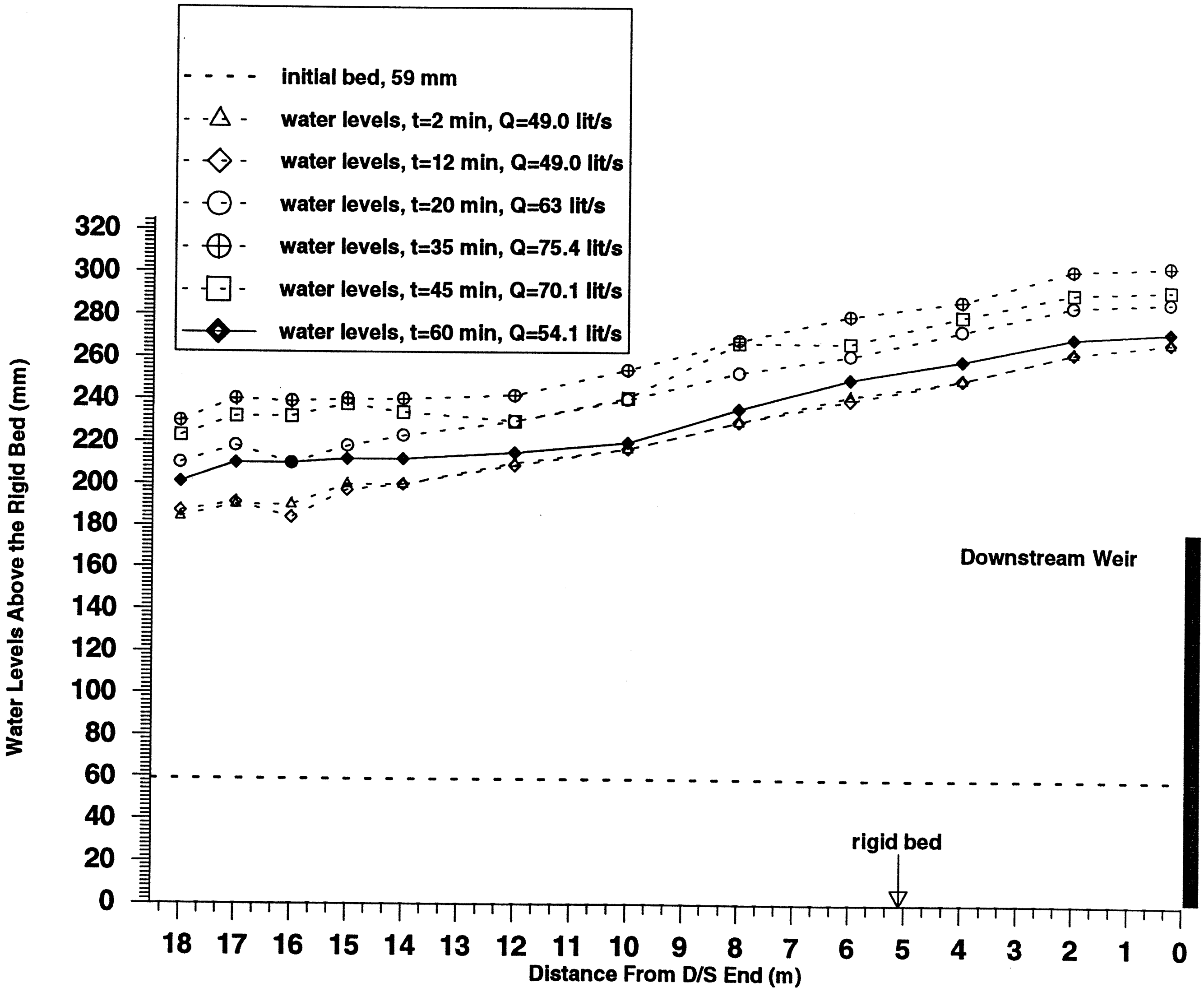

Figure 12 Water Levels in Test 2

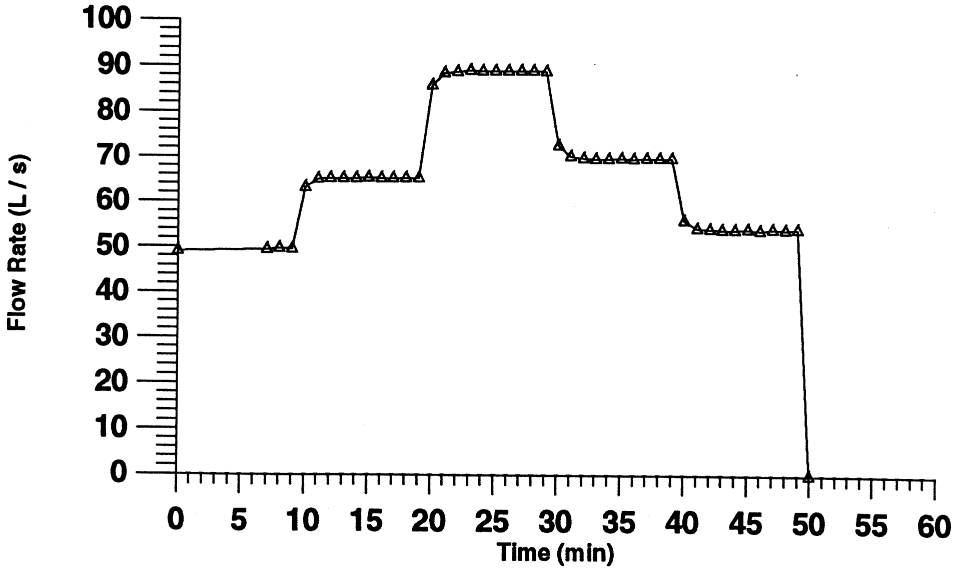

Figure 13(a) Flow Hydrograph in Test 3

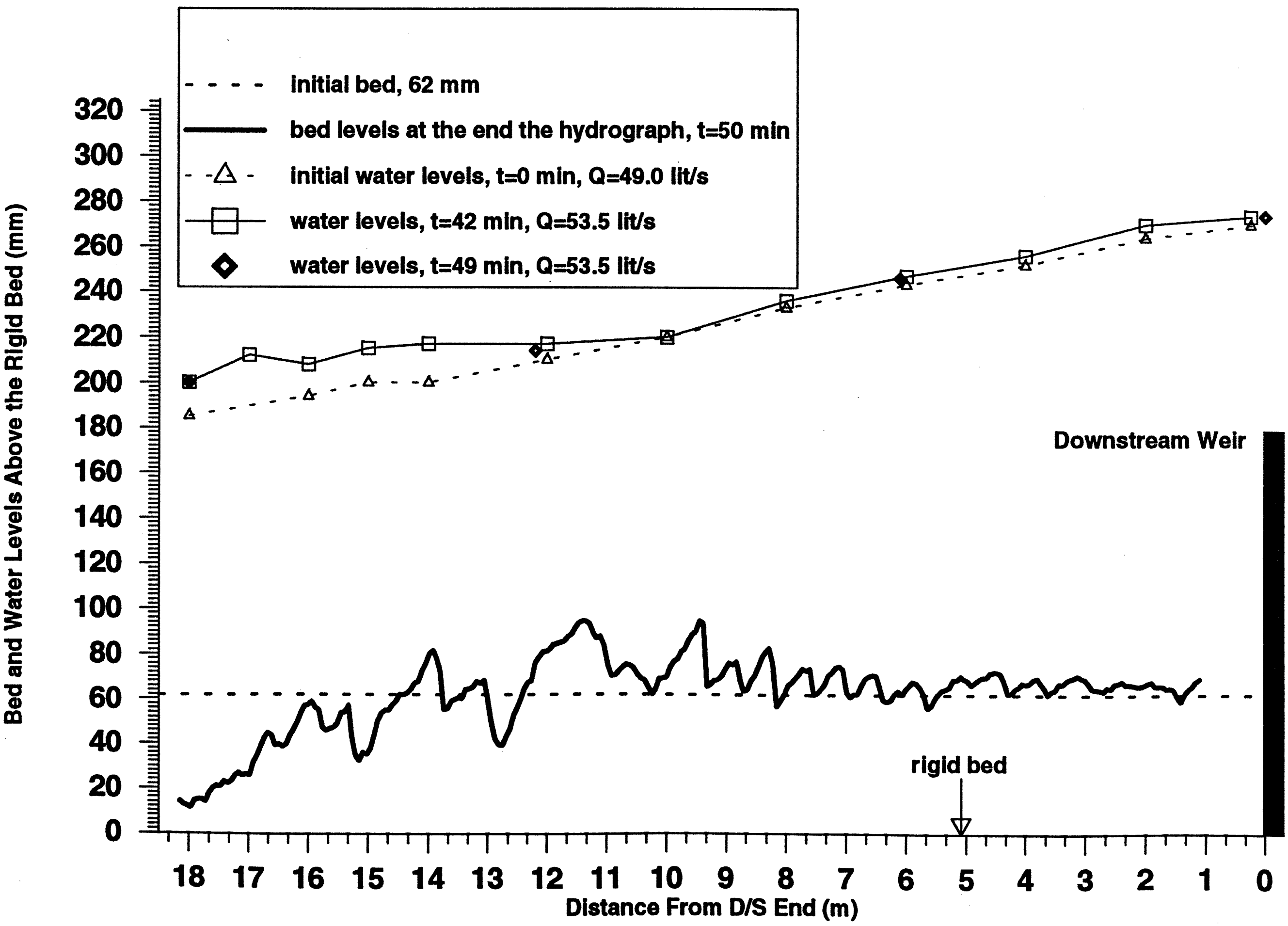

Figure 13(b) Bed and Water Levels in Test 3

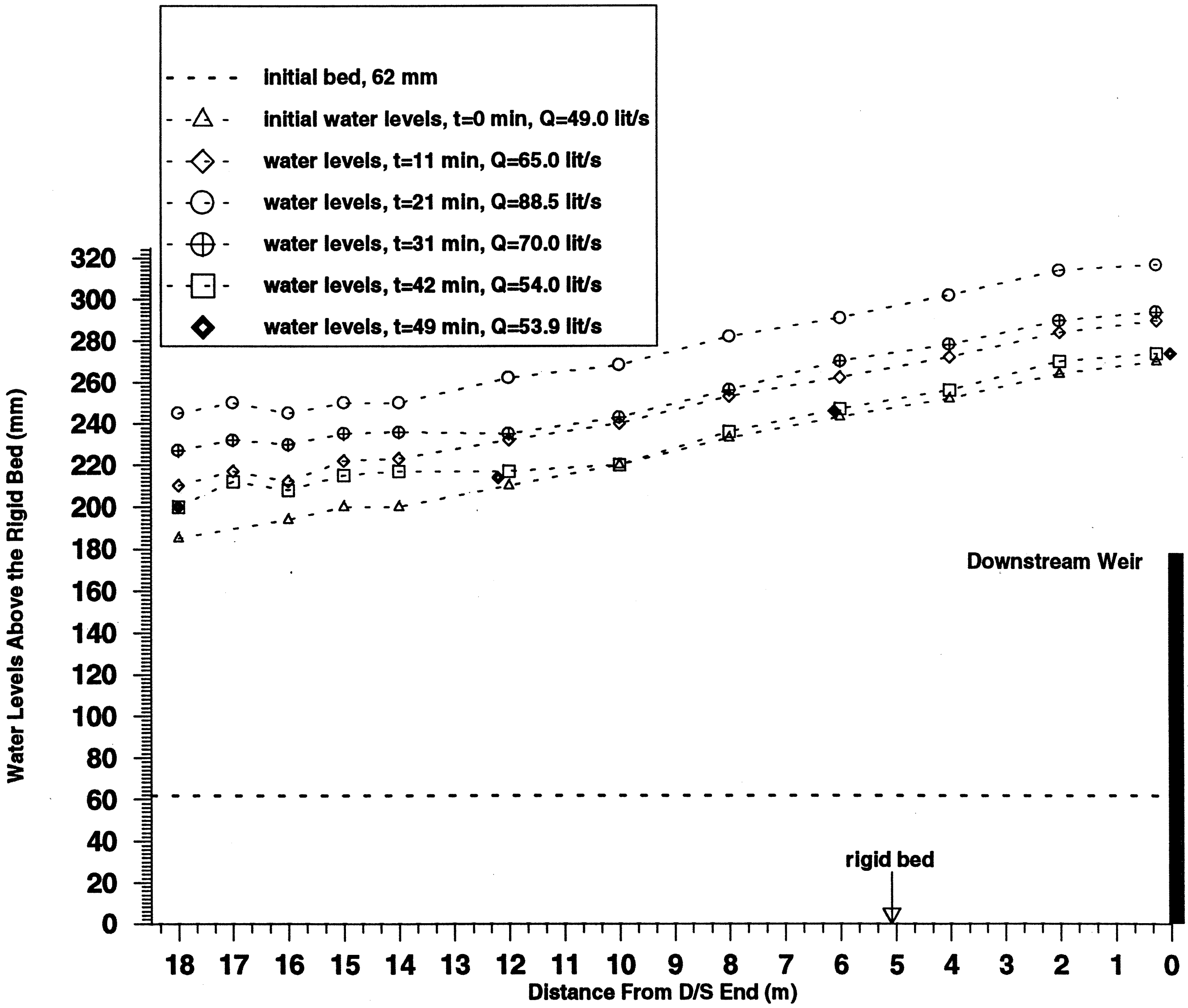

Figure 14 Water Levels in Test 3

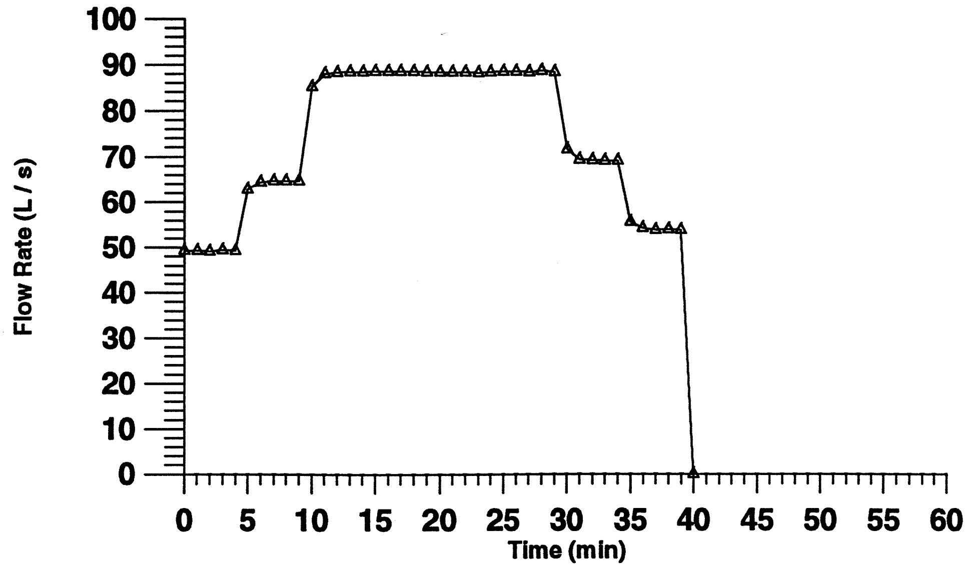

Figure 15(a) Flow Hydrograph in Test 4

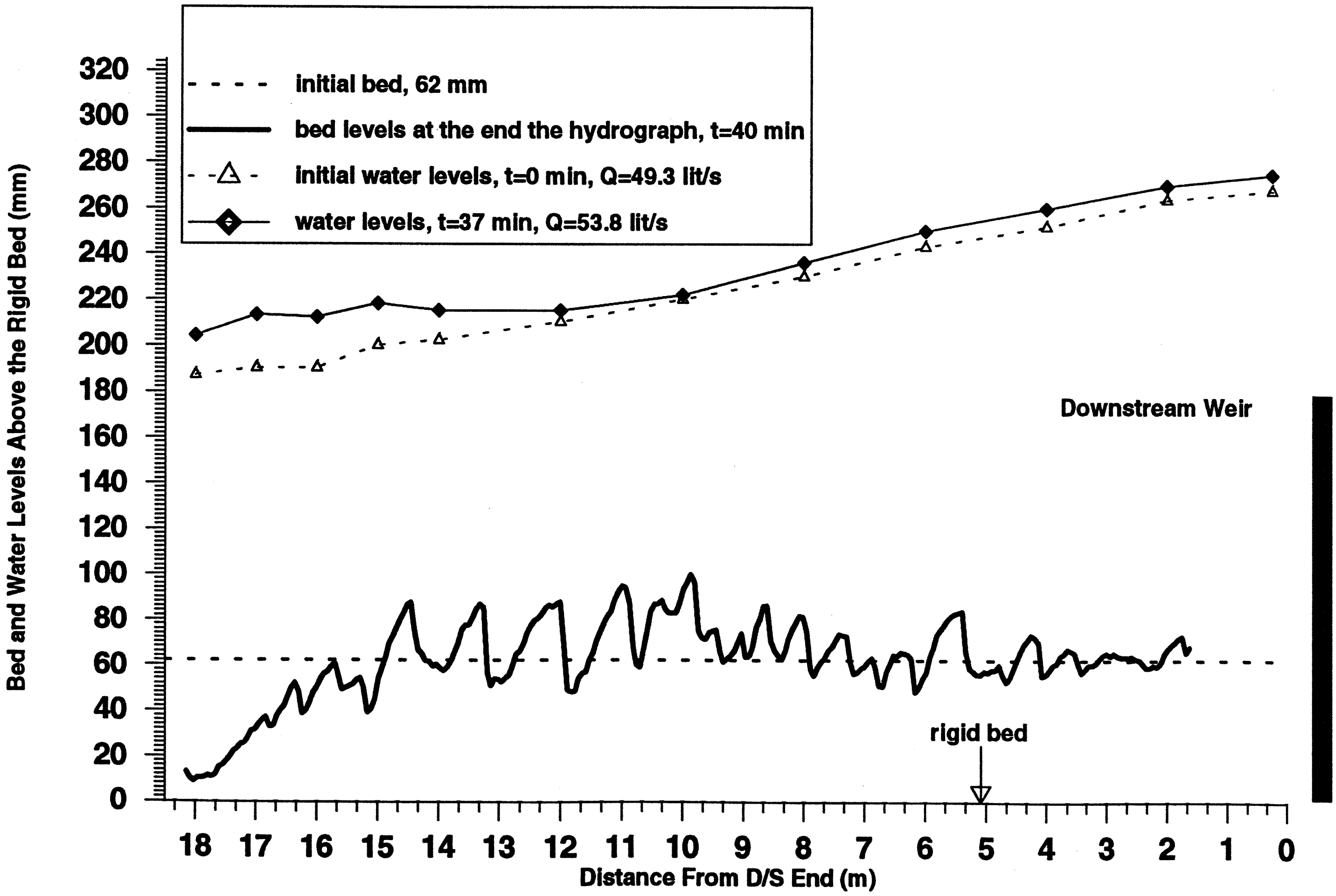

Figure 15(b) Bed and Water Levels in Test 4

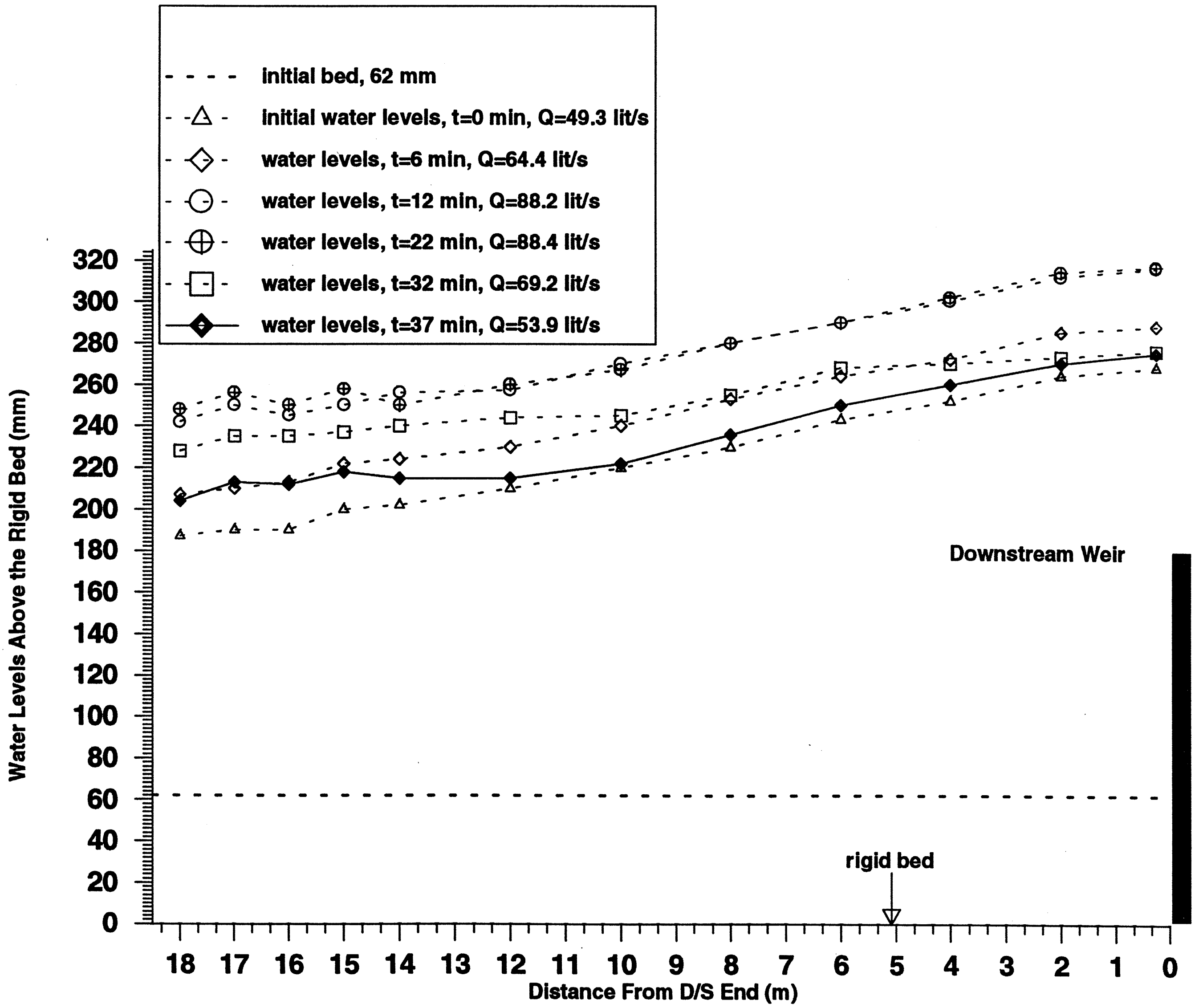

Figure 16 Water Levels in Test 4

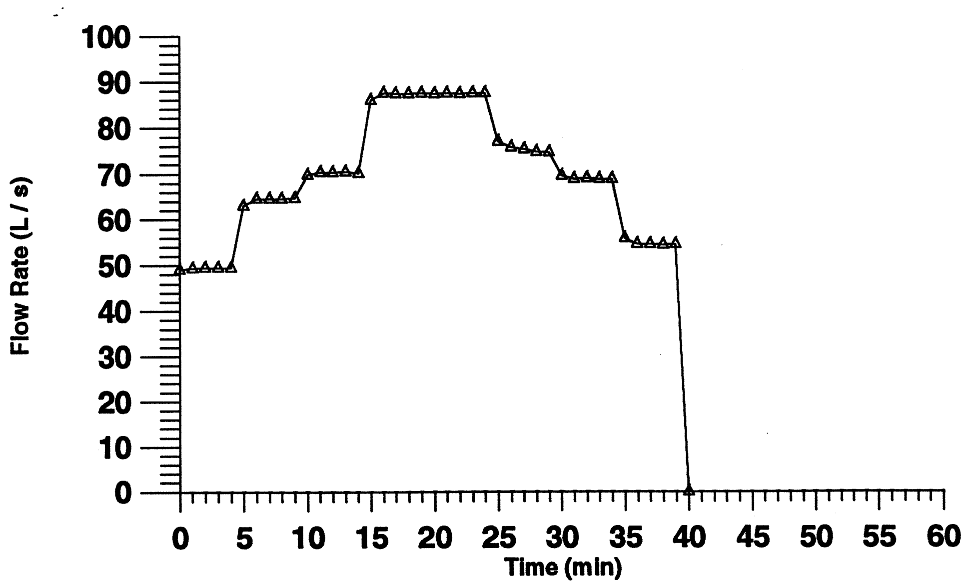

Figure 17(a) Flow Hydrograph in Test 5

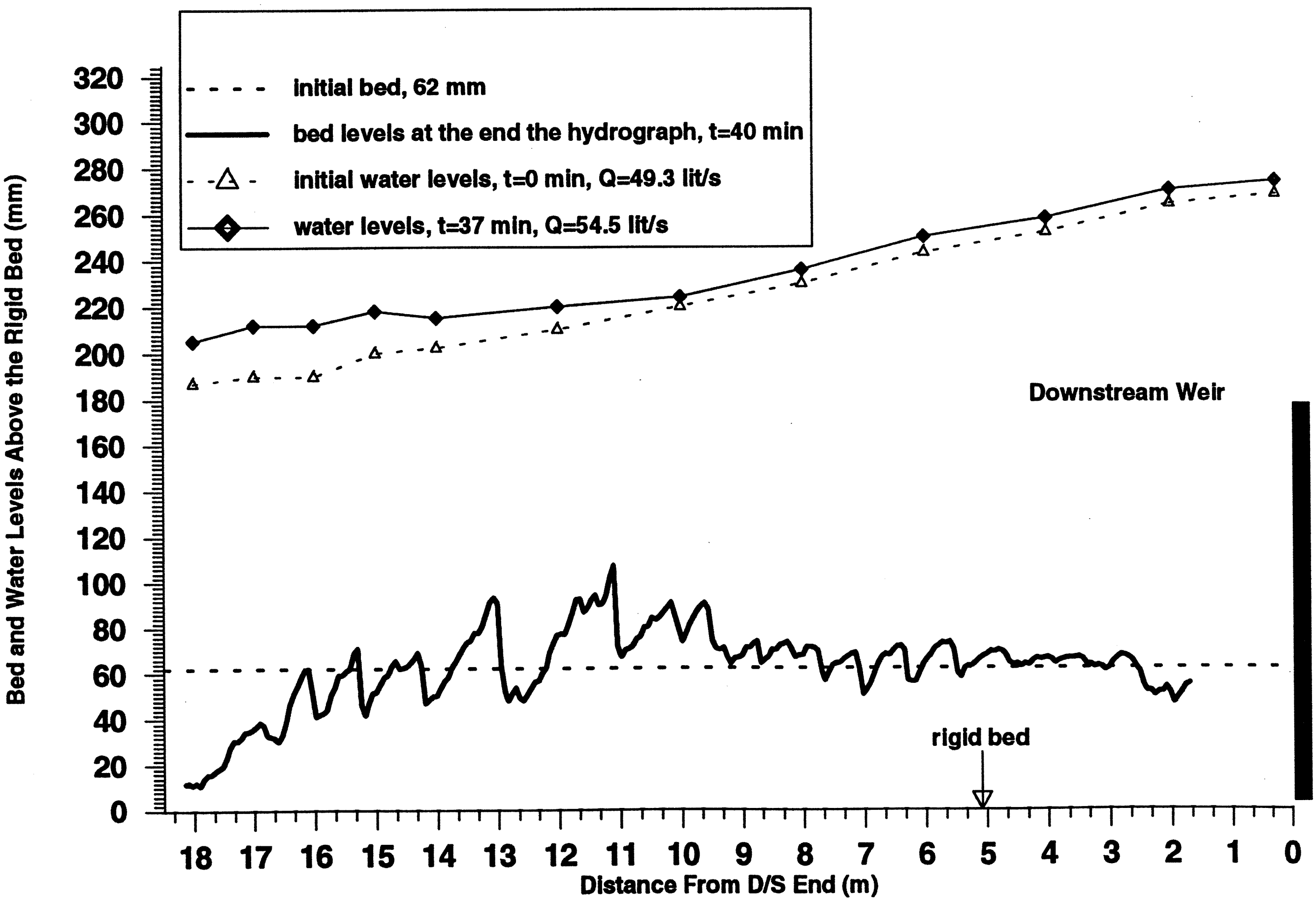

Figure 17(b) Bed and Water Levels in Test 5

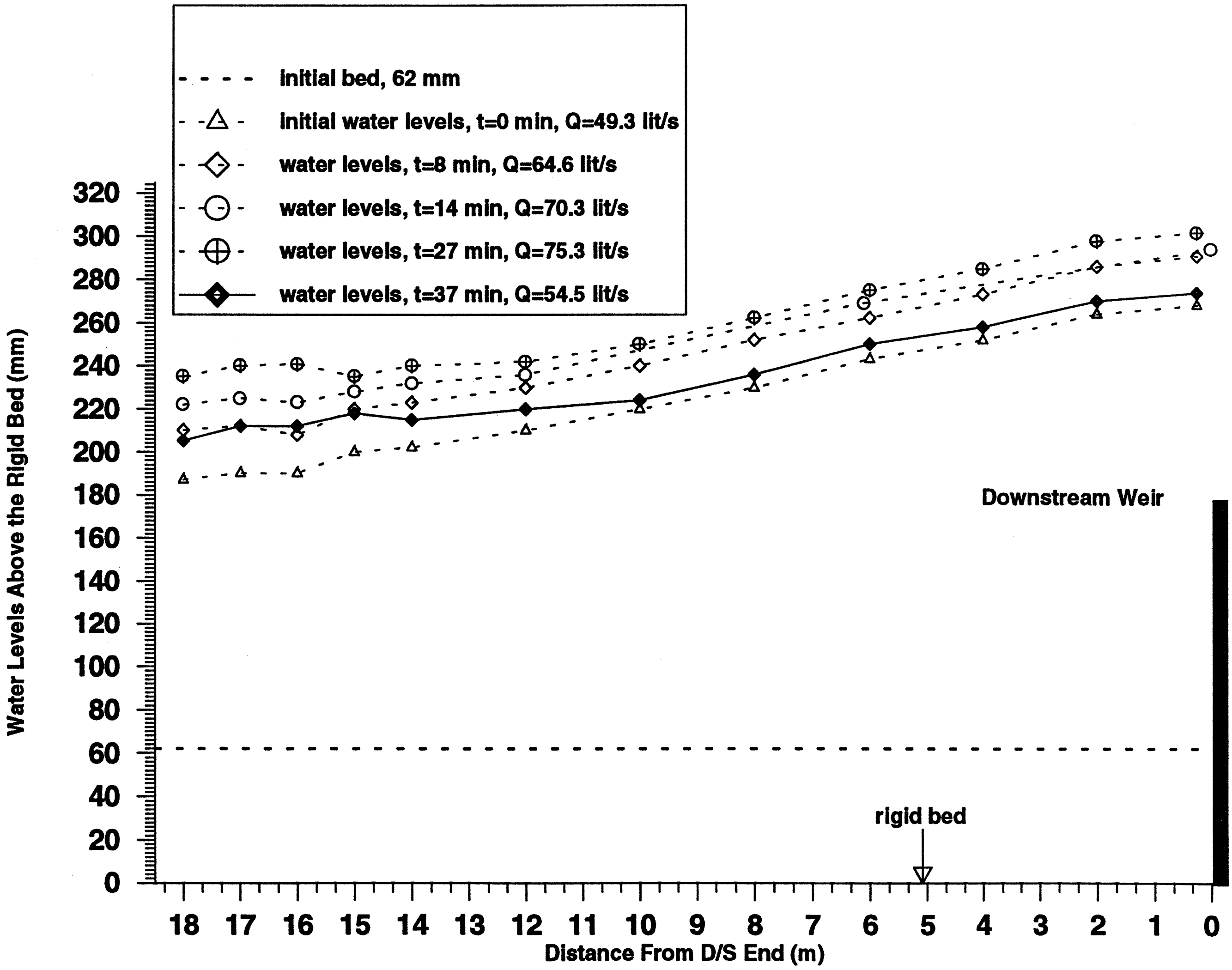

Figure 18 Water Levels in Test 5

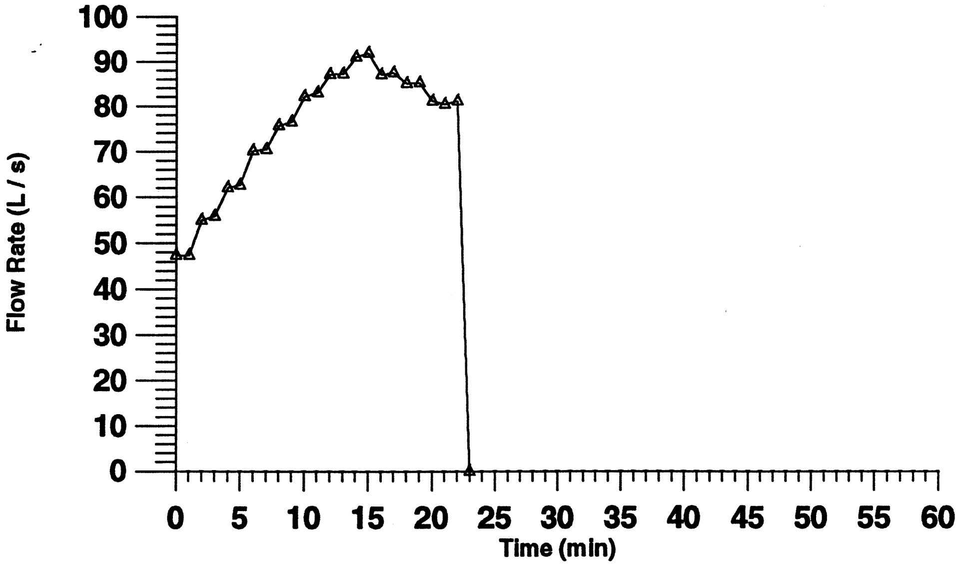

Figure 19(a) Flow Hydrograph in Test 6

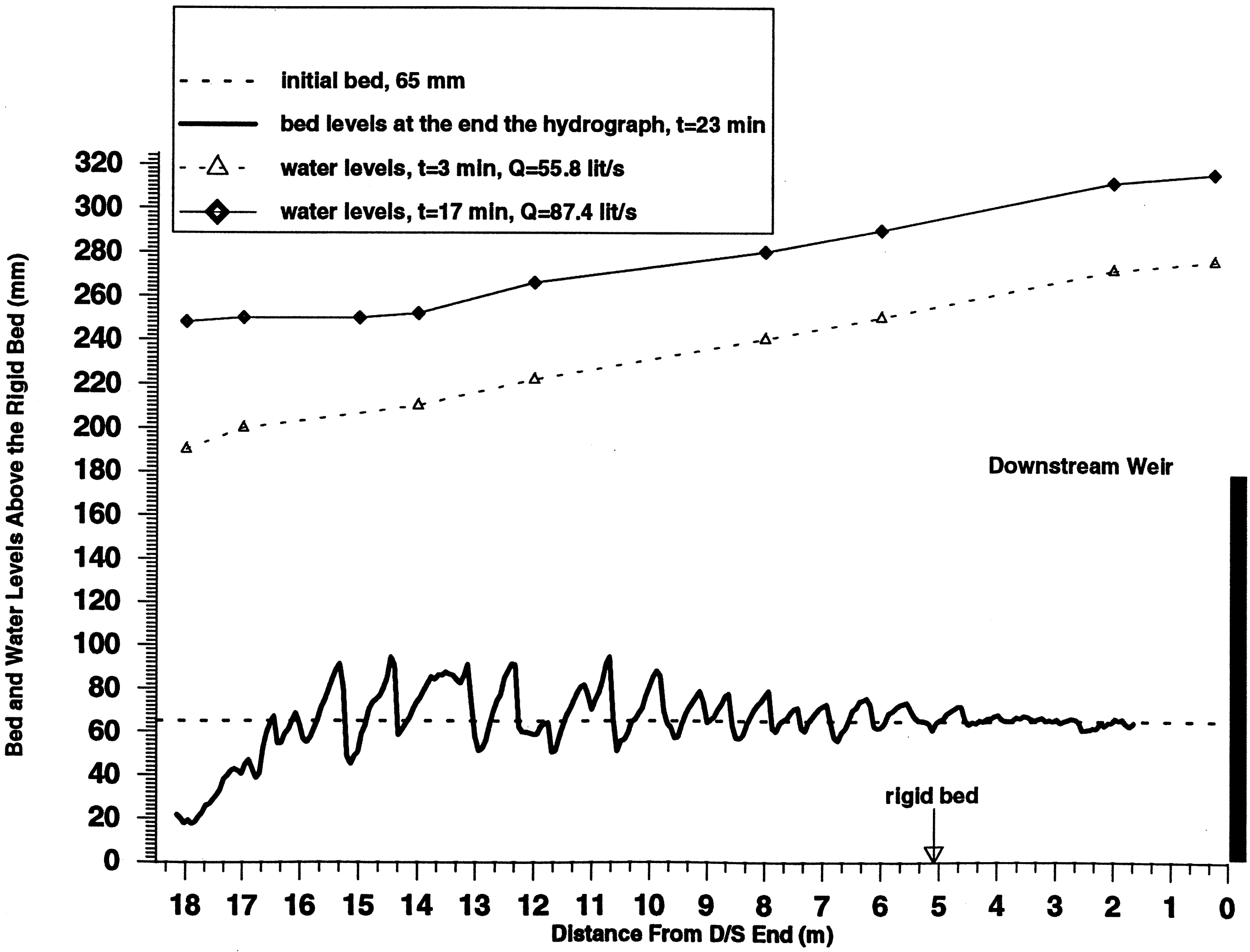

Figure 19(b) Bed and Water Levels in Test 6

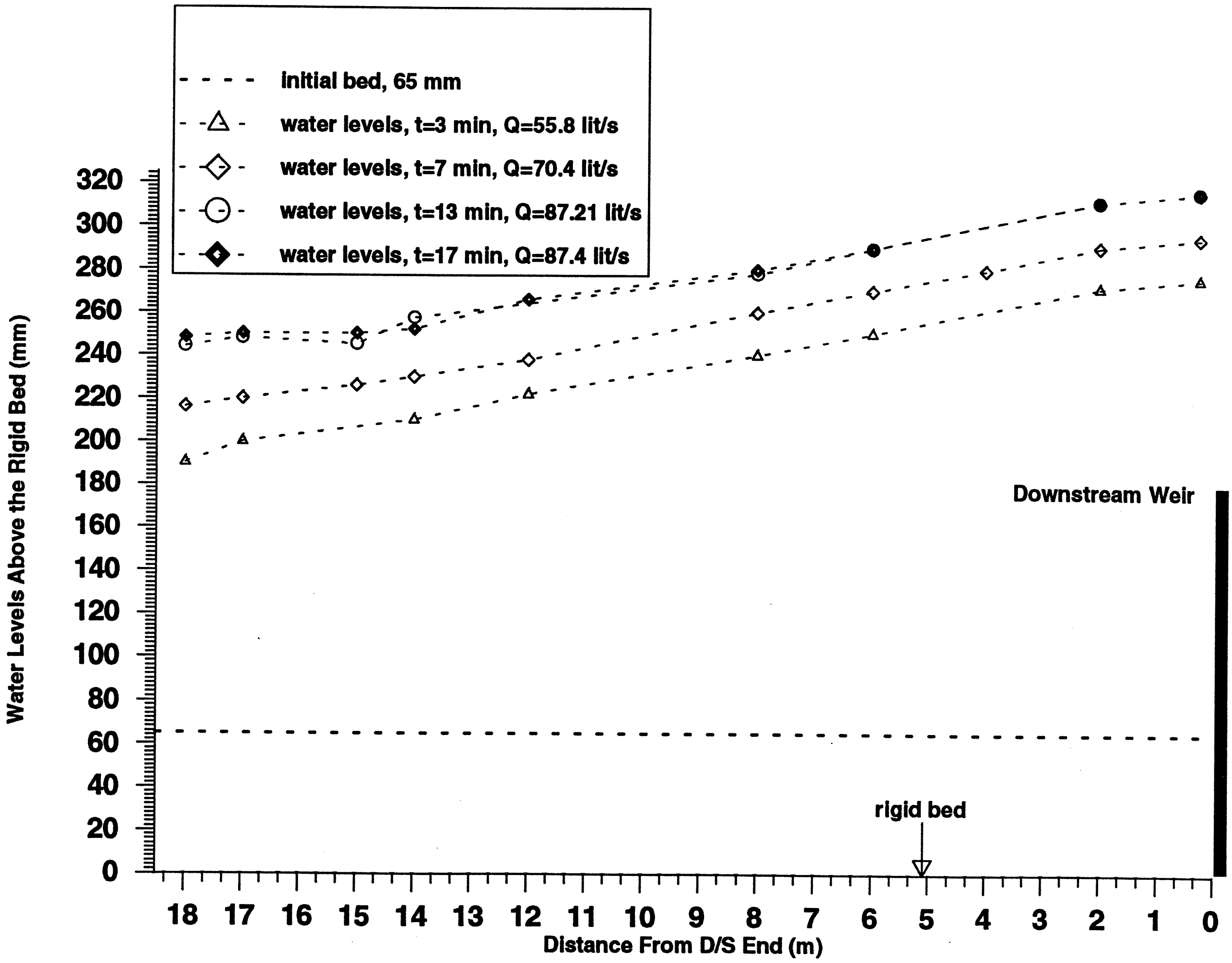

Figure 20 Water Levels in Test 6

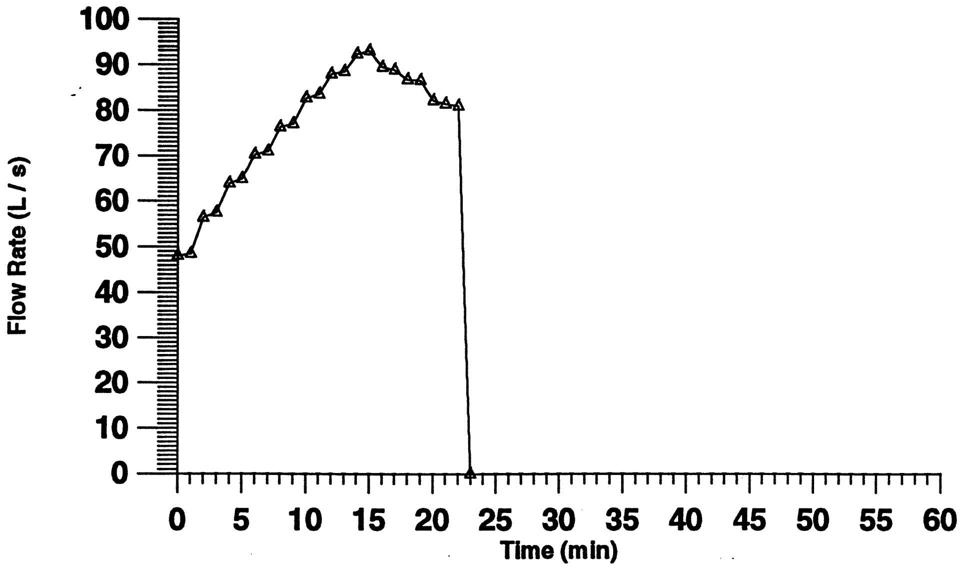

Figure 21(a) Flow Hydrograph in Test 7

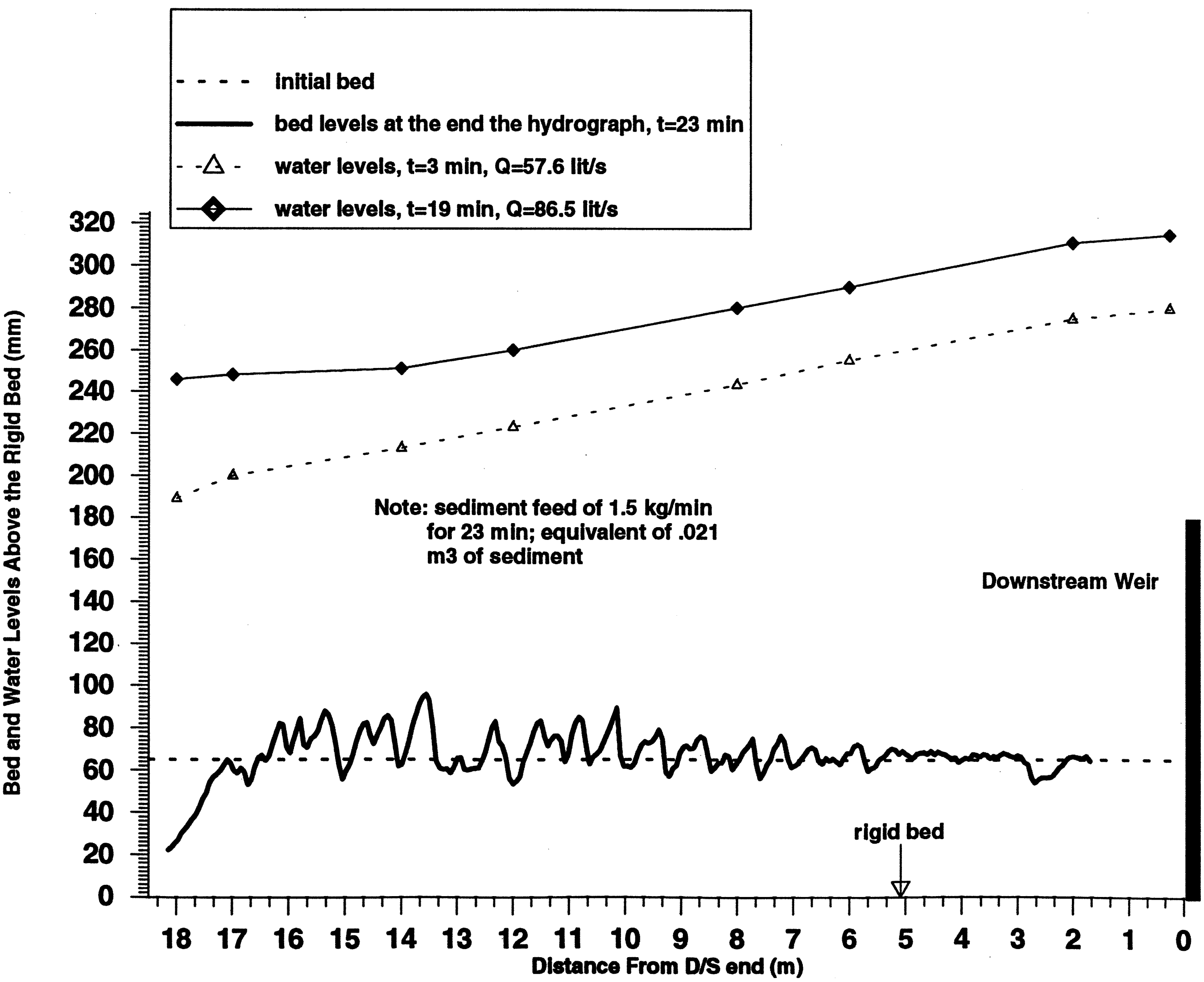

Figure 21(b) Bed and Water Levels in Test 7

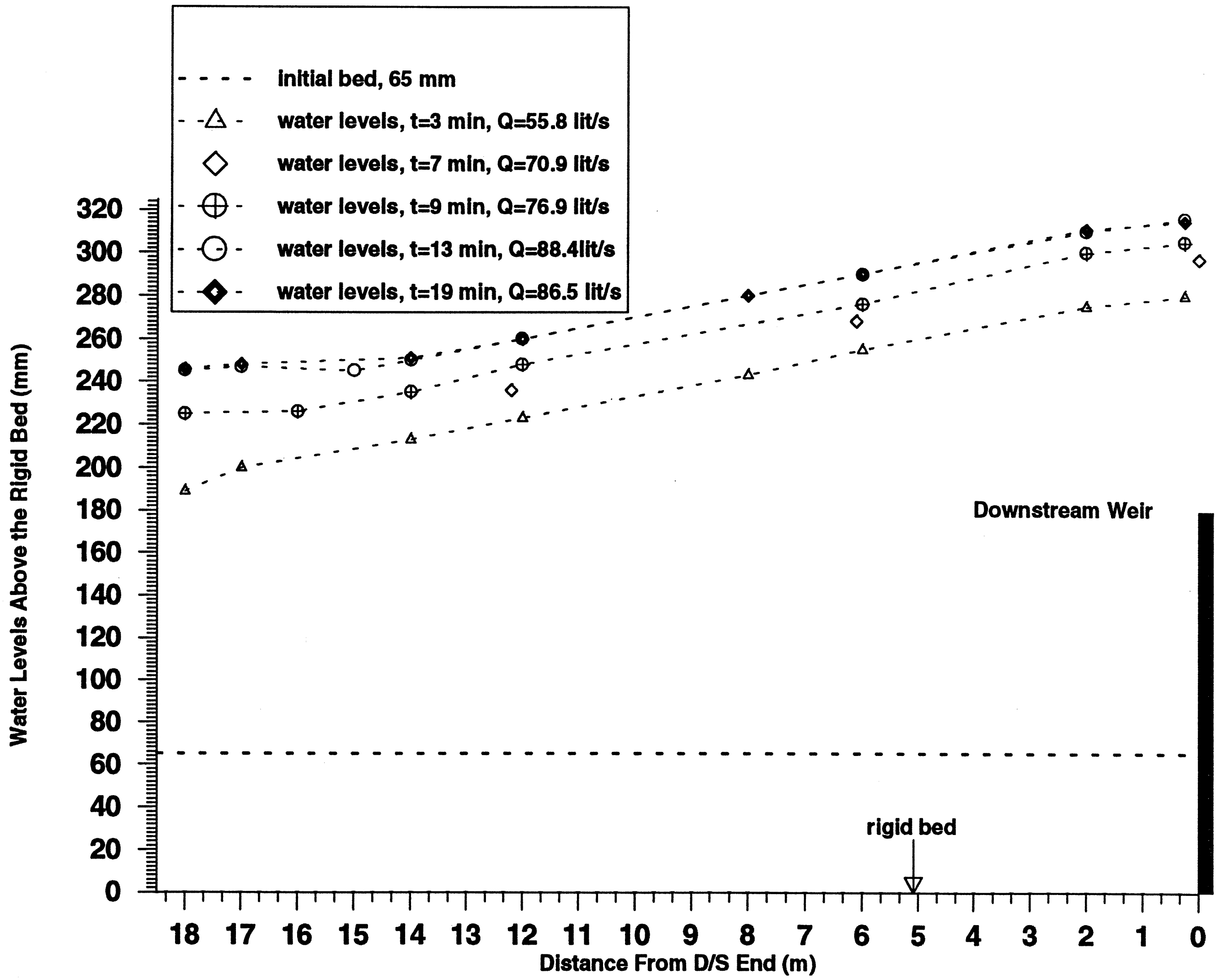

Figure 22 Water Levels in Test 7

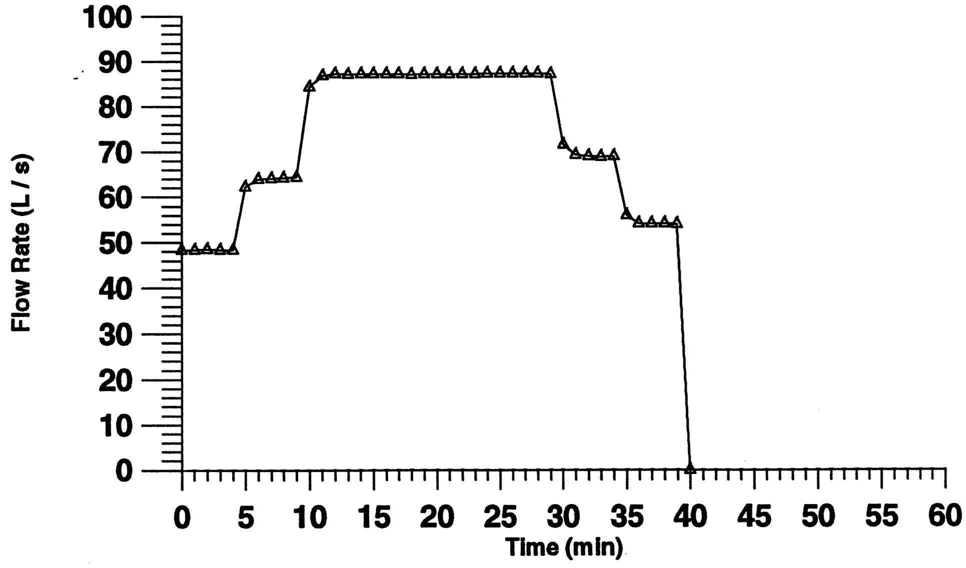

Figure 23(a) Flow Hydrograph in Test 8

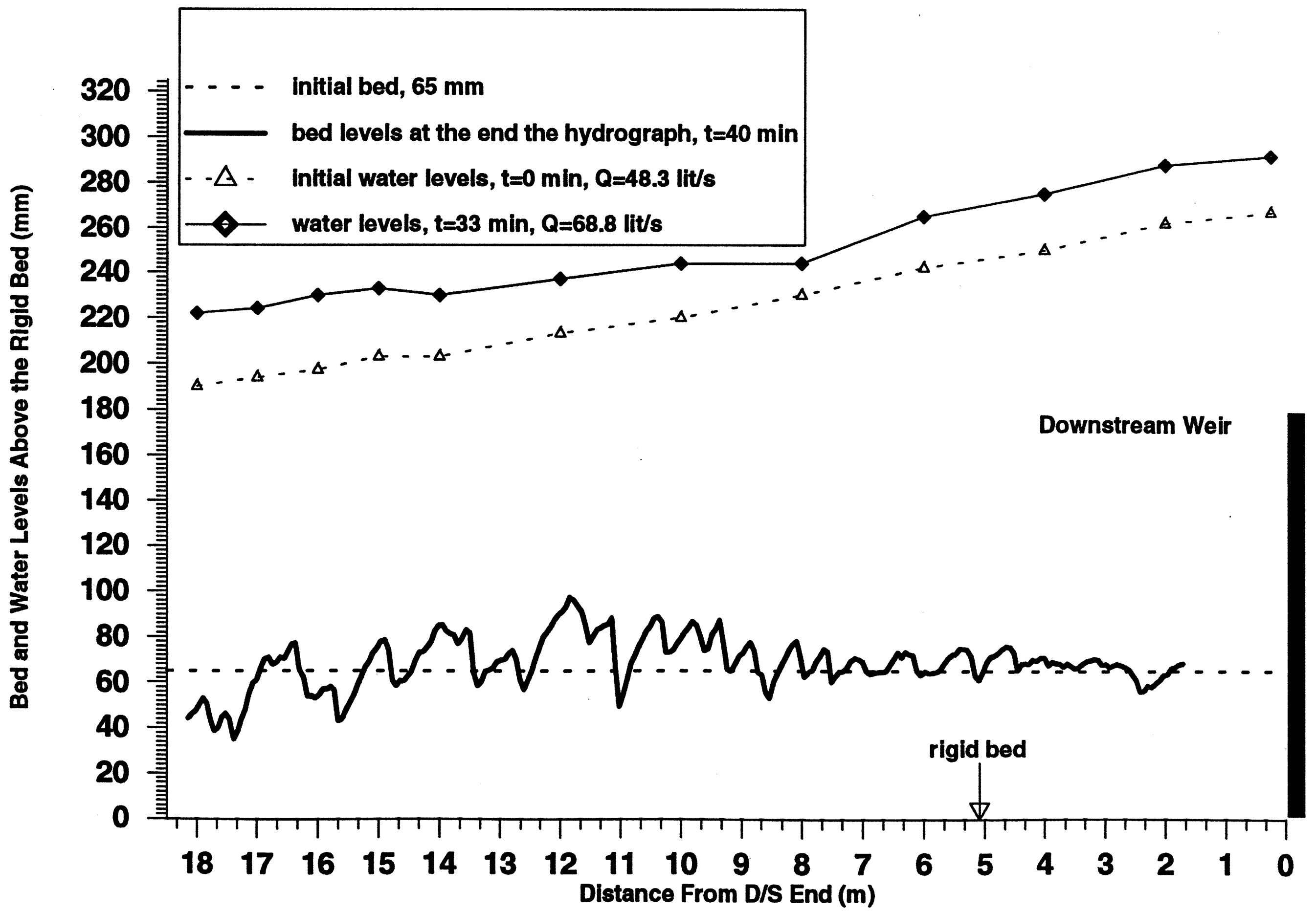

Figure 23(b) Bed and Water Levels in Test 8

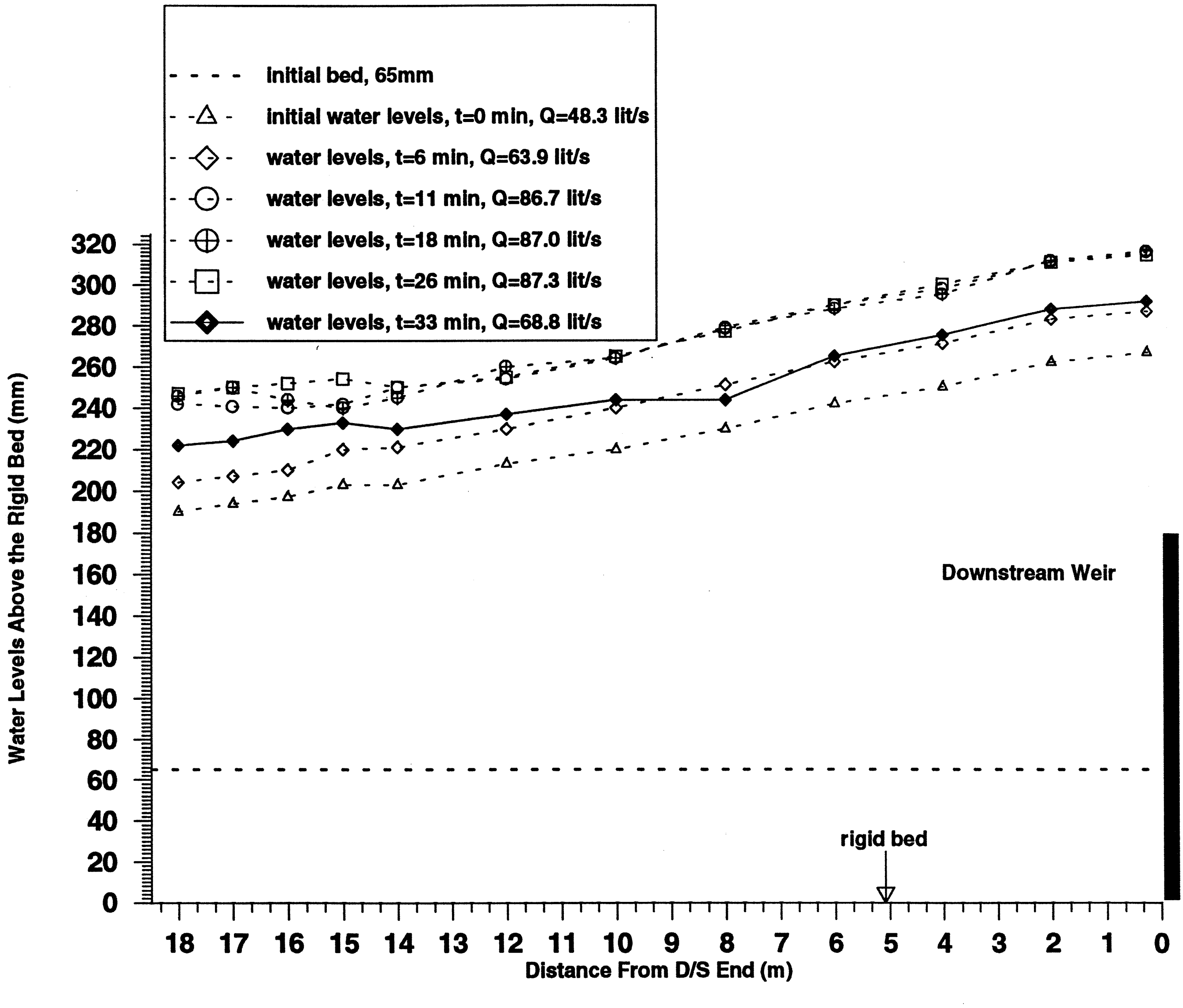

Figure 24 Water Levels in Test 8

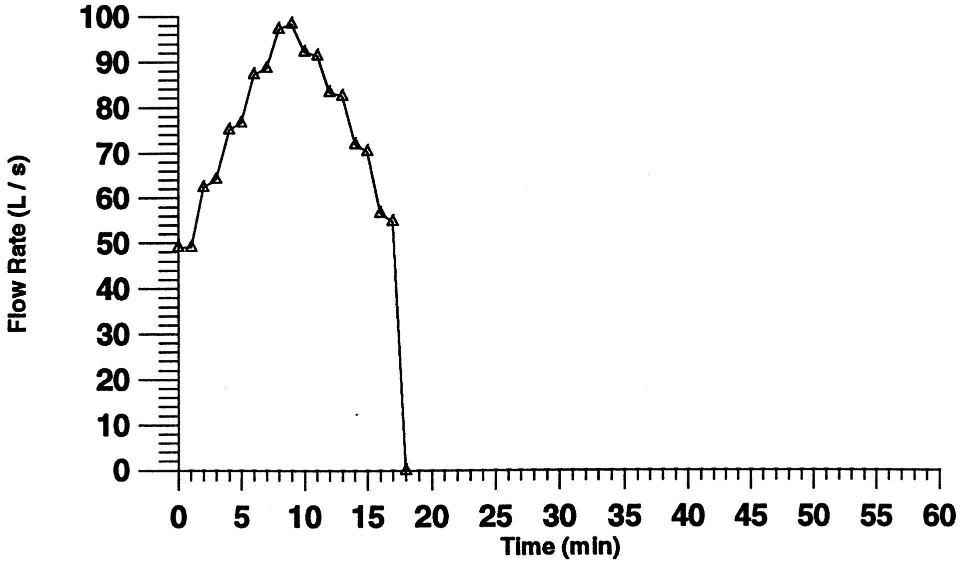

Figure 25(a) Flow Hydrograph in Test 9

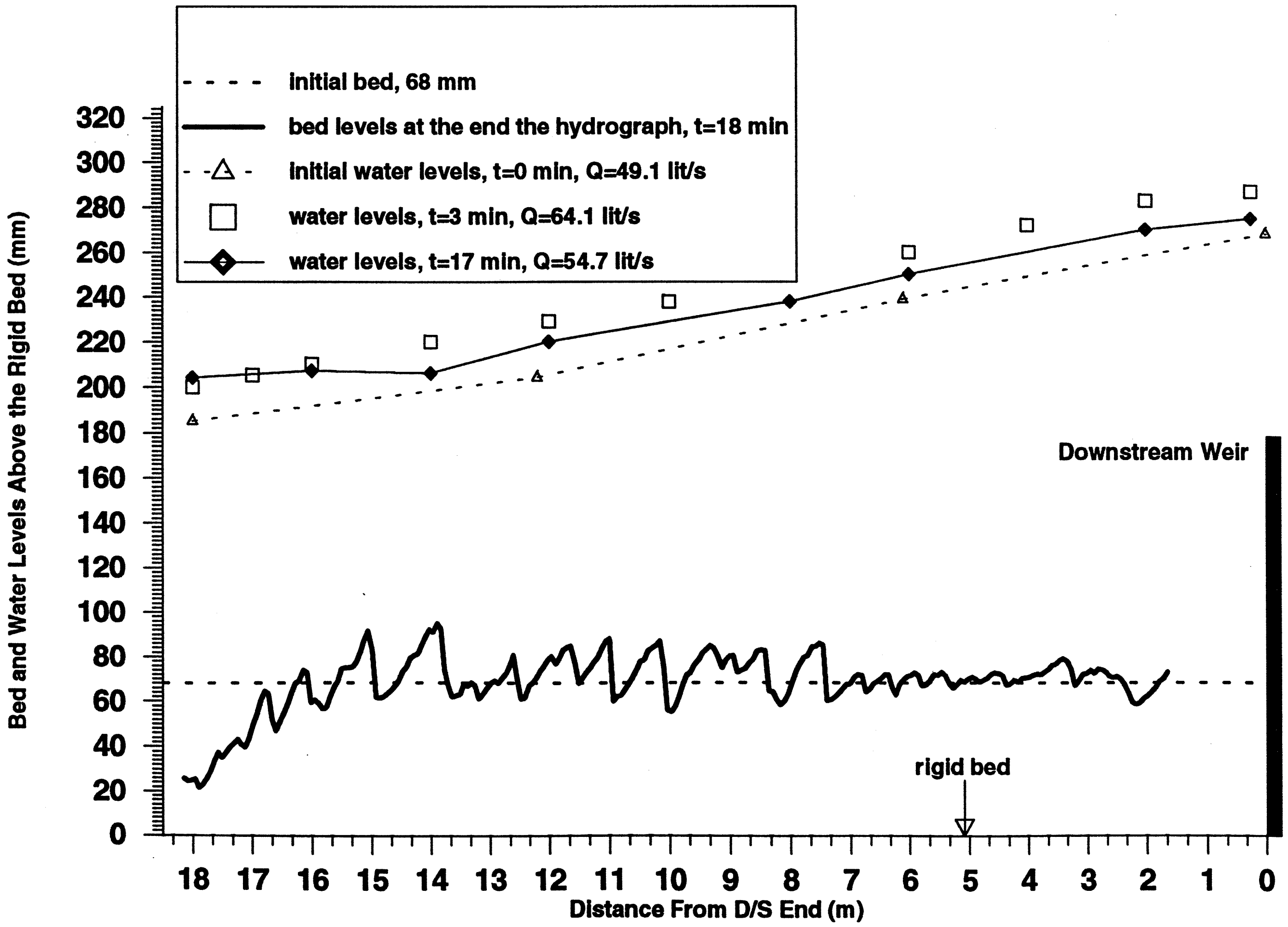

Figure 25(b) Bed and Water Levels in Test 9

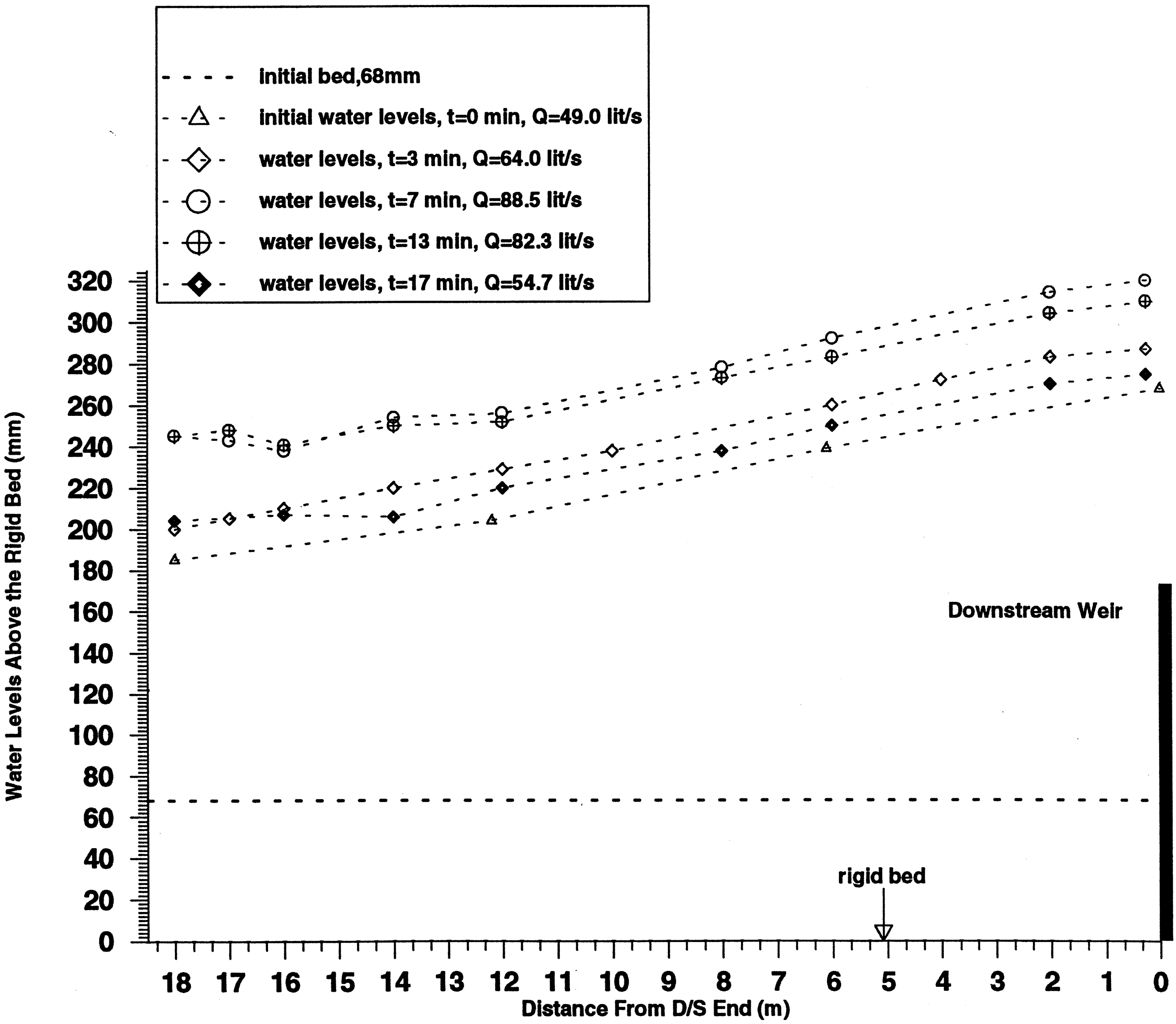

Figure 26 Water Levels in Test 9

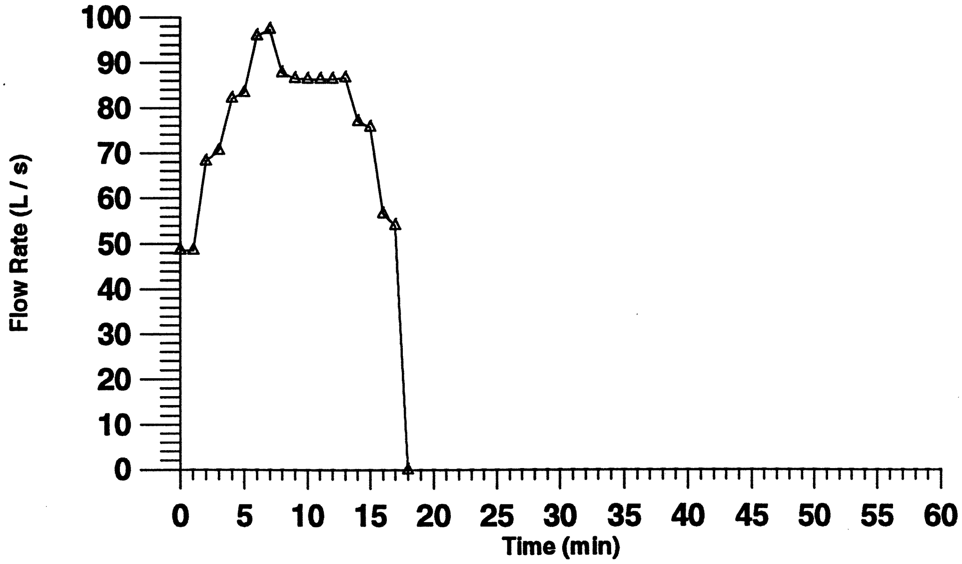

Figure 27(a) Flow Hydrograph in Test 10

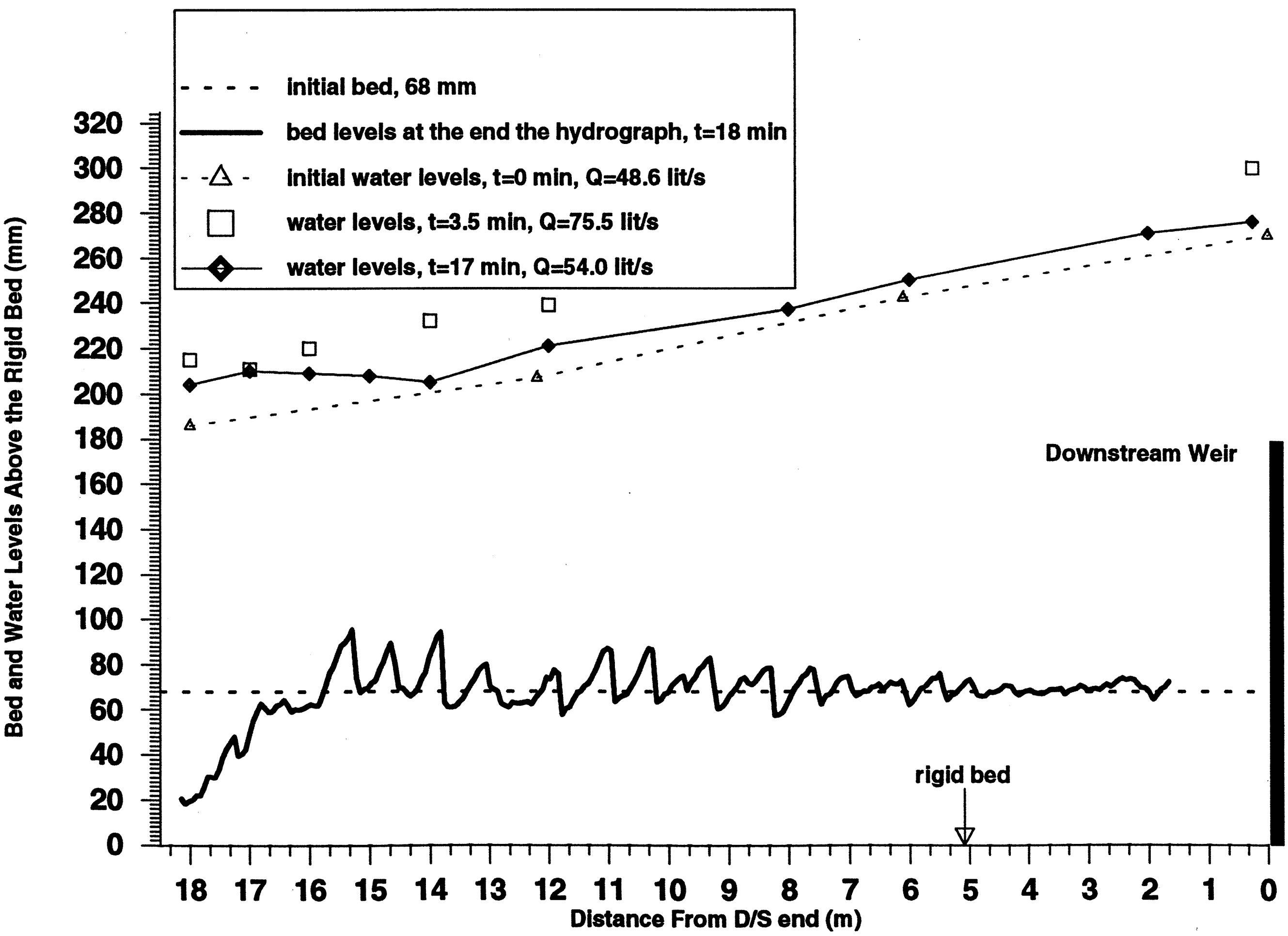

Figure 27(b) Bed and Water Levels in Test 10

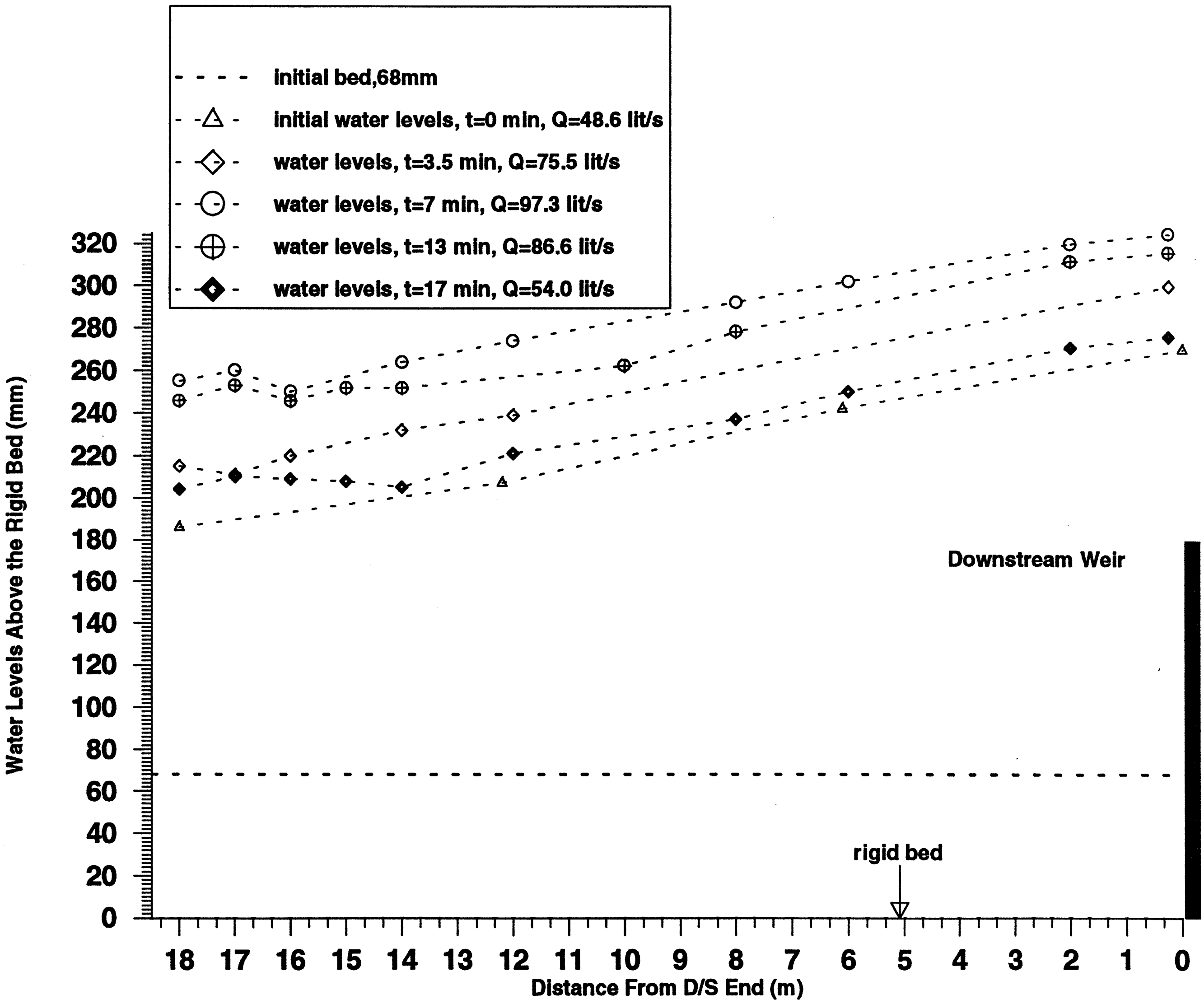

Figure 28 Water Levels in Test 10

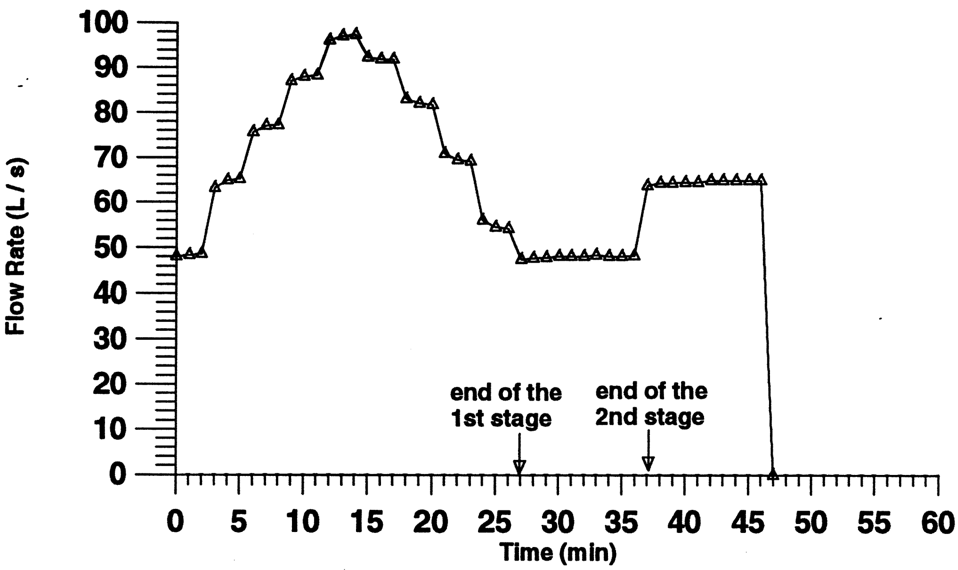

Figure 29(a) Flow Hydrograph in Test 11

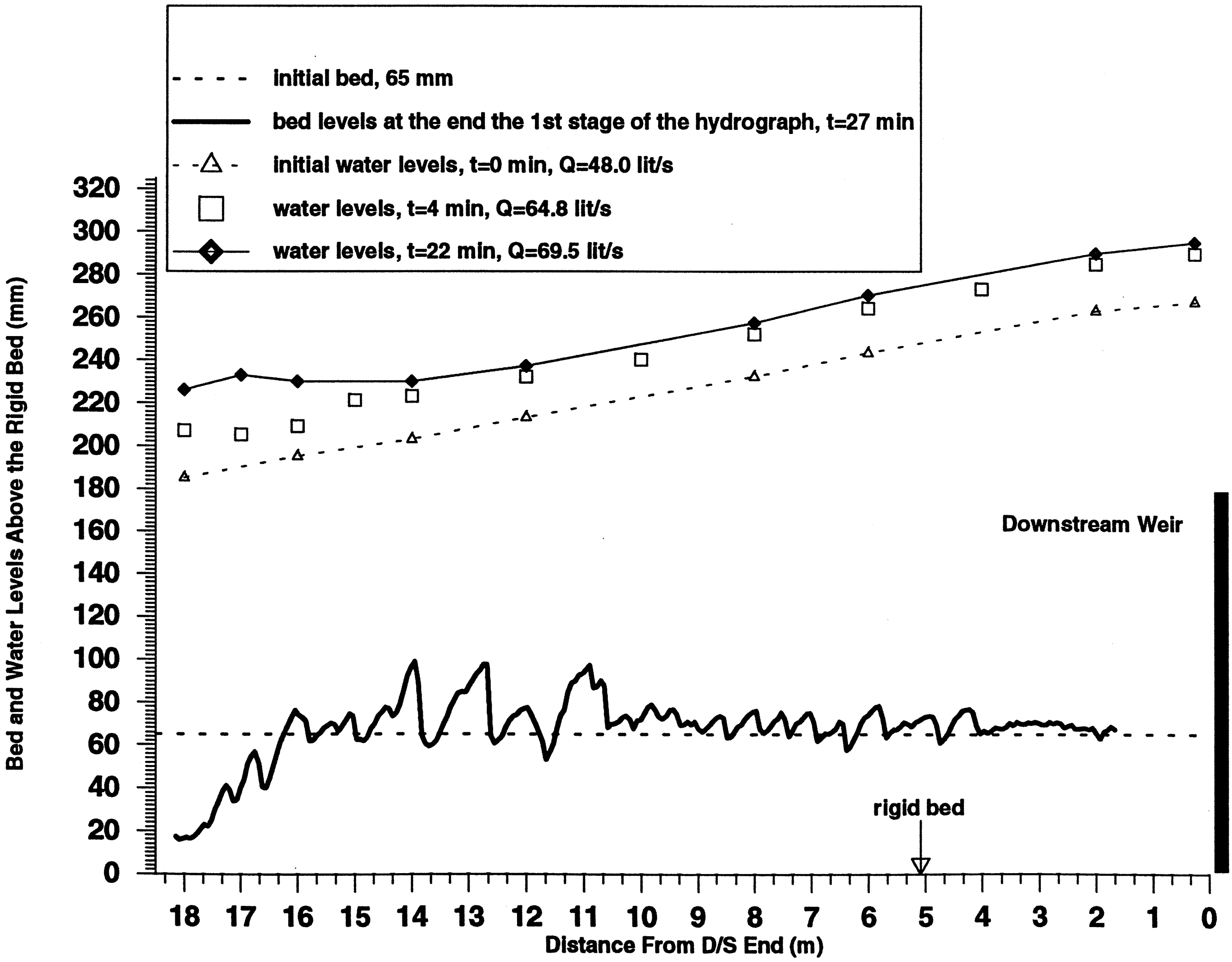

Figure 29(b) Bed and Water Levels in Test 11 (1st stage)

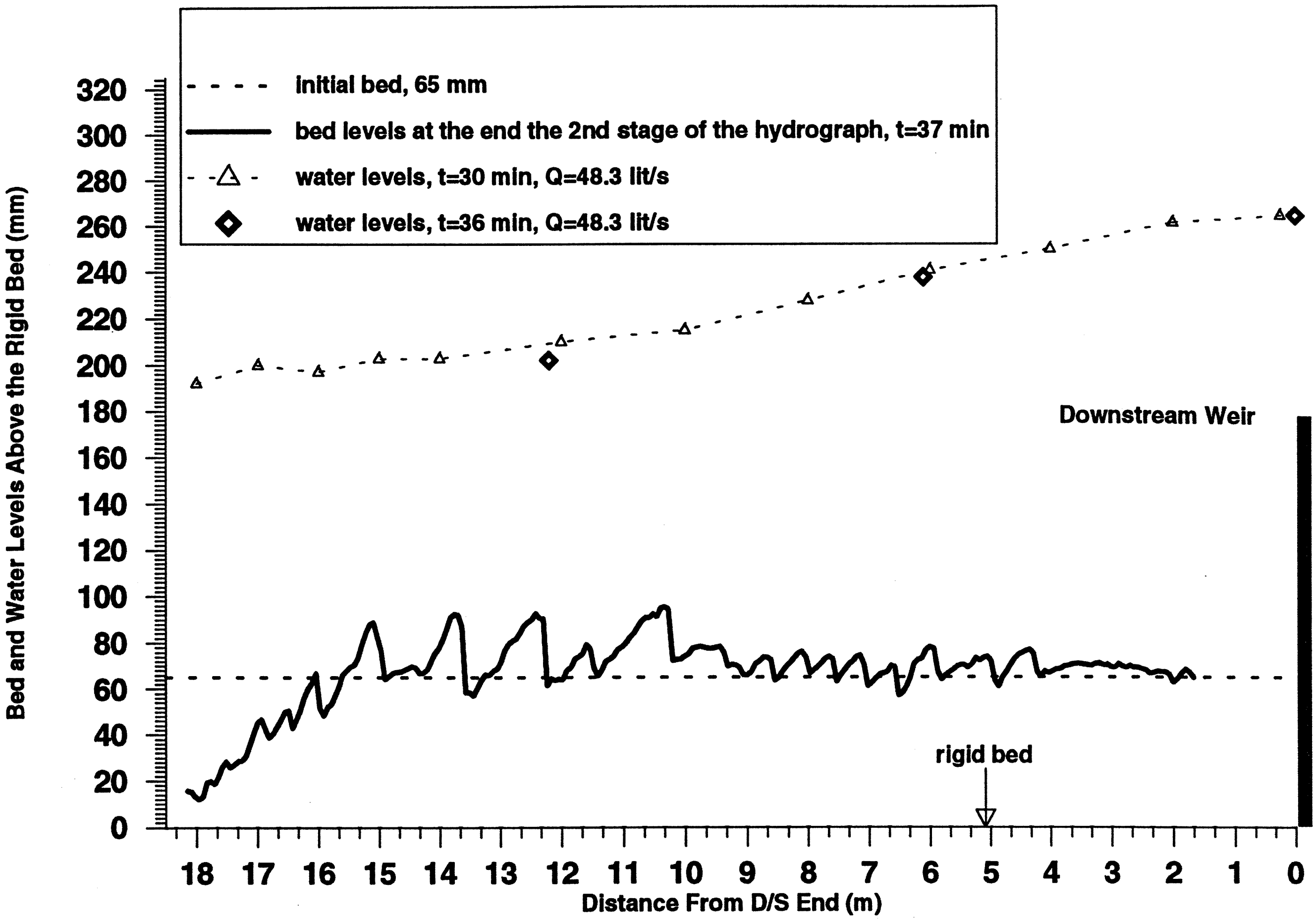

Figure 30(a) Bed and Water Levels in Test 11 (2nd stage)

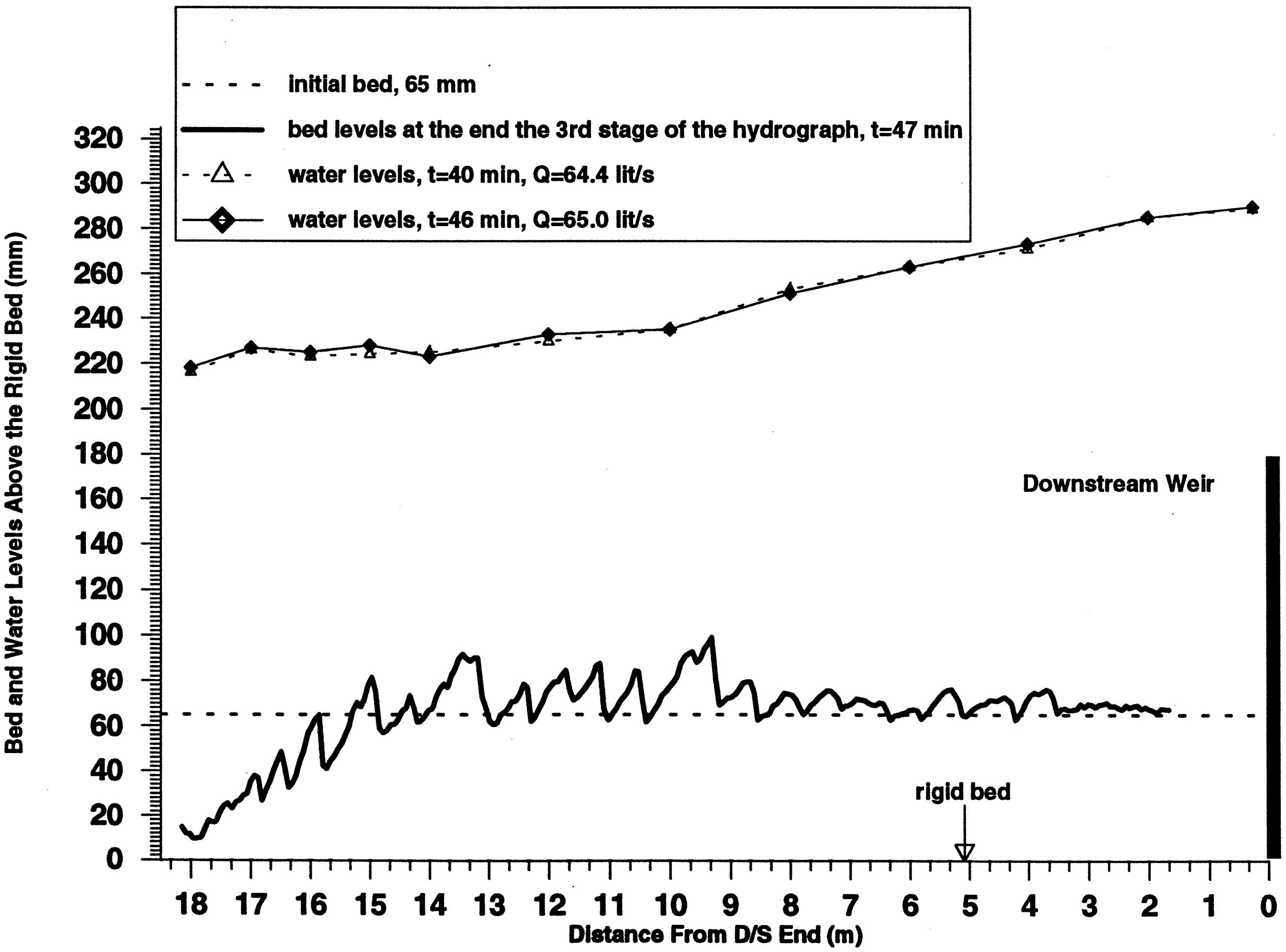

Figure 30(b) Bed and Water Levels in Test 11 (final stage)

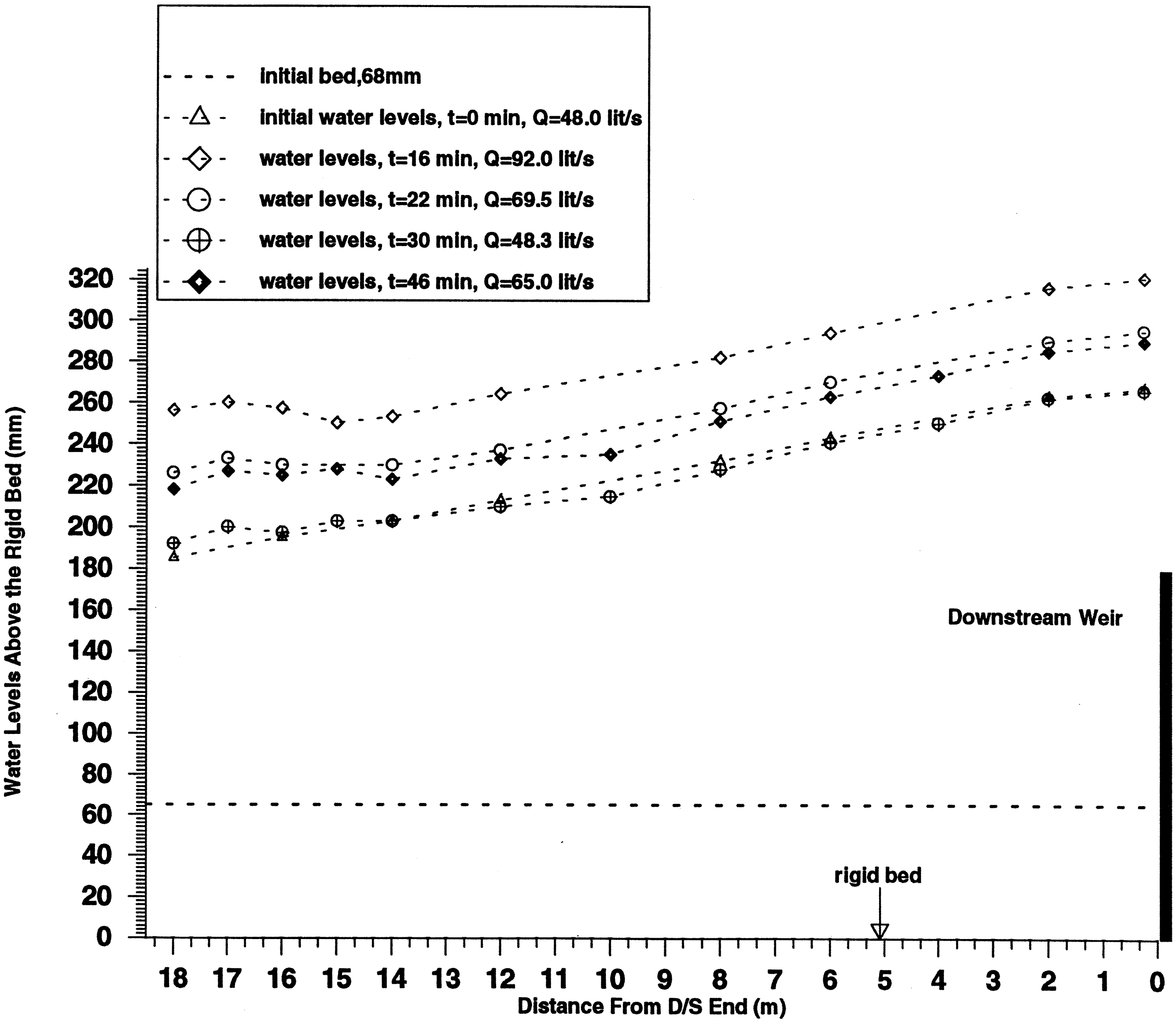

Figure 31 Water Levels in Test 11

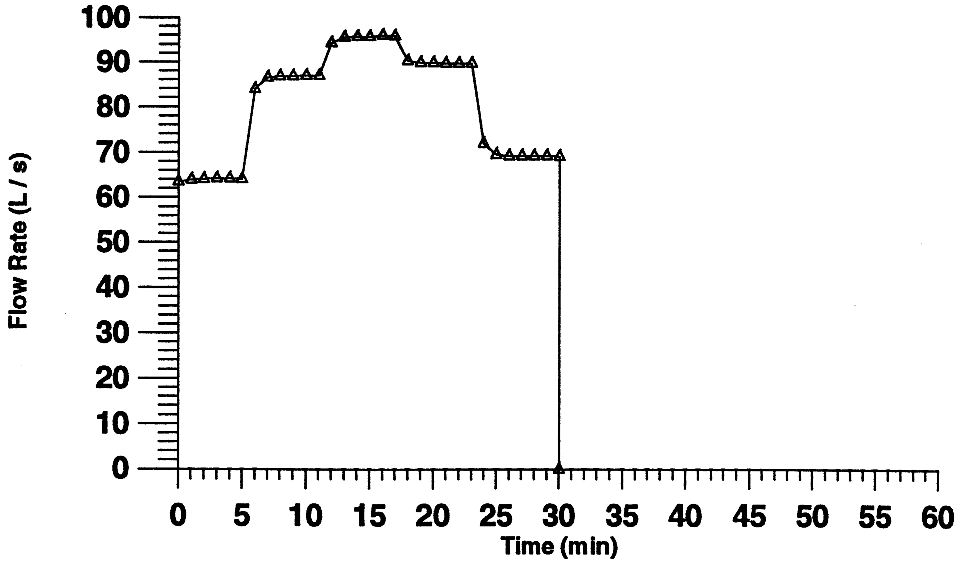

Figure 32(a) Flow Hydrograph in Test 12

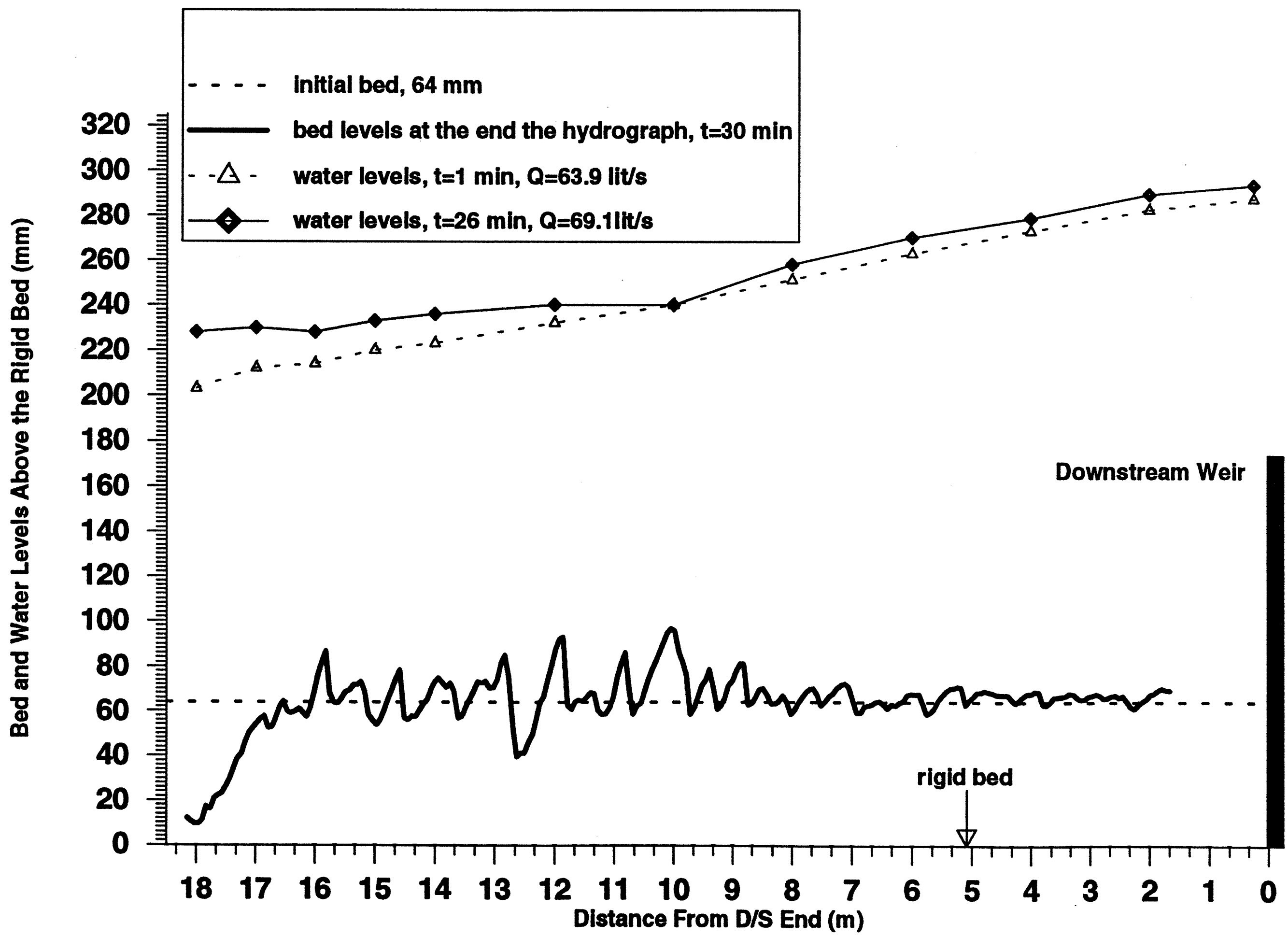

Figure 32(b) Bed and Water Levels in Test 12

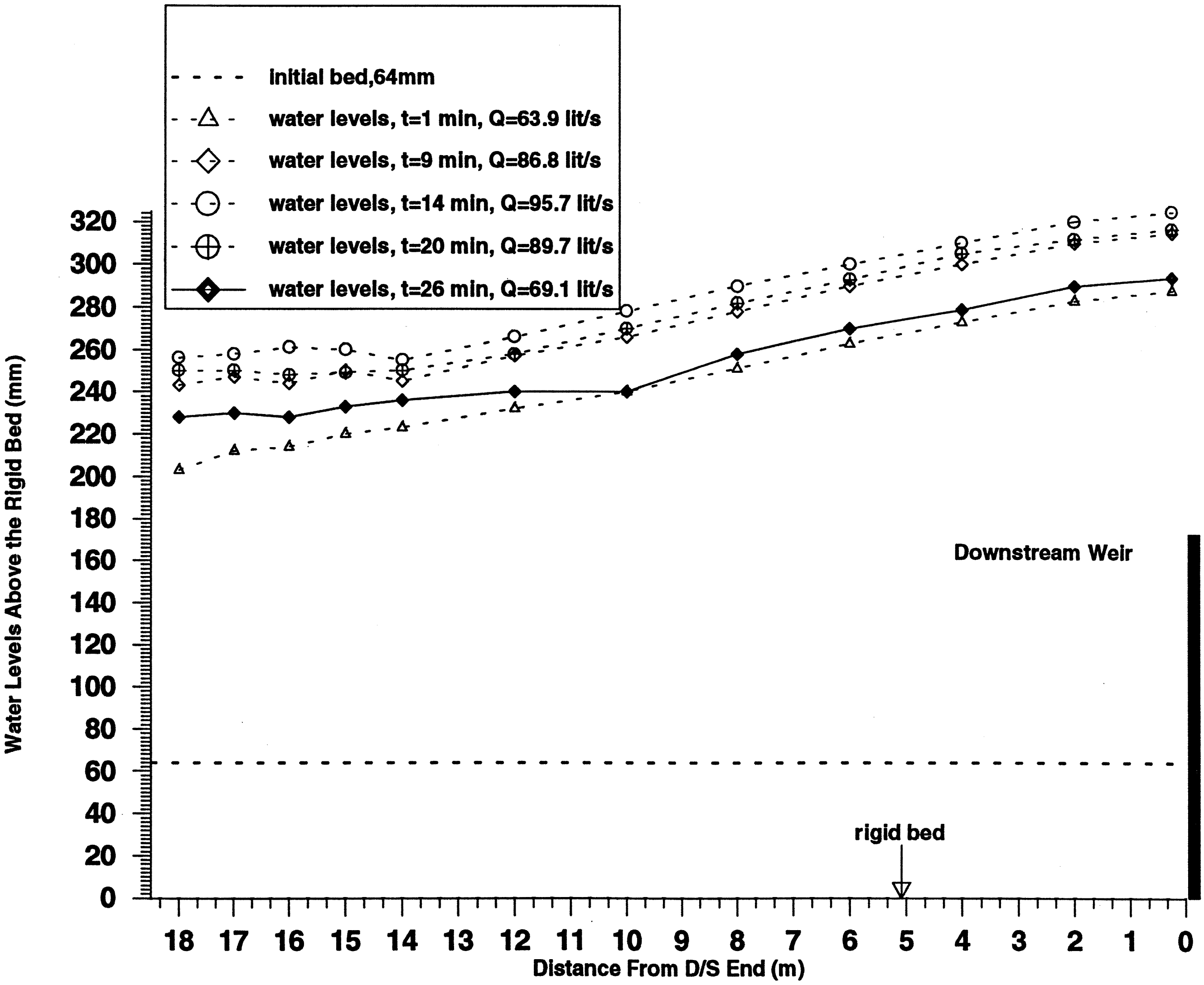

Figure 33 Water Levels in Test 12

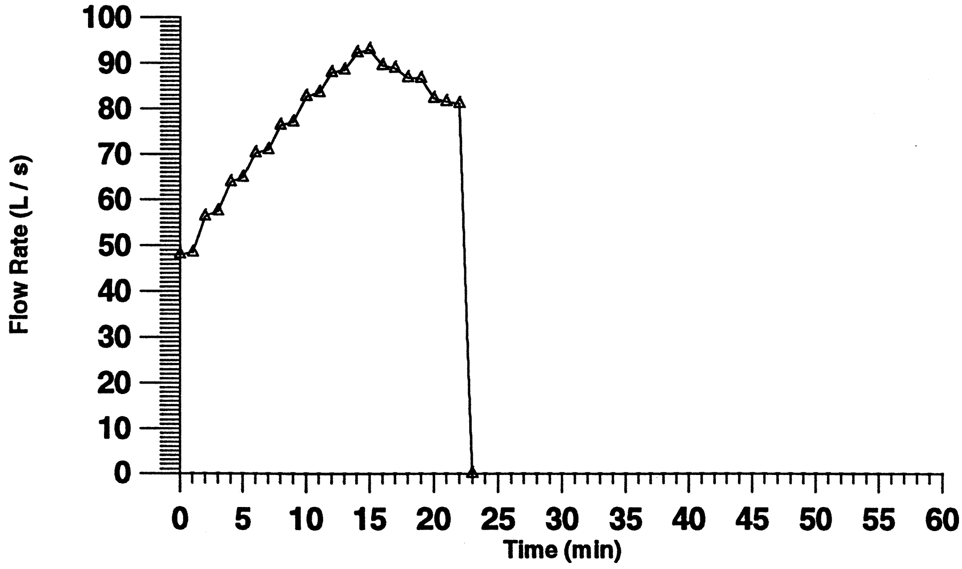

Figure 34(a) Flow Hydrograph in Test 13

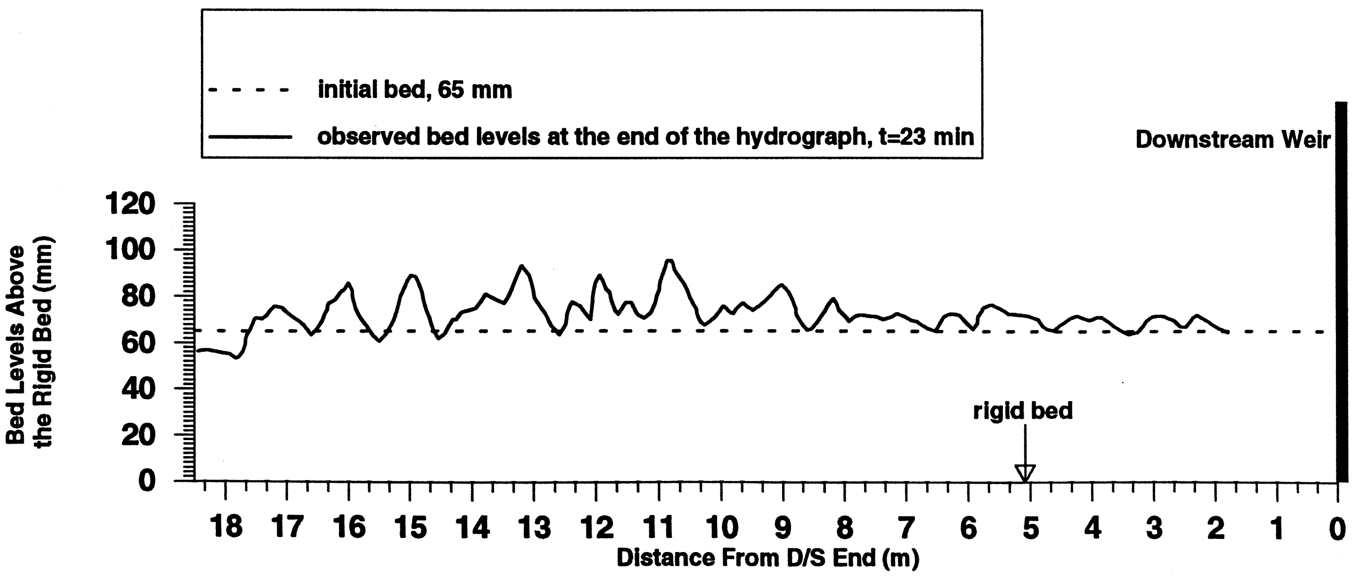

Figure 34(b) Bed Levels in Test 13

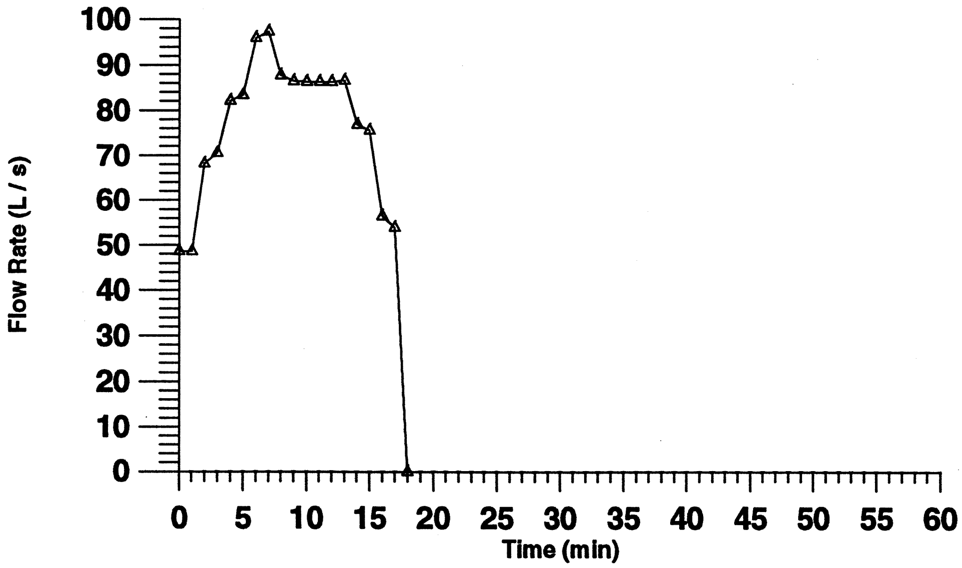

Figure 35(a) Flow Hydrograph in Test 14

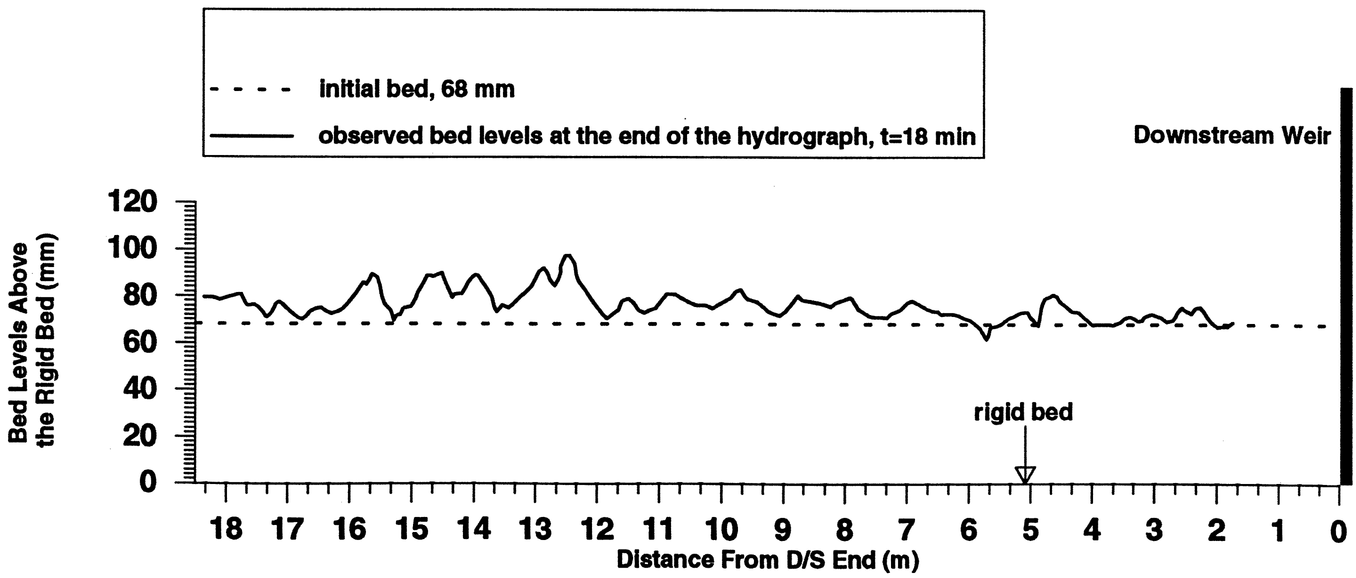

Figure 35(b) Bed Levels in Test 14

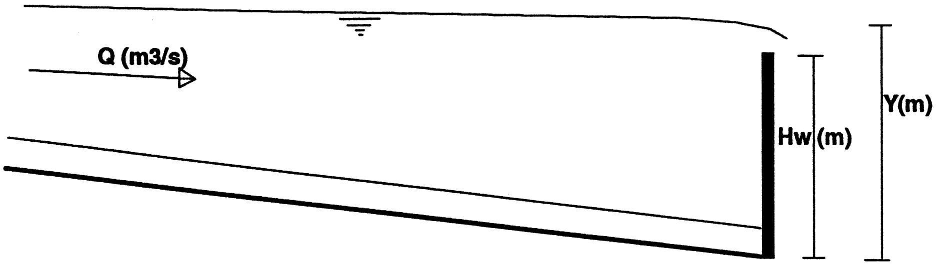

Figure 36(a) Definition Sketch for the Weir Rating Curve

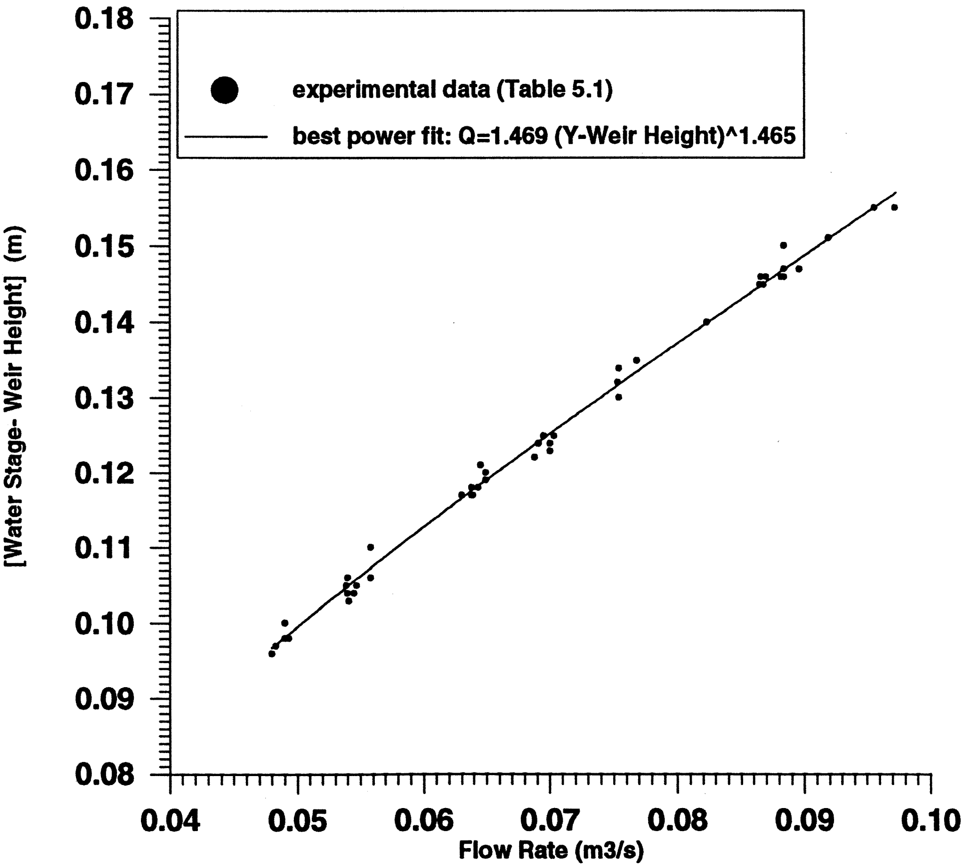

Figure 36(b) Rating Curve for the Downstream Weir

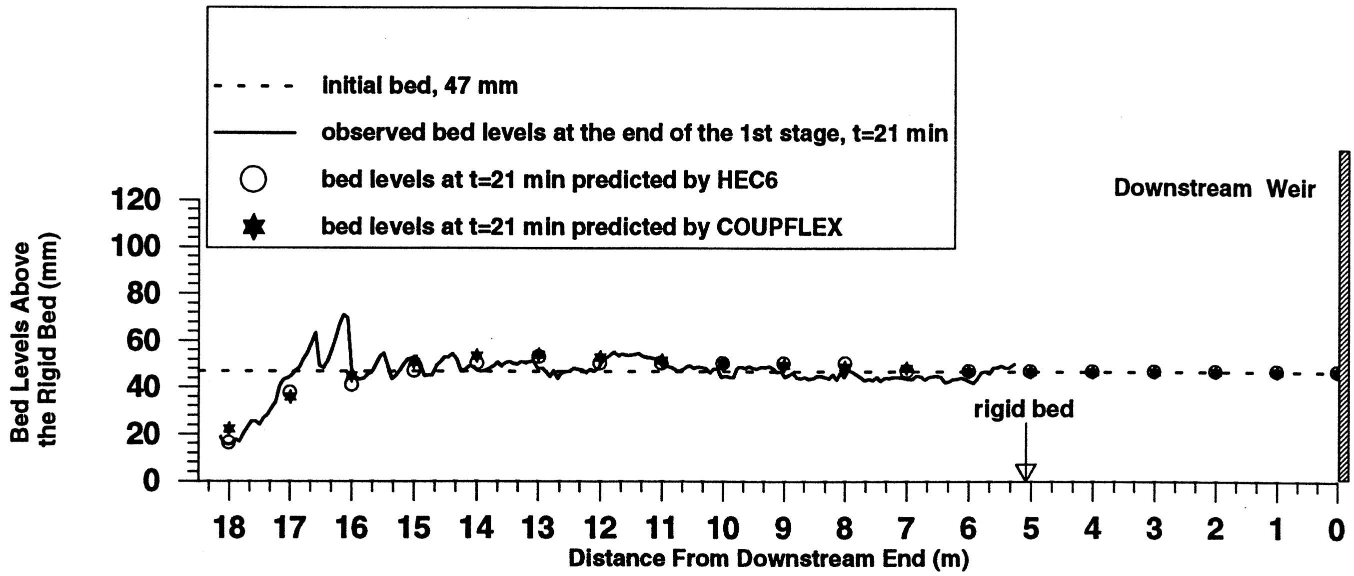

Figure 37(a) Experimental Results and Model Predictions for Test 1

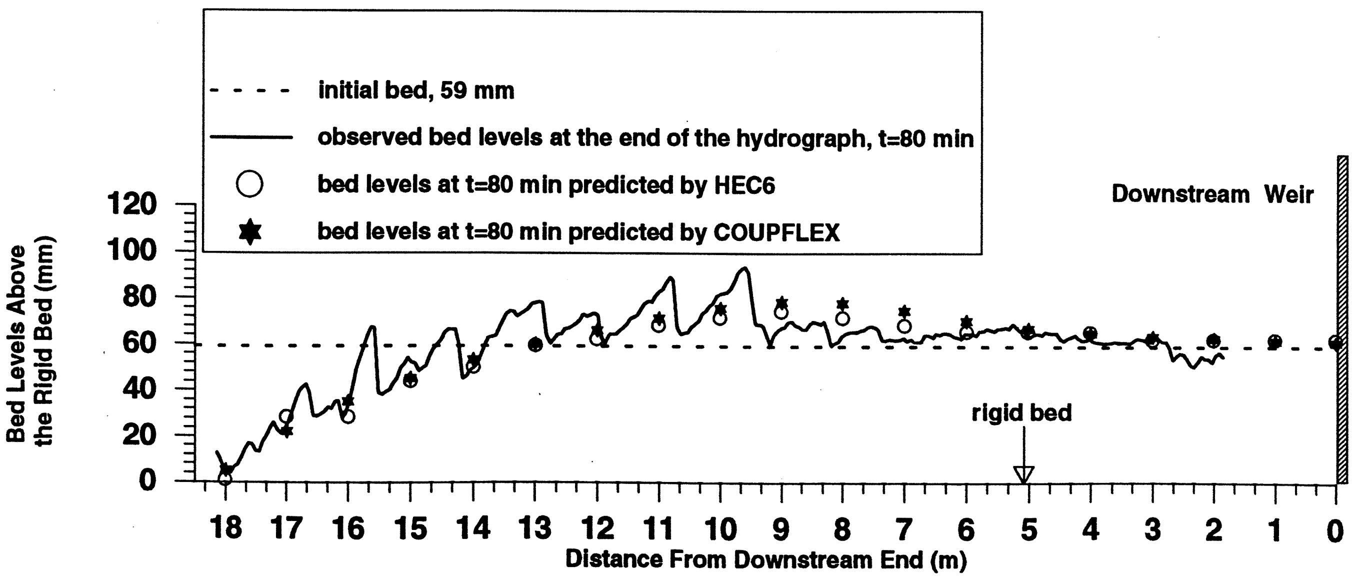

Figure 37(b) Experimental Results and Model Predictions for Test 2

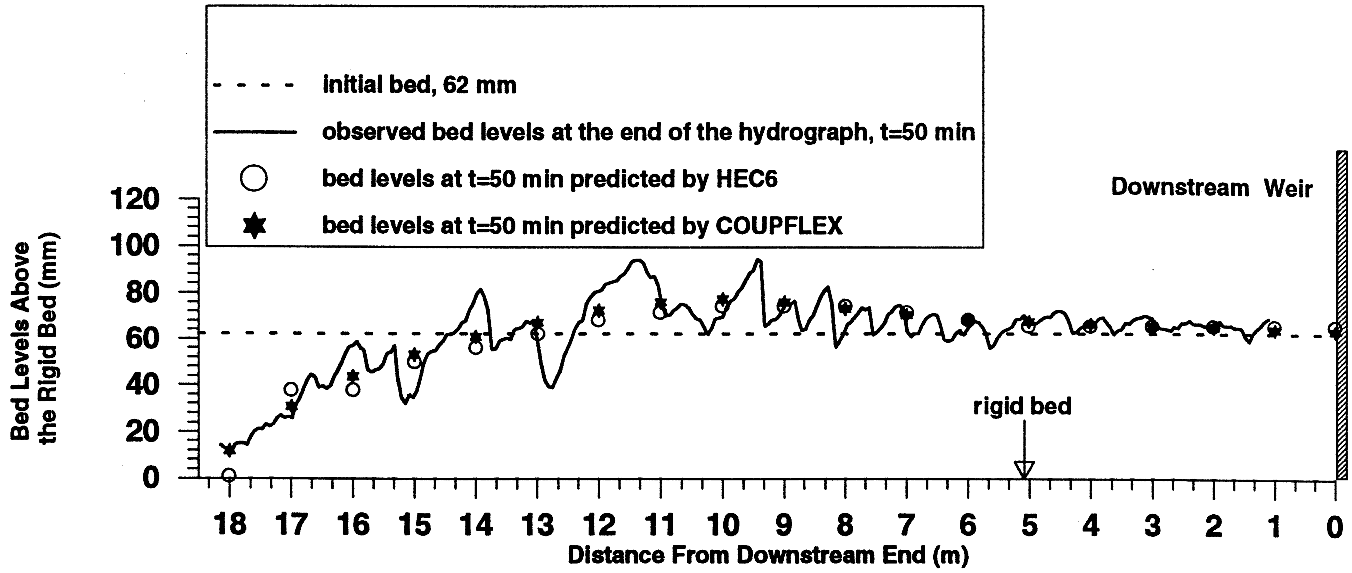

Figure 38(a) Experimental Results and Model Predictions for Test 3

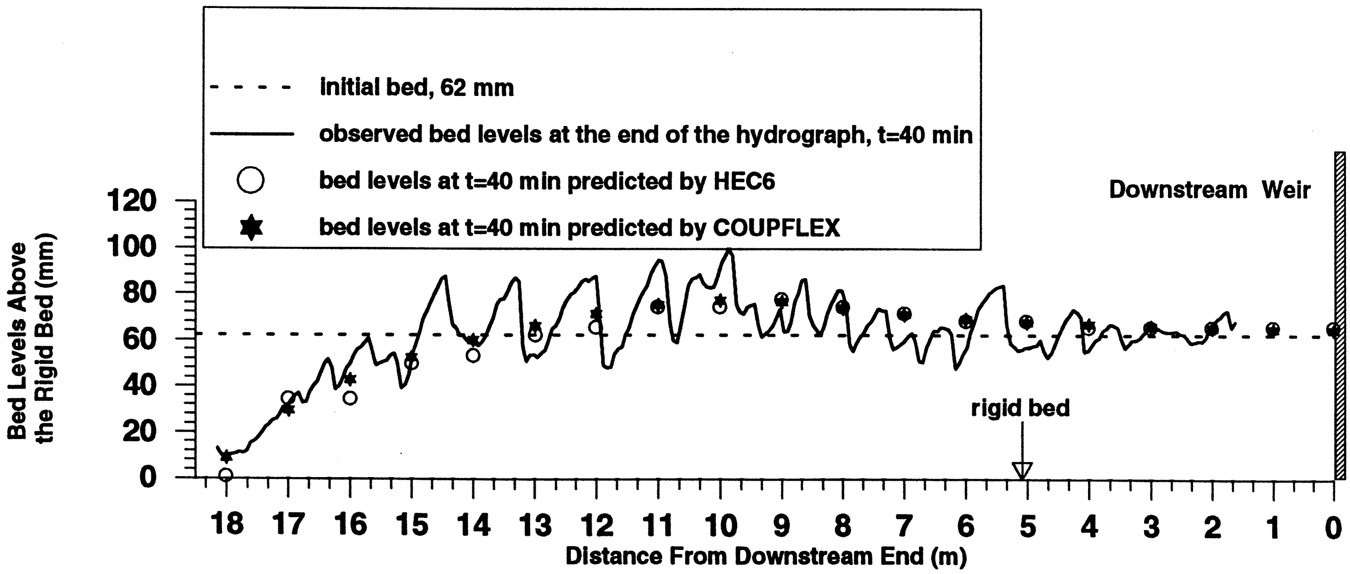

Figure 38(b Experimental Results and Model Predictions for Test 4

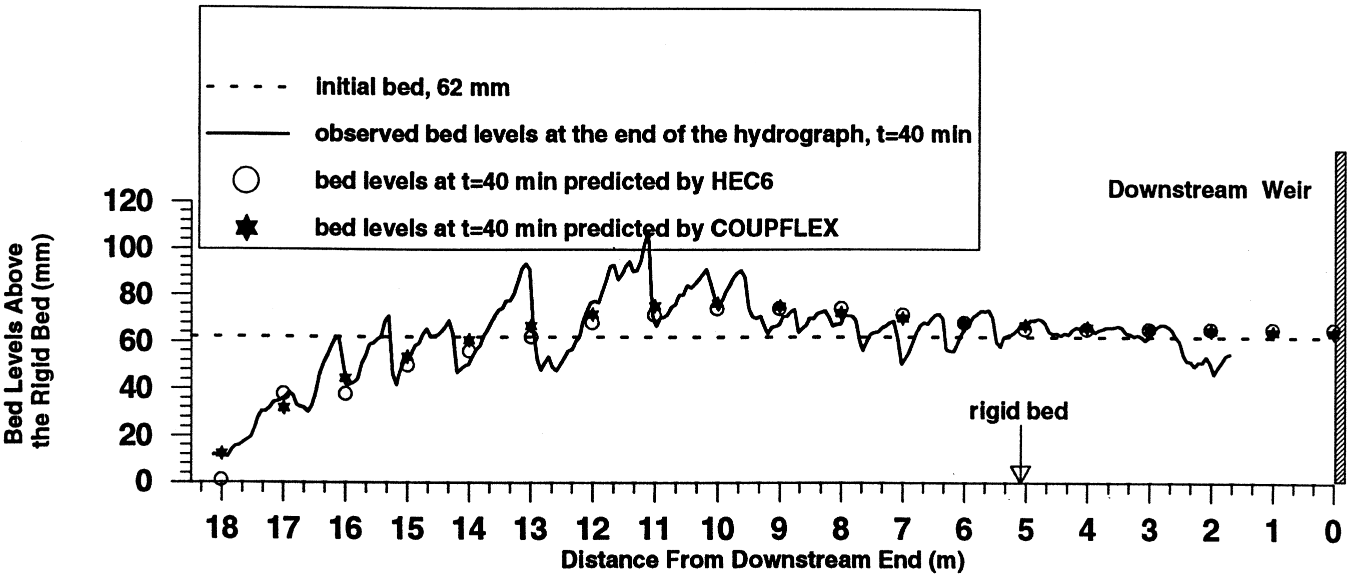

Figure 39(a) Experimental Results and Model Predictions for Test 5

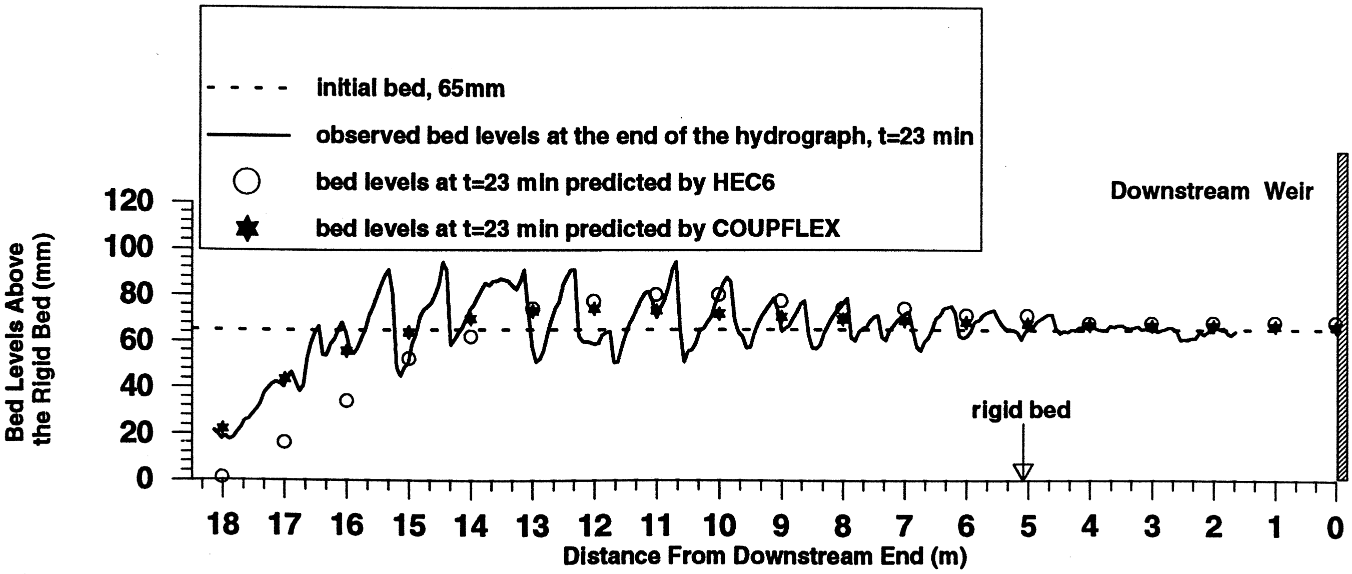

Figure 39(b) Experimental Results and Model Predictions for Test 6

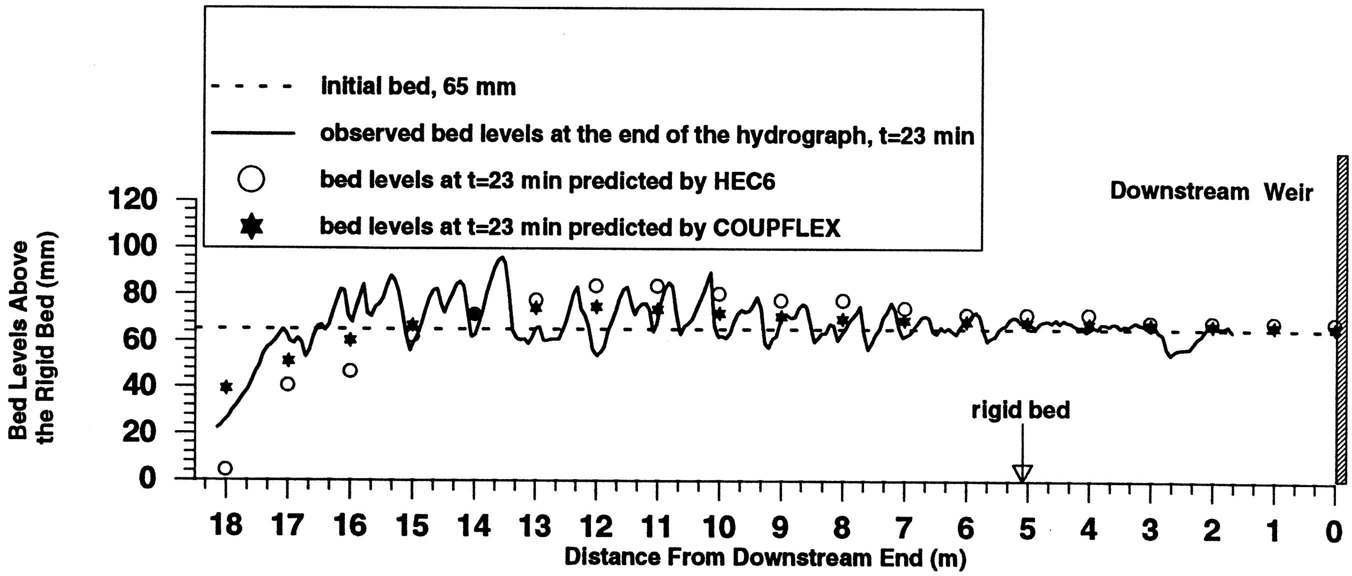

Figure 40(a) Experimental Results and Model Predictions for Test 7

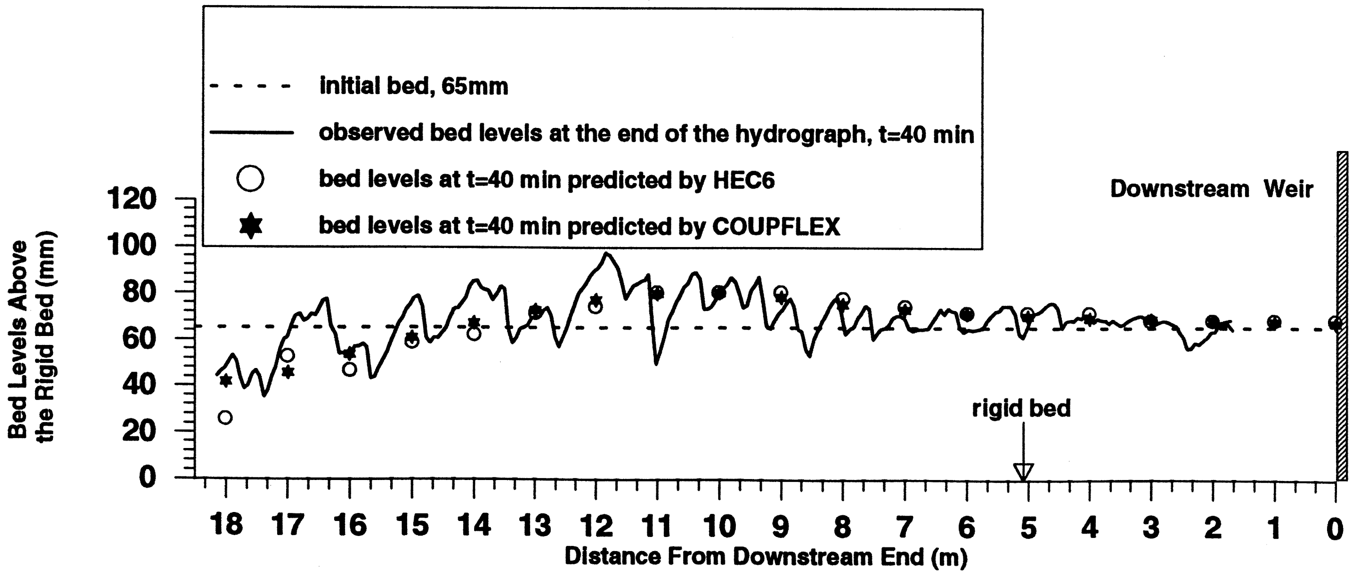

Figure 40(b) Experimental Results and Model Predictions for Test 8

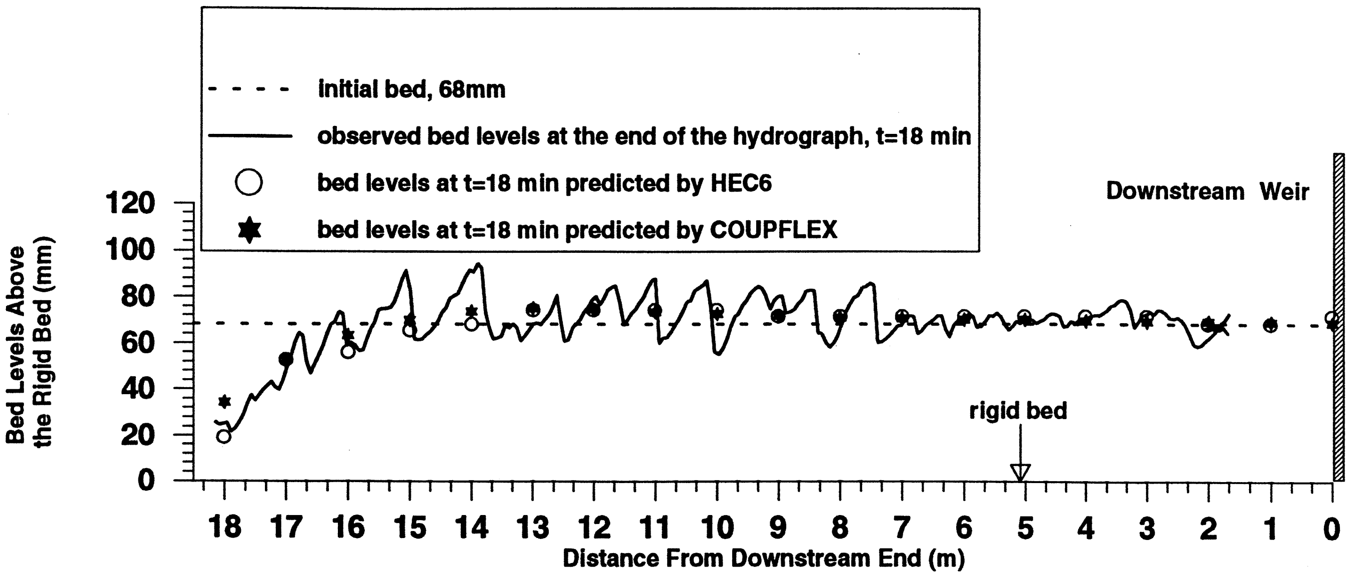

Figure 41(a) Experimental Results and Model Predictions for Test 9

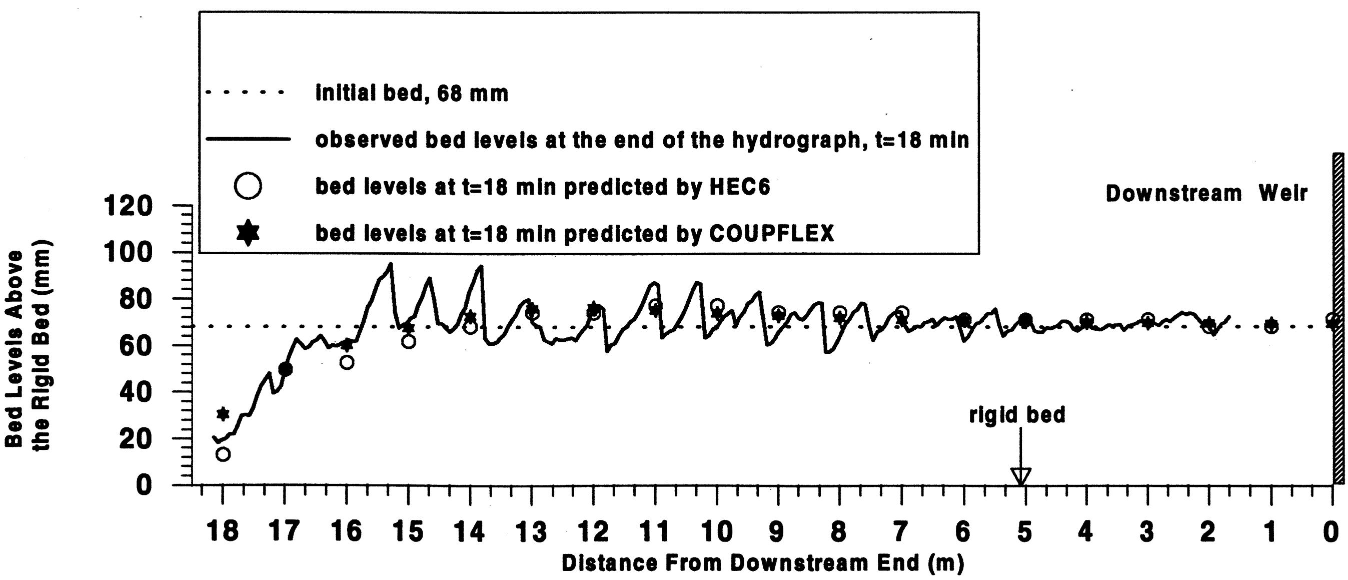

Figure 41(b) Experimental Results and Model Predictions for Test 10

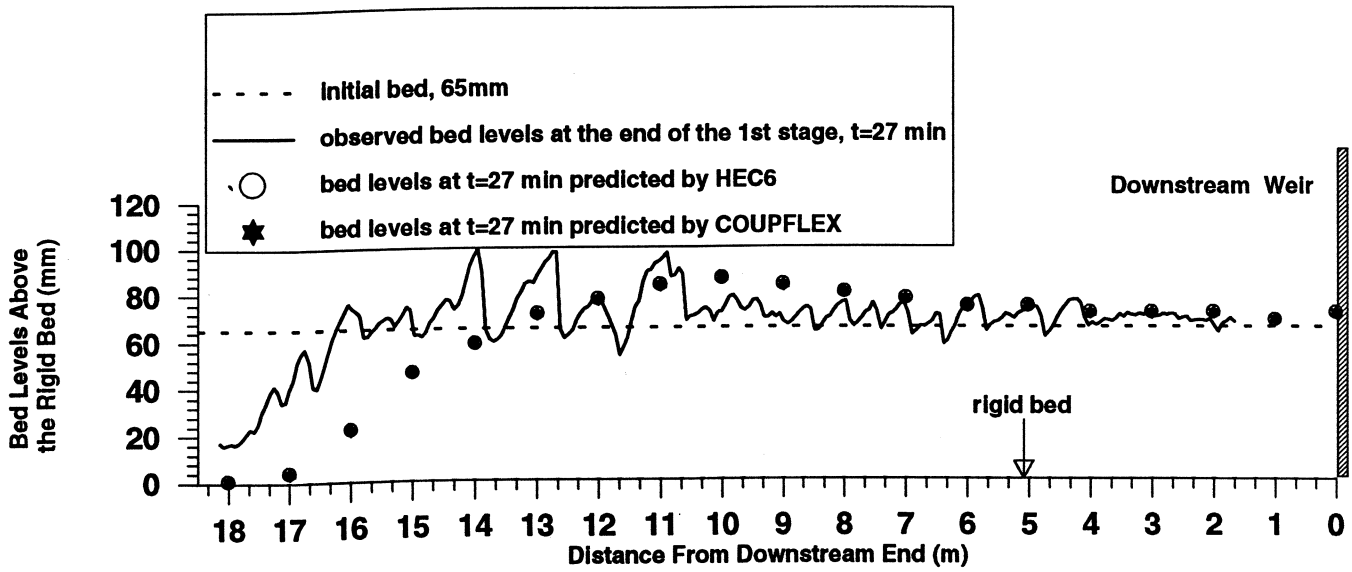

Figure 42(a) Experimental Results and Model Predictions for Test 11 (1st stage)

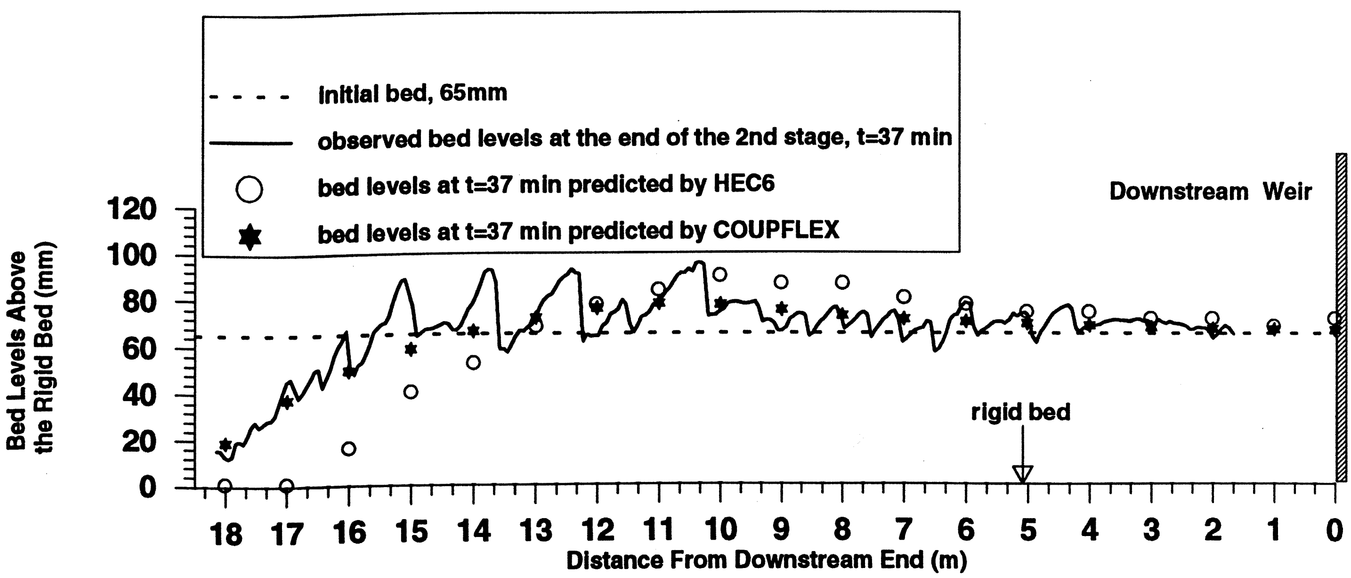

Figure 42(b) Experimental Results and Model Predictions for Test 11 (2nd stage)

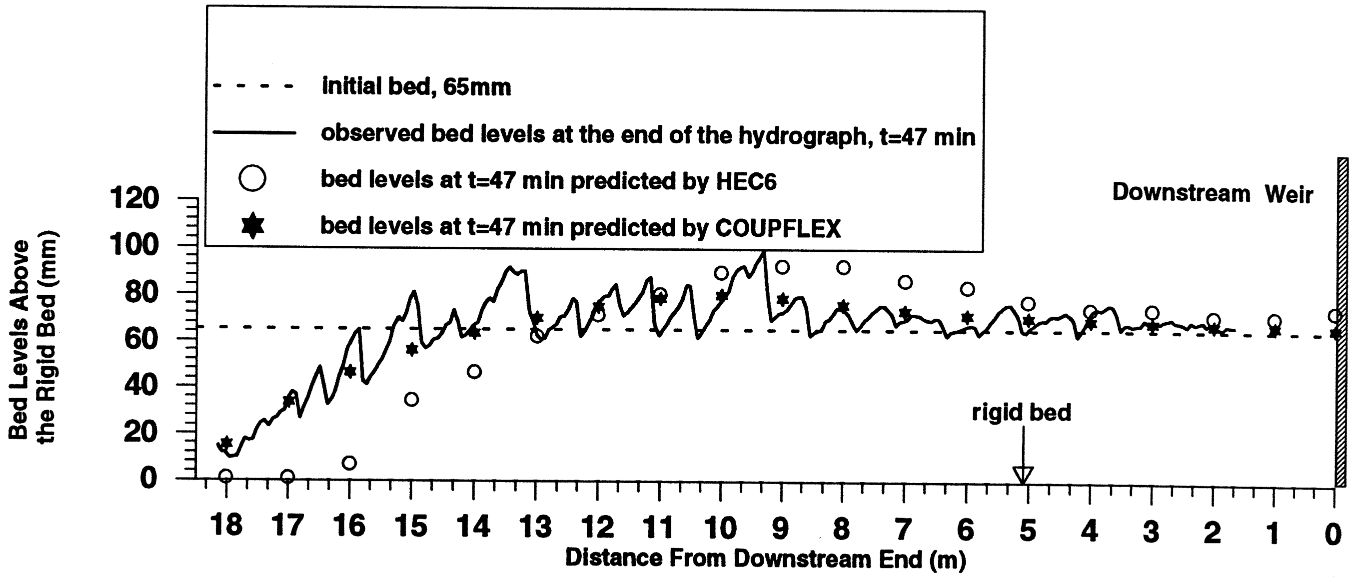

Figure 43(a) Experimental Results and Model Predictions for Test 11 (3rd stage)

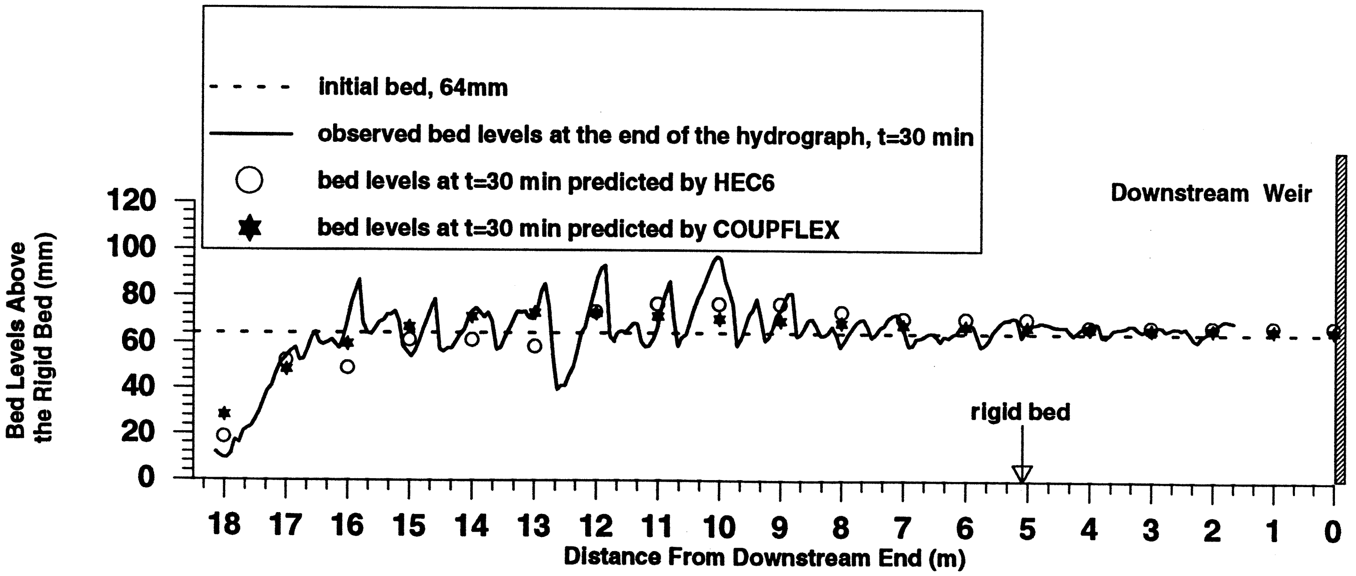

Figure 43(b) Experimental Results and Model Predictions for Test 12

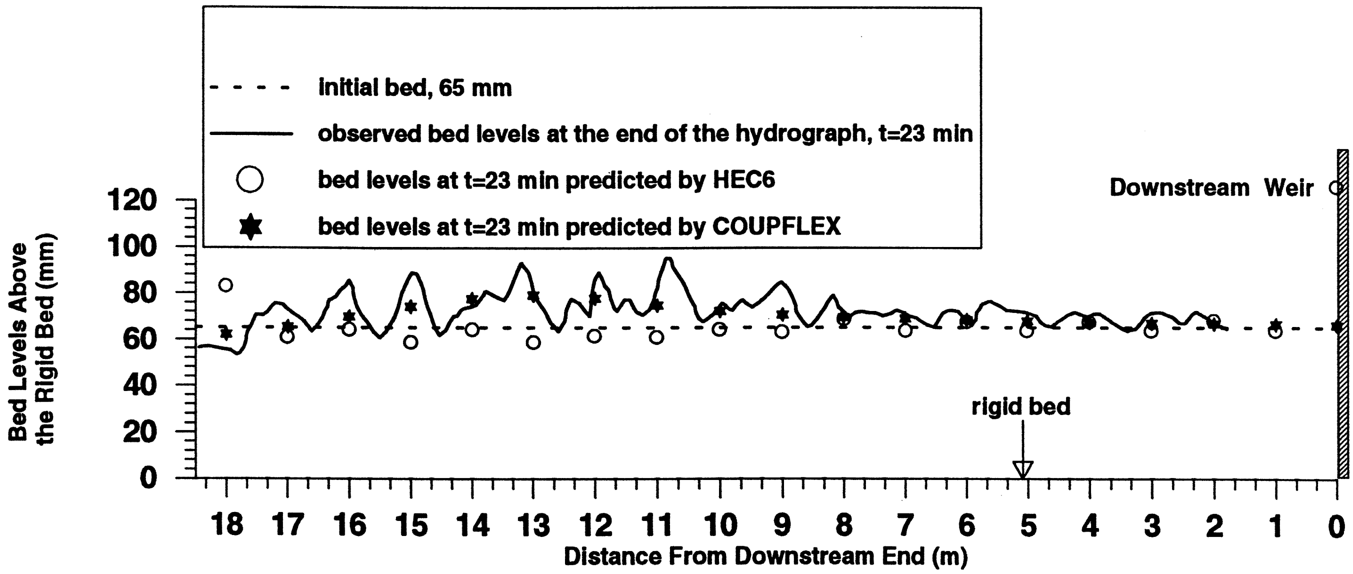

Figure 44(a) Experimental Results and Model Predictions for Test 13

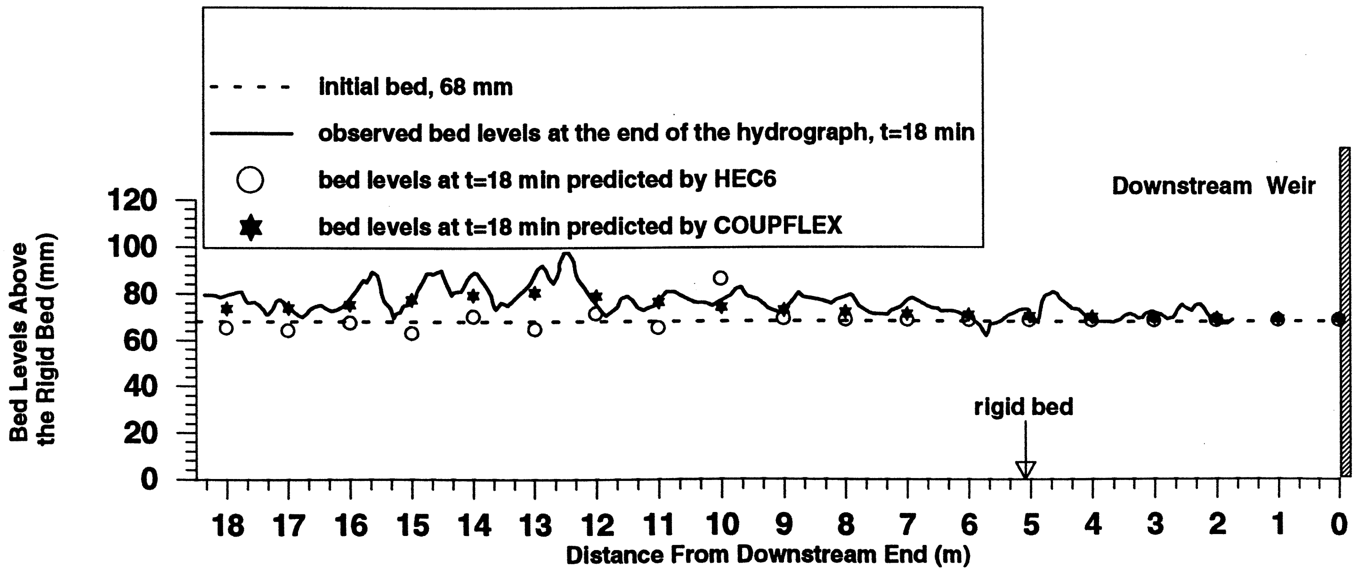

Figure 44(b) Experimental Results and Model Predictions for Test 14

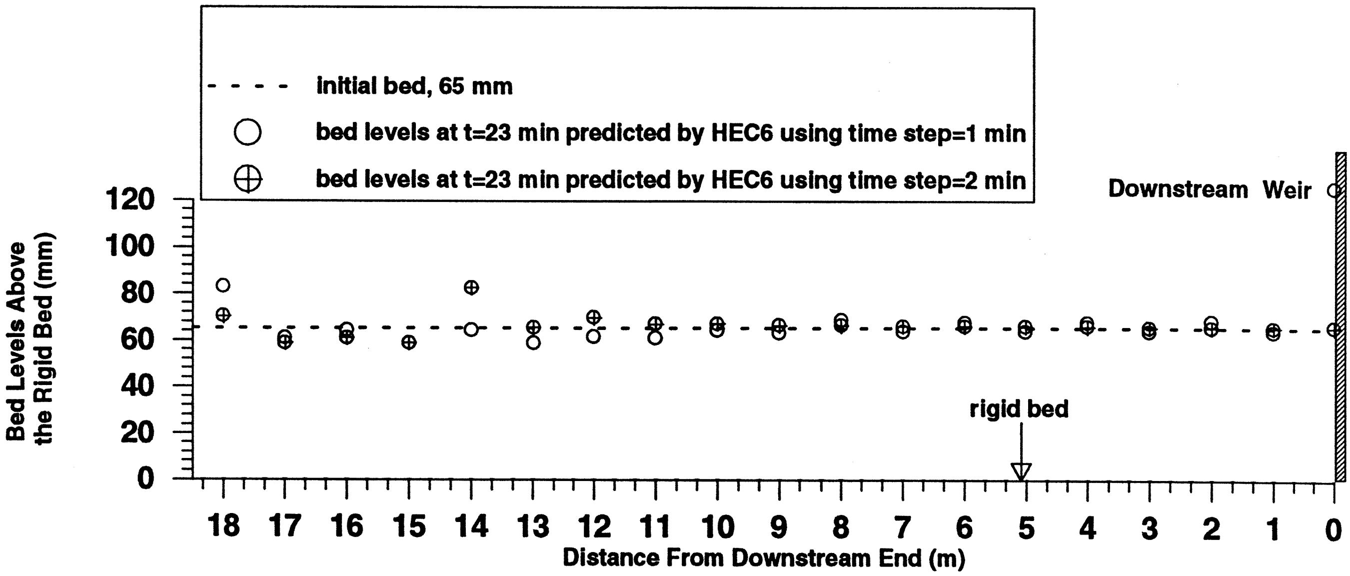

Figure 45(a) Effect of Computational Time Step in Simulation of Test 13

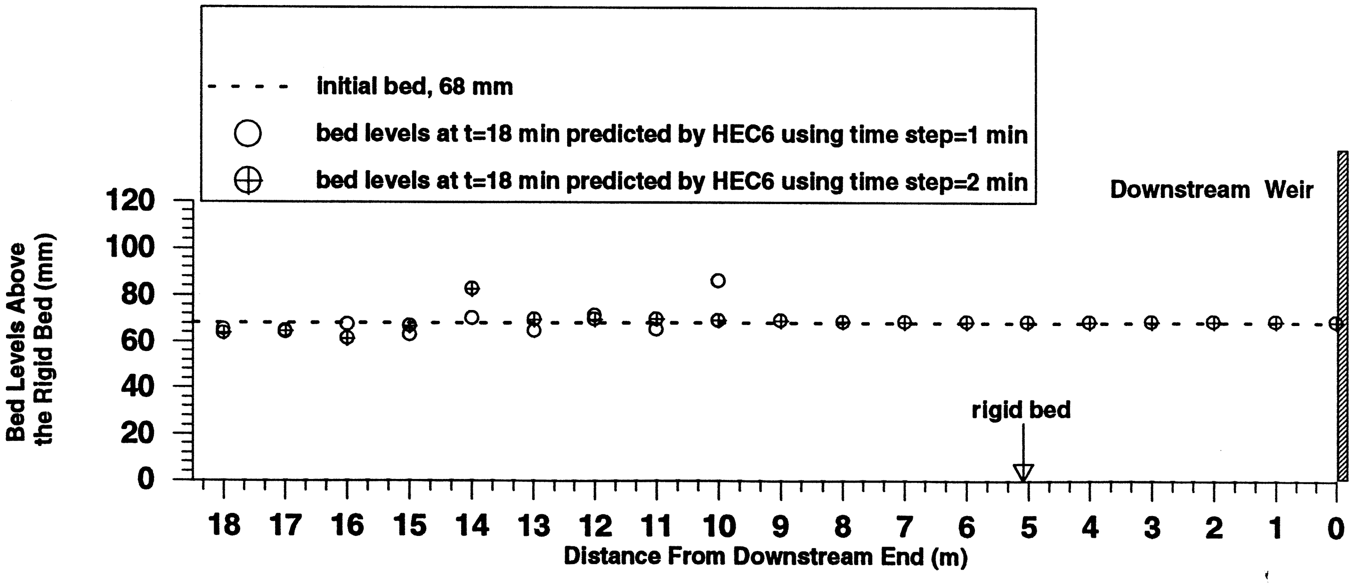

Figure 45(b) Effect of Computational Time Step in Simulation of Test 14

APPENDIX I

INCLUSION OF THE EMPIRICAL FORMULAE IN DIMENSIONLESS FORM

Inclusion of the Empirical Formulae in Dimensionless Form

This is an appendix to Section 2.2.3 and provides examples for nondimensional inclusion of empirical relations for the hydraulic resistance of the flow (S_f), total sediment transport discharge (Q_s), and suspended sediment concentration (C_s) in the model.

(a) Inclusion of S_f in Dimensionless Form

Among several empirical formulae included in the model that of Brownlie (1981) is considered here as an example. Making use of dimensional analysis and by performing regression analysis of parameters from flume and field data, Brownlie obtained the following equation for the friction slope S_f

$$S_f = m_1(s-1)^{m2} F_g^{m3} \left(\frac{R}{D_{50}}\right)^{m4} \sigma^{m5} \tag{I.1}$$

in which $F_g = \dfrac{V}{u_D}$ is the grain Froude number; $u_D = \sqrt{g(s-1)D_{50}}$; D_{50} is the mean grain diameter; σ is the geometric standard deviation of sediment size being one for uniform sediment; R is the hydraulic radius being equal to A / P where P is the wetted perimeter. The coefficients m_1 to m_5 take different values in different flow regimes. For lower regime (ripples and dunes) m_1=0.02054 , m_2=1.286, m_3= 2.572 , m_4 =-0.361 , and m_5 =0.4130. For upper regime (plane bed, standing waves, antidunes) m_1=0.01252, m_2 =1.086, m_3= 2.172 , m_4 =-1.304, and m_5 = 0.2785.

Noting that $V = Q/A$, it is possible to change Equation (I.1) into

$$S_f = m_6 Q^{m3} A^{-m3} R^{m4} \tag{I.2}$$

in which $m6 = m1(s-1)^{m2} \sigma^{m5} u_D^{-m3} D_{50}^{-m4}$ is a constant.

For the dimensional equation (I.1) it can be shown that the relations

$$\frac{\partial S_f}{\partial Q} = m3 \frac{S_f}{Q} \tag{I.3}$$

$$\frac{\partial S_f}{\partial h} = \frac{S_f}{A}\left[(m4 - m3)T - m4R\frac{dP}{dh}\right] \tag{I.4}$$

hold true. Taking the basic quantities Q_0, S_0, A_0 as defined before, and R_0, and P_0, corresponding to h_0 for hydraulic radius and wetted perimeter respectively, the dimensionless variables $Q^* = \dfrac{Q}{Q_o}$, $R^* = \dfrac{R}{R_o}$, $P^* = \dfrac{P}{P_o}$, and $S_f^* = \dfrac{S_f}{S_o}$ can be defined.

After substituting the dimensionless variables, Equations (I.2) and (I.3) become

$$S^*f = \left[\frac{m6}{So} Vo^{m3} Ro^{m4}\right] Q^{*m3} A^{*-m3} R^{*m4} \tag{I.5}$$

$$\frac{\partial Sf^*}{\partial Q^*} = m_3 \frac{Sf^*}{Q^*} \tag{I.6}$$

and Equation (I.4), by multiplying both sides by h_o/S_o and the right hand side by T_o/T_o, becomes

$$\frac{\partial Sf}{\partial h^*} = \frac{Sf^*}{A^*}\left[(m4 - m3)T^* - m4R^* \frac{dP^*}{dh^*}\right] \tag{I.7}$$

Note that dP/dh depends on the geometry of the cross-section (being two for a rectangular and $2\sqrt{1+\eta^2}$ for a trapezoidal cross-section with side slope η.

It is interesting to note that Brownlie's relations, like most other empirical resistance relations, take a similar form, after simplification, to the familiar Manning's friction equation. For example in Brownlie's equations, m_6, which depends on flow regime and sediment parameter, corresponds to n^2 in Manning's relation $Sf = n^2Q^2A^{-2}R^{-4/3}$. In the model, Equations (I.5) to (I.7) are evaluated at time level j, at which all variables are known. A variety of existing empirical formulae for hydraulic resistance has been provided in the model making it possible to choose the most appropriate one for the particular site under study.

(b) Inclusion of Q_s in Dimensionless Form

As an example of incorporating empirical relations for sediment transport capacity in the model the total load formula of Engelund and Hansen (1967) is used here. According to their formula, the volumetric rate of sediment transport can be determined from:

$$Qs = 0.05TV^2\sqrt{\frac{D50}{g(s-1)}}\left[\frac{\tau o}{(\gamma s - \gamma)D50}\right]^{1.5} \tag{I.8}$$

where $\tau_o = \gamma RSf$, γ_s and γ are the weight density of sediment and water respectively, and other variables are as defined before. Some algebraic operations yield

$$Q_s = n_1 TQ^2A^{-2}R^{1.5}Sf^{1.5} \tag{I.9}$$

in which $n_1 = \dfrac{0.05}{\sqrt{gD_{50}}(s-1)^2}$ is a constant for given sediment size and density. The derivatives of Q_s in terms of Q and h are as follows

$$\frac{\partial Qs}{\partial Q} = Qs\left[\frac{2}{Q} + \frac{1.5}{Sf}\frac{\partial Sf}{\partial Q}\right] \tag{I.10}$$

$$\frac{\partial Qs}{\partial h} = Qs\left[\frac{-2}{A}\frac{dA}{dh} + \frac{1.5}{R}\frac{dR}{dh} + \frac{1.5}{Sf}\frac{\partial Sf}{\partial h}\right] \tag{I.11}$$

Noting that $\dfrac{dA}{dh} = T$ and $\dfrac{dR}{dh} = \dfrac{T}{P} - \dfrac{R}{P}\dfrac{dP}{dh}$, Equation (I.11) can be simplified into:

$$\frac{\partial Qs}{\partial h}=\frac{Qs}{A}\left[-0.5T-1.5R\frac{dP}{dh}+\frac{1.5A}{Sf}\frac{\partial Sf}{\partial h}\right] \tag{I.12}$$

Making use of the relevant basic quantities defined before, Equations (I.9), (I.10), and (I.12) can be changed to the following dimensionless relations :

$$Q_s^* = n_2 T^* Q^{*2} A^{*-2} R^{*1.5} S_f^{*1.5} \tag{I.13}$$

$$\frac{\partial Qs^*}{\partial Q^*}=Qs^*\left[\frac{2}{Q^*}+\frac{1.5}{Sf^*}\frac{\partial Sf^*}{\partial Q^*}\right] \tag{I.14}$$

$$\frac{\partial Qs^*}{\partial h^*}=\frac{Qs^*}{A^*}\left[-0.5T^*-1.5R^*\frac{dP^*}{dh^*}+\frac{1.5A^*}{Sf^*}\frac{\partial Sf^*}{\partial h^*}\right] \tag{I.15}$$

where $n_2=\frac{n_1}{Q_o}T_oV_o^2R_o^{1.5}S_o^{1.5}$ is a constant for given sediment size and density.

It should be noted that in Equations (I.13) to (I.15), S_f and its derivatives are obtained using the relevant calculations described in the previous section of this appendix. In the model, several transport formulae used in engineering practice have been provided allowing the user to select the most suitable one for the respective application.

(c) Inclusion of C_s in Dimensionless Form

The volumetric concentration of the suspended sediment part, C_s, of the total sediment load, appears in terms ***11***, ***15***, and ***16*** of Equations (2.2) and (3). The suspended sediment formulation of Celik and Rodi (1991) is employed here as an example of the method of including C_s in dimensionless form in the model. Dealing with a wide rectangular channel, Celik and Rodi (1991) extended their previous investigations on the mechanism of suspended sediment movement and provided the following form of the transport-capacity correlation

$$Cs=1.13\beta c\left[1-\left(\frac{ks}{h}\right)^{nc}\right]\frac{\tau w}{(\rho s-\rho)gh}\frac{V}{ws} \tag{I.16}$$

in which β_c and n_c are empirical coefficients respectively equal to 0.034 and 0.06 for a rough bed , k_s is the equivalent sand-roughness height, τ_w is the wall shear stress, V is the mean water velocity, and w_s is the fall velocity of the sediment. In their formulation $\tau e=\tau w\left[1-\left(\frac{ks}{h}\right)^{nc}\right]$ is the effective shear stress. This corrects the shear stress for the effects of permeability of porous beds on the total shear stress. Celik and Rodi proposed the following relation to estimate k_s when no data is available for the roughness height,

$$\frac{k_s}{h}\approx 30\exp\left(-1-0.4\frac{V}{u_*}\right) \tag{I.17}$$

where $u_* = \sqrt{ghS_o}$ is the shear velocity. Further they recognised a critical shear stress, τ_c, below which no suspension occurs. The relation, in a slightly modified form, is

$$\tau_c = \frac{0.15}{Re_*}\rho g(s-1)D \quad \text{for } Re_* \le 0.6 \tag{I.18a}$$

$$\tau_c = 0.25\rho g(s-1)D \quad \text{for } Re_* > 0.6 \tag{I.18b}$$

in which $Re_* = \frac{u_* D}{\nu}$ is the particle Reynolds number and ν is the kinematic viscosity of water. To formulate the proposed suspended sediment transport capacity in the present model, Equation (I.16) with the criterion defined by Equations (I.18), can be changed to yield:

$$C_s = 0 \qquad \text{for } \tau \le \tau_c \tag{I.19a}$$

$$C_s = 1.13\beta_c\left[1-\left(\frac{k_s}{h}\right)^{nc}\right]\frac{S_f}{(s-1)}\frac{V}{w_s} \qquad \text{for } \tau > \tau_c \tag{I.19b}$$

Noting that $V = \frac{Q}{T \times h}$ and adopting $e_1 = \frac{1.13\beta_c}{(s-1)w_s}$ and $e2 = \left[1-\left(\frac{k_s}{h}\right)^{nc}\right]$, the dimensional form of the relation transforms to

$$C_s = e_1 \times e_2 V \times S_f = e_1 \times e_2 T^{-1} Q \times S_f \times h^{-1} \tag{I.20}$$

Employing the basic characteristic quantities and noting that $C_s = C_{so}C_s^*$, $T = T_oT^*$, $Q = Q_oQ^*$, and $S_f = S_oS_f^*$, Equation (I.20) can be changed to

$$C_s^* = e_3 V^* S_f^* = e_3 T^{*-1} Q^* S_f^* h^{*-1} \tag{I.21}$$

in which $e_3 = e_1 \times e_2 \frac{Q_oS_o}{C_{so}h_o}$ and $V^* = \frac{V}{V_o}$.

The derivatives of C_s in terms of Q and h are

$$\frac{\partial C_s}{\partial Q} = C_s\left[\frac{1}{S_f}\frac{\partial S_f}{\partial Q} + \frac{1}{Q}\right] \tag{I.22}$$

$$\frac{\partial C_s}{\partial h} = C_s\left[\frac{1}{S_f}\frac{\partial S_f}{\partial h} + \frac{1}{h}\right] \tag{I.23}$$

which can be transformed to the following non-dimensional forms by using the relevant basic quantities C_{so}, Q_o, etc.

$$\frac{\partial C_s^*}{\partial Q^*} = C_s^*\left[\frac{1}{S_f^*}\frac{\partial S_f^*}{\partial Q^*} + \frac{1}{Q^*}\right] \tag{I.24}$$

$$\frac{\partial C_s^*}{\partial h^*} = C_s^*\left[\frac{1}{S_f^*}\frac{\partial S_f^*}{\partial h^*} + \frac{1}{h^*}\right] \tag{I.25}$$

Equations (I.21), (I.24), and (I.25) can be used in the respective terms of Equations (2.5) and (2.6) to account for the direct influence of suspended sediment on the motion.

APPENDIX II

SYSTEM COEFFICIENTS AND AUXILIARY PARAMETERS

System Coefficients and Auxiliary Parameters

This is an appendix to Section 2.2.4 of the report describing the final system of discretised equations of COUPFLEX as expressed in Equation (2.9). All the coefficients contain known values at time level j, and all the unknowns are the changes in Q^* ,h^* and z^* from time $j.\Delta t^*$ to $(j+1).\Delta t^*$ at point $i\ \Delta x^*$ or $(i+1)\Delta x^*$. For simplicity, superscript j is dropped in the coefficients.

$$C_1 = Fr_o\frac{\theta}{\Delta x^*};\quad C_2 = -C_1;\quad C_3 = \overline{T}\frac{\phi}{\Delta t^*};\quad C_4 = \frac{1-\phi}{\phi}C_3;$$

$$C_5 = \overline{T}\frac{\phi}{\Delta t^*};\qquad C_6 = \frac{1-\phi}{\phi}C_5;\quad D_1 = Fr_o[\frac{\tilde{Q}}{\Delta x^*} - \tilde{q}_L];$$

$$C_{11} = Fr_o\frac{\phi}{\Delta t^*} + 2\theta Fr_o^2\{\frac{1}{\Delta x^*}[\overline{\beta}V_1 + \phi\tilde{Q}\times u_8] + \phi[V_2\frac{1}{\Delta x^*}\tilde{\beta} - u_4\times u_{13}]\}$$
$$+\varepsilon_o[\theta\phi\overline{A}(\frac{\partial S^*_f}{\partial Q^*})_{i+1}] + Fr_o^2[\theta\phi\tilde{q}_L\frac{1}{A^*_{i+1}}]$$
$$+Cs_o\alpha_1\alpha_s[\frac{\theta}{\Delta x^*}\overline{A}\times\overline{h}(\frac{\partial C^*_s}{\partial Q^*})_{i+1}];$$

$$C_{22} = Fr_o\frac{1-\phi}{\Delta t^*} + 2\theta Fr_o^2\{\frac{1}{\Delta x^*}[-\overline{\beta}V_1 + (1-\phi)\tilde{Q}\times u_7] + (1-\phi)[V_1\frac{1}{\Delta x^*}\tilde{\beta} - u_3\times u_{13}]\}$$
$$+\varepsilon_o[\theta(1-\phi)\overline{A}(\frac{\partial S^*_f}{\partial Q^*})_i] + Fr_o^2[\theta(1-\phi)\tilde{q}_L\frac{1}{A^*_i}]$$
$$+Cs_o\alpha_1\alpha_s[-\frac{\theta}{\Delta x^*}\overline{A}\times\overline{h}(\frac{\partial C^*_s}{\partial Q^*})_i];$$

$$C_{33} = \theta Fr_o^2\{2\phi[u_6\times u_{13} - u_2\frac{1}{\Delta x^*}\tilde{Q}] - \frac{1}{\Delta x^*}[\overline{\beta}_{v2}T_4 + \phi u_{10}\tilde{\beta}]\}$$
$$+\theta Fr_o^2[-\phi\tilde{q}_L u_{12}] + Cs_o\alpha_1\alpha_s\frac{\theta}{\Delta x^*}[\tilde{C}_s\phi(\overline{A} + T_{i+1}\overline{h}) + \overline{A}\times\overline{h}(\frac{\partial C^*_s}{\partial h^*})_{i+1}]$$
$$+\frac{\theta}{\Delta x^*}[\phi T_{i+1}\overline{h} + \overline{A}) + \theta\phi\varepsilon_o[T_{i+1}\overline{S}_f + \overline{A}(\frac{\partial S^*_f}{\partial h^*})_{i+1}] + \frac{\theta}{\Delta x^*}[\phi\tilde{z}T^*_{i+1}];$$

$$C_{44} = \theta Fr_o^2\{2(1-\phi)[u_5\times u_{13} - u_1\frac{1}{\Delta x^*}\tilde{Q}] - \frac{1}{\Delta x^*}[\overline{\beta}_{v2}T_3 + (1-\phi)u_9\tilde{\beta}]\}$$
$$+\theta Fr_o^2[-(1-\phi)\tilde{q}_L u_{11}] + Cs_o\alpha_1\alpha_s\frac{\theta}{\Delta x^*}[\tilde{C}_s(1-\phi)(\overline{A} + T^*_{i+1}\overline{h}) - \overline{A}\times\overline{h}(\frac{\partial C^*_s}{\partial h^*})_i]$$
$$+\frac{\theta}{\Delta x^*}[(1-\phi)T^*_i\overline{h} - \overline{A}) + \theta(1-\phi)\varepsilon_o[T^*_i\overline{S}_f + \overline{A}(\frac{\partial S^*_f}{\partial h^*})_i] + \frac{\theta}{\Delta x^*}[(1-\phi)\tilde{z}T^*_i];$$

$$C_{55} = \{\frac{\theta}{\Delta x^*}\overline{A} + \frac{\phi}{\Delta t^*}Fr_o\overline{V}\times\overline{T}\};\qquad C_{66} = \{-\frac{\theta}{\Delta x^*}\overline{A} + \frac{(1-\phi)}{\Delta t^*}Fr_o\overline{V}\times\overline{T}\};$$

$$D_{11} = Fr_o^2\{\frac{1}{\Delta x^*}[2\overline{\beta V_1}\tilde{Q} + \tilde{\beta}\overline{V_Q}] - \overline{\beta V_2}u_{13}\} + \frac{1}{\Delta x^*}\overline{A}[\tilde{h} + \tilde{z}]$$

$$+\varepsilon_o\overline{A} \times \overline{S_f} - Fr_o^2\tilde{q}_L[\tilde{V}_1 Cos[\alpha_L] - \overline{V}] + Cs_o\alpha_1\alpha_s\frac{1}{\Delta x^*}\overline{A} \times \overline{h} \times \overline{Cs}$$

$$C_{111} = C_o Fr_o\frac{\theta}{\Delta x^*}(\frac{\partial Q^*s}{\partial Q^*})_{i+1} + Cs_o\frac{\phi}{\Delta t^*}\overline{A}(\frac{\partial C^*s}{\partial Q^*})_{i+1}$$

$$C_{222} = -C_o Fr_o\frac{\theta}{\Delta x^*}(\frac{\partial Q^*s}{\partial Q^*})_i + Cs_o\frac{1-\phi}{\Delta t^*}\overline{A}(\frac{\partial C^*s}{\partial Q^*})_i$$

$$C333 = CoFro\frac{\theta}{\Delta x^*}(\frac{\partial Q^*s}{\partial h^*})_{i+1} + Cso\frac{\phi}{\Delta t^*}\left[\overline{T} \times \overline{Cs} + \overline{A}(\frac{\partial C^*s}{\partial h^*})_{i+1}\right]$$

$$C444 = -CoFro\frac{\theta}{\Delta x^*}(\frac{\partial Q^*s}{\partial h^*})_i + Cso\frac{1-\phi}{\Delta t^*}\left[\overline{T} \times \overline{Cs} + \overline{A}(\frac{\partial C^*s}{\partial h^*})_i\right]$$

$$C_{555} = (1-p)\frac{\phi}{\Delta t^*}\overline{T}; \quad C_{666} = \frac{1-\phi}{\phi}C_{555}; \quad D111 = CoFro\left[\frac{\tilde{Q}s}{\Delta x^*} - \tilde{q}_{Ls}\right]$$

It should be noted that α_S, defined previously, is close to s-1 for most practical cases because usually C_S<<1.

In defining the coefficients used in (2.9), the following auxiliary parameters were used to avoid cluttering the equations. They are all evaluated at the time level j , at which all variables are known.

$$\overline{T} = [\phi T^*_{i+1} + (1-\phi)T^*_i]; \quad \overline{A} = [\phi A^*_{i+1} + (1-\phi)A^*_i]; \quad \overline{h} = [\phi h^*_{i+1} + (1-\phi)h^*_i];$$

$$\overline{\beta V_1} = [\phi(\frac{\beta Q^*}{A^*})_{i+1} + (1-\phi)(\frac{\beta Q^*}{A^*})_i]; \quad \overline{\beta V_2} = [\phi(\frac{\beta Q^{*2}}{A^{*2}})_{i+1} + (1-\phi)(\frac{\beta Q^{*2}}{A^{*2}})_i];$$

$$V_1 = (\frac{Q^*}{A^*})_i; \; V_2 = (\frac{Q^*}{A^*})_{i+1}; \; \overline{V} = \phi V_2 + (1-\phi)V_1; \; \overline{S_f} = [\phi S_f{}^*_{i+1} + (1-\phi)S_f{}^*_i];$$

$$\overline{A_x} = [\phi A^h_{x\,i+1} + (1-\phi)A^h_{x\,i}]; \quad \overline{Cs} = [\phi Cs^*_{i+1} + (1-\phi)Cs^*_i];$$

$$\overline{V_Q} = \phi(\frac{Q^{*2}}{A^*})_{i+1} + (1-\phi)(\frac{Q^{*2}}{A^*})_i \; ; \; u_1 = (\frac{\beta Q^* T^*}{A^{*2}})_i \; ; \; u_2 = (\frac{\beta Q^* T^*}{A^{*2}})_{i+1} \; ;$$

$$u_3 = (\frac{\beta Q^*}{A^{*2}})_i \; ; \; u_4 = (\frac{\beta Q^*}{A^{*2}})_{i+1} \; ; \; u_5 = (\frac{\beta Q^{*2} T^*}{A^{*3}})_i \; ; \; u_6 = (\frac{\beta Q^{*2} T^*}{A^{*3}})_{i+1}$$

$$u_7 = (\frac{\beta}{A^*})_i \; ; \; u_8 = (\frac{\beta}{A^*})_{i+1} \; ; \; u_9 = (\frac{Q^{*2} T^*}{A^{*2}})_i \; ; \; u_{10} = (\frac{Q^{*2} T^*}{A^{*2}})_{i+1}$$

$$u_{11} = (\frac{Q^* T^*}{A^{*2}})_i \; ; \; u_{12} = (\frac{Q^* T^*}{A^{*2}})_{i+1} \; ; \; u_{13} = \overline{A_x} + \overline{T}\tilde{h}\frac{1}{\Delta x^*}$$

$$\tilde{Q} = Q^*_{i+1} - Q^*_i \; ; \; \tilde{h} = h^*_{i+1} - h^*_i \; ; \; \tilde{C}s = Cs^*_{i+1} - Cs^*_i \; ; \; \tilde{z} = z^*_{i+1} - z^*_i$$

$$\tilde{\beta} = \beta_{i+1} - \beta_i \; ; \; \tilde{Q}s = Qs^*_{i+1} - Qs^*_i \; ; \; T_1 = (\frac{dT^*}{dh^*})_i \; ; \; T_2 = (\frac{dT^*}{dh^*})_{i+1} \; ;$$

$$T_3 = [(1-\phi)\tilde{h}T_1 - \overline{T}] \; ; \; T_4 = [\phi\tilde{h}T_2 + \overline{T}] \; ;$$

$$\tilde{q}_L = q_{L_{i+1/2}} \; ; \; \tilde{q}_{Ls} = q_{Ls_{i+1/2}} \; ; \; \tilde{V}_L = V_{L_{i+1/2}}$$

where A_x^h=departure from a prismatic channel, or, derivative of A with respect to x when h is held constant ($\frac{\partial A}{\partial x} = T\frac{\partial h}{\partial x} + A_x^h$; A_x^h=0 for prismatic channels and is positive for channels expanding with x) and subscript i+1/2 shows the average value of the relevant variable in the section between nodes i and i+1.

APPENDIX III

SOME SCHEMES IN UNCOUPLED APPROACH

Some Schemes in Uncoupled Approach

This is an appendix to Section 2.2.4 of the report describing the discretisation of the equations of COUPFLEX.

A feature common to all uncoupled alluvial river models is separation of flow and bed level variations to different degrees. However, to discretise the equation of continuity for sediment, model developers have used different schemes. Let us consider the sediment continuity equation, Equation (2.3), in its simplest form, and assuming zero porosity. The equation for unit width of the channel is

$$\frac{\partial q_s}{\partial x} + \frac{\partial z}{\partial t} = 0 \qquad \text{(III.1)}$$

where q_s is the dimensional volumetric sediment flow rate per unit width. Uncoupled approaches may be classified into different classes based on the way this equation is discretised. In the following, several different discretisation schemes are briefly described.

Scheme 1.

The sediment continuity equation is fully discretised, like other equations in the coupled approach, but is solved separately from the flow equations. This is the uncoupled approach closest to the coupled approach. Starting from the upstream boundary, the third equation of (2.9) is solved for Δz_{i+1} using

$$\Delta z_{i+1} = -\frac{1}{C_{555}}\left[C_{111}\Delta Q_{i+1} + C_{222}\Delta Q_i + C_{333}\Delta h_{i+1} + C_{444}\Delta h_i + C_{666}\Delta z_i + D_{111}\right] \qquad \text{(III.2)}$$

This scheme differs from all the following schemes in that q_s is discretised using the third relation in Equation (2.8) and the weighting factors (θ and ϕ) used for sediment continuity equation are the same as those for the flow equations.

Scheme 2.

This scheme uses the following equation

$$\frac{\theta}{\Delta x}\left[q_{s\,i+1}^{\,j+1} - q_{s\,i}^{\,j+1}\right] + \frac{1-\theta}{\Delta x}\left[q_{s\,i+1}^{\,j} - q_{s\,i}^{\,j}\right] + \frac{1}{2\Delta t}\left[\Delta z_{i+1} + \Delta z_i\right] = 0 \qquad \text{(III.3)}$$

An example of this scheme has been used by Cunge and Perdreau (1973) among others. They employed Manning-Strickler's S_f, Meyer-Peter and Muller's (1948) Q_s, and the full dynamic equation of water flow and applied their model to an aggradation case in a hypothetical river.

Scheme 3

The equation

$$\frac{1}{2\Delta x}\left[qs^{j}_{i+1}+qs^{j+1}_{i+1}\right]-\frac{1}{2\Delta x}\left[qs^{j}_{i}+qs^{j+1}_{i}\right]+\frac{1}{\Delta t}\left[\Delta z_{i+1}\right]=0 \quad \text{(III.4)}$$

has been used by Chang (1982, pp. 680-681) to simulate bed changes in a reach of the San Diego River during the March 1978 flood. Chang employed Manning's S_f, Graf's (1971) Q_s, and the full dynamic equation of water flow.

Scheme 4

The equation of this scheme is

$$\frac{1}{\Delta x}\left[qs^{j}_{i+1}-qs^{j}_{i}\right]+\frac{1}{\Delta t}\left[\Delta z_{i+1}\right]=0 \quad \text{(III.5)}$$

Examples of application can be found in Michiue and Suzuki (1982, p.250) who used Manning's S_f, Ashida and Michiue's (1972) Q_s and a quasi-steady flow model to apply to a soil consolidation work study of Hii River, and in Gysel et al (1992) who used Manning's S_f, three empirical relations for Q_s and the full dynamic water flow model. Gysel et al applied their model to three examples quoted in Cunge et al (1980).

Scheme 5

$$\frac{1}{2\Delta x}\left[qs^{j}_{i+1}-qs^{j}_{i-1}\right]+\frac{1}{\Delta t}\left[z^{j+1}_{i}-\left\{(1-\alpha)z^{j}_{i}+\frac{\alpha}{2}\left[z^{j}_{i+1}+z^{j}_{i-1}\right]\right\}\right]=0 \quad \text{(III.6)}$$

This scheme has been introduced and described by Vries (1981, pp.36-39) and later has been used and assessed by many investigators. α is a damping factor for an otherwise unstable explicit scheme. If $\mu = c\frac{\Delta t}{\Delta x}$ and $\beta_o = \alpha - \mu$, the criteria for selection of α are $\mu^2 < \alpha < 1$ and $\beta_o = 0.001 - 0.05$, where c is the celerity of small bed disturbances (see pp.292-3 of Cunge et al. 1980). Examples of the application of this scheme can be found in Tingsanchali and Panvanich (1981, p.521) and Morse and Townsend (1990, p.1348), and others.

Scheme 6

This scheme adopts

$$\frac{1}{2\Delta x}\left[qs^{j}_{i+1}-qs^{j}_{i-1}\right]+\frac{1}{\Delta t}\left[\Delta z_{i}\right]=0 \quad \text{(III.7)}$$

Examples of its application have been presented by several investigators including Gessler (1971, pp.4-18) who employed a Chezy and Darcy-Weisbach type equation for S_f, Meyer-

Peter and Muller's (1948) Q_S and investigated aggradation and degradation of coarse sediment in a hypothetical flume, and by Thomas and Prasuhn (1977, p.855) who used Manning's S_f and a quasi-steady flow model. The latter verified their model using some laboratory and field data. This scheme has been used in different versions of the well-known HEC-6 sedimentation program (see Thomas 1982).

Scheme 7

The equation for this scheme is

$$\frac{1}{\Delta x}\left[{q_s}_{i+1}^{j+1} - {q_s}_{i}^{j+1}\right] + \frac{1}{\Delta t}[\Delta z_i] = 0 \qquad \text{(III.8)}$$

This scheme has been used, for example, by Hosseinipour (1989, p.478) who employed Yang's (1973) Q_S, Manning's S_f and the full dynamic equation for water.

These schemes, all used in uncoupled approaches, may be unsuccessful when modelling rapid river changes, or if successful, may be limited in selection of the magnitude of Δt because of the explicit nature of the solution.

APPENDIX IV

HYDROGRAPHS OF THE EXPERIMENTAL TESTS

Hydrographs of the Experimental Tests

This appendix refers to Section 4.1 and provides a quick comparison of the input flow hydrographs of the experimental tests.

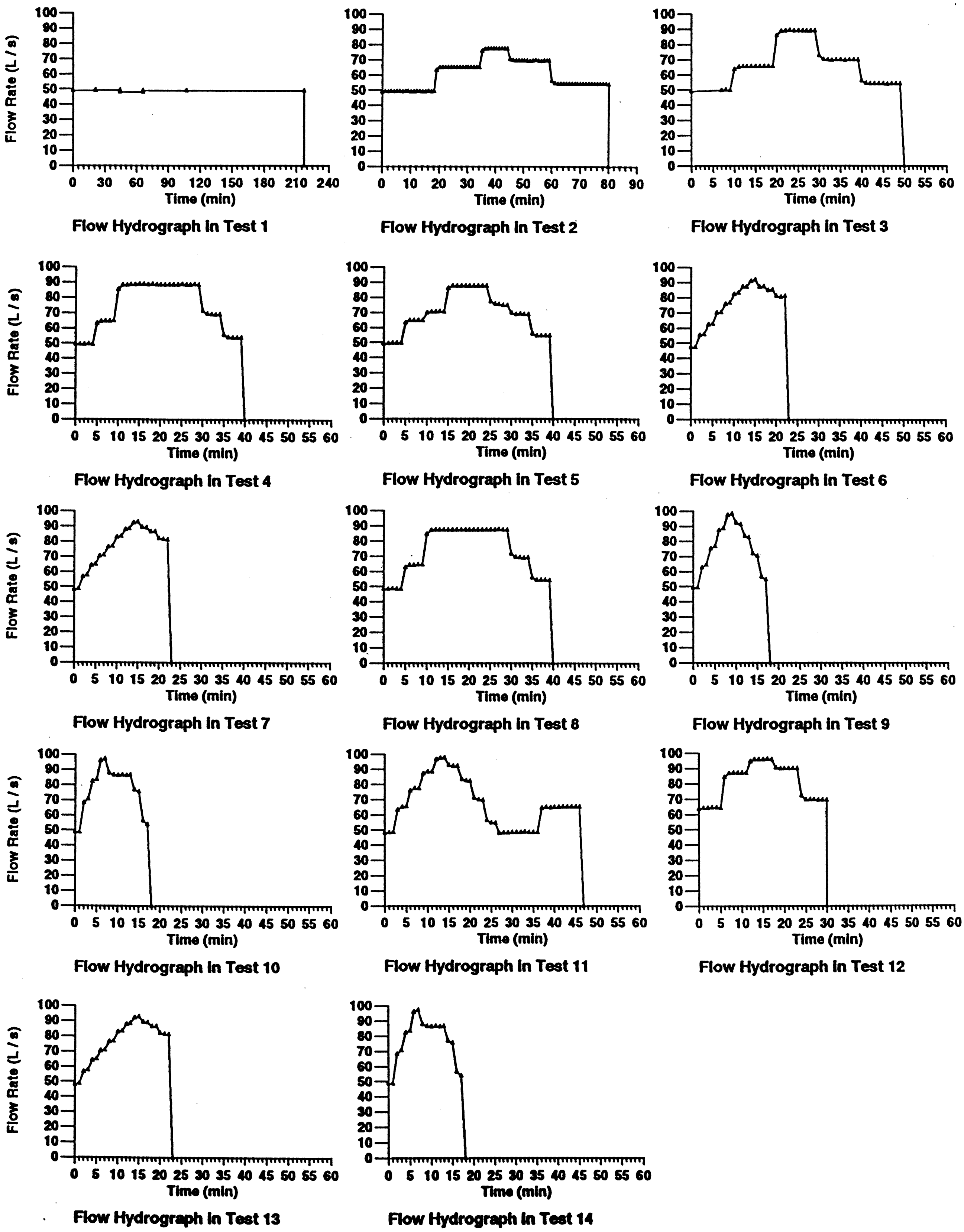

Fig. IV.1. Comparison of Flow Hydrographs in All Tests

APPENDIX V

SAMPLE COMPUTER INPUT AND OUTPUT FILES

Sample Computer Input and Output Files

This appendix gives some sample computer files for the simulation of the tests using HEC6 program. The first and second input and output files belong to the simulation of Test 2 using Δt=1 min and Test 14 using Δt=2 min, respectively.

Input File for the Simulation of Test 2
Time Step = 1 min

```
T1        saied: Test 2
T2        base flow (assume T=328 ft),q=8.03m3/s=(49 lit/s for 0.61 m)=284 cfs,
T3       slope=0.005,n=0.013, D/S BC water=variable
NC   .013   .013    .013
X1    0.0      4       20.    348.      0.       0.       0.
GR   128.     20.      0.     20.     0.      348.   128.     348.
HD    0.0     0.193
X1    1.0      0.      20.    348.    3.28     3.28     3.28     0.   0.0164
HD    1.0     0.193
X1    2.0      0.      20.    348.    3.28     3.28     3.28     0.   0.0164
HD    2.0     0.193
X1    3.0      0.      20.    348.    3.28     3.28     3.28     0.   0.0164
HD    3.0     0.193
X1    4.0      0.      20.    348.    3.28     3.28     3.28     0.   0.0164
HD    4.0     0.193
X1    5.0      0.      20.    348.    3.28     3.28     3.28     0.   0.0164
HD    5.0     0.193
X1    6.0      0.      20.    348.    3.28     3.28     3.28     0.   0.0164
HD    6.0     0.193
X1    7.0      0.      20.    348.    3.28     3.28     3.28     0.   0.0164
HD    7.0     0.193
X1    8.0      0.      20.    348.    3.28     3.28     3.28     0.   0.0164
HD    8.0     0.193
X1    9.0      0.      20.    348.    3.28     3.28     3.28     0.   0.0164
HD    9.0     0.193
X1    10.0     0.      20.    348.    3.28     3.28     3.28     0.   0.0164
HD    10.0    0.193
X1    11.0     0.      20.    348.    3.28     3.28     3.28     0.   0.0164
HD    11.0    0.193
X1    12.0     0.      20.    348.    3.28     3.28     3.28     0.   0.0164
HD    12.0    0.193
X1    13.0     0.      20.    348.    3.28     3.28     3.28     0.   0.0164
HD    13.0    0.193
X1    14.0     0.      20.    348.    3.28     3.28     3.28     0.   0.0164
HD    14.0    0.193
X1    15.0     0.      20.    348.    3.28     3.28     3.28     0.   0.0164
HD    15.0    0.193
X1    16.0     0.      20.    348.    3.28     3.28     3.28     0.   0.0164
HD    16.0    0.193
X1    17.0     0.      20.    348.    3.28     3.28     3.28     0.   0.0164
HD    17.0    0.193
X1    18.0     0.      20.    348.    3.28     3.28     3.28     0.   0.0164
HD    18.0    0.193
EJ
T4   all sediment info between EJ and $HYD
T5   U/S BC for sediment Qs=constant=0    t/day
T6   SEDIMENT TRANSPORT : user-specified
T7   D50=2.0    mm
T8   D/S BC for sediment free escape ?!
I1             1
I4   sand      2       6       6       2.6      0.7      0.5      30       102
J          0.006     1.35    18e-5
K           75e6      0.
LQ             1     532
LT total     0.0       0.0
```

```
LF   VFG     1.0     1.0
PF EXAMP     0.0      1.0      8.0      2.1    100.0      2.0      0.0
$HYD
*    AB   PROFILE 1 = 1st segment of the hydrograph
Q  284
R   0.730
T  43
X                   0.0140      20.
*    AB   PROFILE 2 = 2nd segment of the hydrograph
Q  376
R   0.750
T  43
X                   0.0104      15.
*    AB   PROFILE 3 = 3rd segment of the hydrograph
Q  446
R   0.800
T  43
X                   0.0070      10.
*    AB   PROFILE 4 = 4th segment of the hydrograph
Q  400
R   0.767
T  43
X                   0.0140      20.
*    AB   PROFILE 5 = 5th segment of the hydrograph
Q  313
R   0.707
T  43
X                   0.0140      20.
$$END
```

A Summary of the Output File for the Simulation
of Test 2 by HEC6,Time Step = 1 min

TABLE SB-2: STATUS OF THE BED PROFILE AT TIME = 0.014 DAYS

SECTION NUMBER	BED CHANGE (ft)	WS ELEV (ft)	THALWEG (ft)	Q (cfs)	TRANSPORT RATE (tons/day) SAND
18.000	-0.06	0.73	0.24	284.	89.
17.000	-0.02	0.72	0.26	284.	141.
16.000	-0.01	0.72	0.26	284.	177.
15.000	0.01	0.72	0.25	284.	181.
14.000	0.01	0.72	0.24	284.	153.
13.000	0.01	0.72	0.22	284.	118.
12.000	0.01	0.72	0.20	284.	85.
11.000	0.01	0.72	0.19	284.	58.
10.000	0.00	0.72	0.17	284.	37.
9.000	0.00	0.72	0.15	284.	21.
8.000	0.00	0.72	0.13	284.	8.
7.000	0.00	0.73	0.12	284.	1.
6.000	0.00	0.73	0.10	284.	0.
5.000	0.00	0.73	0.08	284.	0.
4.000	0.00	0.73	0.07	284.	0.
3.000	0.00	0.73	0.05	284.	0.
2.000	0.00	0.73	0.03	284.	0.
1.000	0.00	0.73	0.02	284.	0.
0.000	0.00	0.73	0.00	284.	0.

TIME STEP # 2
* AB PROFILE 2 = 2nd segment of the hydrograph
COMPUTING FROM TIME= 0.0140 DAYS TO TIME= 0.0244 DAYS IN 15 COMPUTATION STEPS

TABLE SB-1: SEDIMENT LOAD PASSING THE BOUNDARIES OF STREAM SEGMENT # 1

SEDIMENT INFLOW at the Upstream Boundary:

GRAIN SIZE	LOAD (tons/day)	GRAIN SIZE	LOAD (tons/day)
VERY FINE GRAVEL..	0.00		
		TOTAL =	0.00

SEDIMENT OUTFLOW from the Downstream Boundary

GRAIN SIZE	LOAD (tons/day)	GRAIN SIZE	LOAD (tons/day)
VERY FINE GRAVEL..	10.26		
		TOTAL =	10.26

TABLE SB-2: STATUS OF THE BED PROFILE AT TIME = 0.024 DAYS

SECTION NUMBER	BED CHANGE (ft)	WS ELEV (ft)	THALWEG (ft)	Q (cfs)	TRANSPORT RATE (tons/day) SAND
18.000	-0.14	0.77	0.16	376.	155.
17.000	-0.04	0.74	0.24	376.	255.
16.000	-0.03	0.74	0.23	376.	386.
15.000	-0.01	0.73	0.24	376.	456.

14.000	0.01	0.73	0.24	376.	497.
13.000	0.02	0.73	0.23	376.	494.
12.000	0.02	0.73	0.22	376.	434.
11.000	0.02	0.73	0.20	376.	357.
10.000	0.02	0.73	0.18	376.	285.
9.000	0.01	0.74	0.16	376.	225.
8.000	0.01	0.74	0.14	376.	177.
7.000	0.01	0.74	0.12	376.	138.
6.000	0.01	0.74	0.10	376.	106.
5.000	0.00	0.74	0.09	376.	81.
4.000	0.00	0.75	0.07	376.	61.
3.000	0.00	0.75	0.05	376.	44.
2.000	0.00	0.75	0.04	376.	30.
1.000	0.00	0.75	0.02	376.	19.
0.000	0.00	0.75	0.00	376.	10.

==

TIME STEP # 3
* AB PROFILE 3 = 3rd segment of the hydrograph
COMPUTING FROM TIME= 0.0244 DAYS TO TIME= 0.0314 DAYS IN 10 COMPUTATION STEPS

TABLE SB-1: SEDIMENT LOAD PASSING THE BOUNDARIES OF STREAM SEGMENT # 1

SEDIMENT INFLOW at the Upstream Boundary:

GRAIN SIZE	LOAD (tons/day)	GRAIN SIZE	LOAD (tons/day)
VERY FINE GRAVEL..	0.00		
		TOTAL =	0.00

SEDIMENT OUTFLOW from the Downstream Boundary

GRAIN SIZE	LOAD (tons/day)	GRAIN SIZE	LOAD (tons/day)
VERY FINE GRAVEL..	53.07		
		TOTAL =	53.07

TABLE SB-2: STATUS OF THE BED PROFILE AT TIME = 0.031 DAYS

SECTION NUMBER	BED CHANGE (ft)	WS ELEV (ft)	THALWEG (ft)	Q (cfs)	TRANSPORT RATE (tons/day) SAND
18.000	-0.18	0.83	0.11	446.	91.
17.000	-0.06	0.80	0.22	446.	222.
16.000	-0.05	0.80	0.21	446.	385.
15.000	-0.02	0.78	0.23	446.	477.
14.000	0.00	0.78	0.23	446.	553.
13.000	0.02	0.78	0.23	446.	590.
12.000	0.03	0.77	0.22	446.	595.
11.000	0.03	0.77	0.21	446.	535.
10.000	0.03	0.78	0.19	446.	453.
9.000	0.02	0.78	0.17	446.	368.
8.000	0.02	0.79	0.15	446.	298.
7.000	0.02	0.79	0.13	446.	241.
6.000	0.01	0.79	0.11	446.	195.
5.000	0.01	0.79	0.09	446.	158.
4.000	0.01	0.80	0.07	446.	129.
3.000	0.01	0.80	0.06	446.	104.
2.000	0.01	0.80	0.04	446.	83.
1.000	0.00	0.80	0.02	446.	67.
0.000	0.01	0.80	0.01	446.	53.

==

TIME STEP # 4
* AB PROFILE 4 = 4th segment of the hydrograph
COMPUTING FROM TIME= 0.0314 DAYS TO TIME= 0.0454 DAYS IN 20 COMPUTATION STEPS

TABLE SB-1: SEDIMENT LOAD PASSING THE BOUNDARIES OF STREAM SEGMENT # 1

SEDIMENT INFLOW at the Upstream Boundary:

GRAIN SIZE	LOAD (tons/day)	GRAIN SIZE	LOAD (tons/day)
VERY FINE GRAVEL..	0.00		
		TOTAL =	0.00

SEDIMENT OUTFLOW from the Downstream Boundary

GRAIN SIZE	LOAD (tons/day)	GRAIN SIZE	LOAD (tons/day)
VERY FINE GRAVEL..	33.09		
		TOTAL =	33.09

TABLE SB-2: STATUS OF THE BED PROFILE AT TIME = 0.045 DAYS

SECTION NUMBER	BED CHANGE (ft)	WS ELEV (ft)	THALWEG (ft)	Q (cfs)	TRANSPORT RATE (tons/day) SAND
18.000	-0.19	0.79	0.11	400.	2.
17.000	-0.09	0.77	0.19	400.	109.
16.000	-0.09	0.77	0.18	400.	224.
15.000	-0.04	0.76	0.21	400.	295.
14.000	-0.02	0.75	0.21	400.	373.
13.000	0.00	0.75	0.22	400.	424.
12.000	0.02	0.74	0.22	400.	464.
11.000	0.03	0.74	0.21	400.	479.
10.000	0.04	0.74	0.21	400.	458.
9.000	0.04	0.74	0.19	400.	390.
8.000	0.04	0.74	0.17	400.	312.
7.000	0.03	0.75	0.15	400.	239.
6.000	0.02	0.75	0.12	400.	182.
5.000	0.02	0.75	0.10	400.	138.
4.000	0.01	0.76	0.08	400.	105.
3.000	0.01	0.76	0.06	400.	80.
2.000	0.01	0.76	0.04	400.	59.
1.000	0.01	0.76	0.02	400.	44.
0.000	0.01	0.76	0.01	400.	33.

TIME STEP # 5
* AB PROFILE 5 = 5th segment of the hydrograph
COMPUTING FROM TIME= 0.0454 DAYS TO TIME= 0.0594 DAYS IN 20 COMPUTATION STEPS

TABLE SB-1: SEDIMENT LOAD PASSING THE BOUNDARIES OF STREAM SEGMENT # 1

SEDIMENT INFLOW at the Upstream Boundary:

GRAIN SIZE	LOAD (tons/day)	GRAIN SIZE	LOAD (tons/day)
VERY FINE GRAVEL..	0.00		
		TOTAL =	0.00

SEDIMENT OUTFLOW from the Downstream Boundary

GRAIN SIZE	LOAD (tons/day)	GRAIN SIZE	LOAD (tons/day)
VERY FINE GRAVEL..	0.00		
		TOTAL =	0.00

TABLE SB-2: STATUS OF THE BED PROFILE AT TIME = 0.059 DAYS

SECTION NUMBER	BED CHANGE (ft)	WS ELEV (ft)	THALWEG (ft)	Q (cfs)	TRANSPORT RATE (tons/day) SAND
18.000	-0.19	0.73	0.11	313.	0.
17.000	-0.10	0.71	0.18	313.	40.
16.000	-0.10	0.71	0.16	313.	95.
15.000	-0.05	0.70	0.20	313.	130.
14.000	-0.03	0.70	0.20	313.	177.
13.000	0.00	0.69	0.21	313.	209.
12.000	0.01	0.69	0.21	313.	240.
11.000	0.03	0.69	0.21	313.	258.
10.000	0.04	0.68	0.21	313.	266.
9.000	0.05	0.68	0.20	313.	241.
8.000	0.05	0.68	0.18	313.	195.
7.000	0.05	0.69	0.16	313.	137.
6.000	0.03	0.69	0.13	313.	89.
5.000	0.03	0.69	0.11	313.	54.
4.000	0.02	0.70	0.09	313.	30.
3.000	0.02	0.70	0.07	313.	14.
2.000	0.01	0.70	0.05	313.	4.
1.000	0.01	0.70	0.03	313.	0.
0.000	0.01	0.70	0.01	313.	0.

$$END

0 DATA ERRORS DETECTED.

TOTAL NO. OF TIME STEPS READ = 5
TOTAL NO. OF WS PROFILES = 85
ITERATIONS IN EXNER EQ = 1615

COMPUTATIONS COMPLETED
RUN TIME = 0 HOURS, 0 MINUTES & 37.00 SECONDS

```
----------------------------------------
Input File for the Simulation of Test 14
          Time Step = 2 min
----------------------------------------
```

```
T1       saied: Test 14
T2       base flow (assume T=328 ft),
T3      slope=0.005,n=0.013, D/S BC water=variable
NC  .013   .013    .013
X1   0.0      4      20.    348.     0.      0.      0.
GR  128.     20.     0.     20.     0.     348.  128.     348.
HD   0.0    0.223
X1   1.0     0.      20.    348.   3.28    3.28    3.28    0.   0.0164
HD   1.0    0.223
X1   2.0     0.      20.    348.   3.28    3.28    3.28    0.   0.0164
HD   2.0    0.223
X1   3.0     0.      20.    348.   3.28    3.28    3.28    0.   0.0164
HD   3.0    0.223
X1   4.0     0.      20.    348.   3.28    3.28    3.28    0.   0.0164
HD   4.0    0.223
X1   5.0     0.      20.    348.   3.28    3.28    3.28    0.   0.0164
HD   5.0    0.223
X1   6.0     0.      20.    348.   3.28    3.28    3.28    0.   0.0164
HD   6.0    0.223
X1   7.0     0.      20.    348.   3.28    3.28    3.28    0.   0.0164
HD   7.0    0.223
X1   8.0     0.      20.    348.   3.28    3.28    3.28    0.   0.0164
HD   8.0    0.223
X1   9.0     0.      20.    348.   3.28    3.28    3.28    0.   0.0164
HD   9.0    0.223
X1   10.0    0.      20.    348.   3.28    3.28    3.28    0.   0.0164
HD   10.0   0.223
X1   11.0    0.      20.    348.   3.28    3.28    3.28    0.   0.0164
HD   11.0   0.223
X1   12.0    0.      20.    348.   3.28    3.28    3.28    0.   0.0164
HD   12.0   0.223
X1   13.0    0.      20.    348.   3.28    3.28    3.28    0.   0.0164
HD   13.0   0.223
X1   14.0    0.      20.    348.   3.28    3.28    3.28    0.   0.0164
HD   14.0   0.223
X1   15.0    0.      20.    348.   3.28    3.28    3.28    0.   0.0164
HD   15.0   0.223
X1   16.0    0.      20.    348.   3.28    3.28    3.28    0.   0.0164
HD   16.0   0.223
X1   17.0    0.      20.    348.   3.28    3.28    3.28    0.   0.0164
HD   17.0   0.223
X1   18.0    0.      20.    348.   3.28    3.28    3.28    0.   0.0164
HD   18.0   0.223
EJ
T4  all sediment info between EJ and $HYD
T5  U/P BC for sediment Qs=constant=0   t/day
T6  SEDIMENT TRANSPORT : user-specified
T7  D50=2.0   mm
T8  D/S BC for sediment free escape ?!
I1          1
I4  sand    2      6      6      2.6     0.7     0.5     30     102
J        0.006    1.35   18e-5
K         75e6     0.
```

```
LQ            200   566
LT total     1600  1600
LF    VFG     1.0   1.0
PF EXAMP      0.0     1.0      8.0      2.1   100.0       2.0       0.0
$HYD
*   AB  PROFILE 1 = 1st segment of the hydrograph
Q  278
R   0.663
T  43
X                  0.0014       1.
*   AB  PROFILE 2 = 2nd segment of the hydrograph
Q  400
R   0.722
T  43
X                  0.0014       1.
*   AB  PROFILE 3 = 3rd segment of the hydrograph
Q  479
R   0.794
T  43
X                  0.0014       1.
*   AB  PROFILE 4 = 4th segment of the hydrograph
Q  559
R   0.843
T  43
X                  0.0014       1.
*   AB  PROFILE 5 = 5th segment of the hydrograph
Q  501
R   0.813
T  43
X                  0.0042       3
*   AB  PROFILE 6 = 6th segment of the hydrograph
Q  442
R   0.761
T  43
X                  0.0014       1.
*   AB  PROFILE 7 = 7th segment of the hydrograph
Q  318
R   0.682
T  43
X                  0.0014       1.
$$END
```

A Summary of the Output File for the Simulation of Test 14 by HEC6,Time Step = 2 min

TABLE SB-2: STATUS OF THE BED PROFILE AT TIME = 0.001 DAYS

SECTION NUMBER	BED CHANGE (ft)	WS ELEV (ft)	THALWEG (ft)	Q (cfs)	TRANSPORT RATE (tons/day) SAND
18.000	0.05	0.63	0.34	278.	678.
17.000	0.00	0.64	0.28	278.	641.
16.000	0.00	0.64	0.27	278.	508.
15.000	0.00	0.64	0.25	278.	402.
14.000	0.00	0.64	0.23	278.	318.
13.000	0.00	0.65	0.21	278.	250.
12.000	0.00	0.65	0.20	278.	195.
11.000	0.00	0.65	0.18	278.	150.
10.000	0.00	0.65	0.16	278.	113.
9.000	0.00	0.65	0.15	278.	83.
8.000	0.00	0.65	0.13	278.	58.
7.000	0.00	0.65	0.12	278.	38.
6.000	0.00	0.66	0.10	278.	23.
5.000	0.00	0.66	0.08	278.	11.
4.000	0.00	0.66	0.07	278.	2.
3.000	0.00	0.66	0.05	278.	0.
2.000	0.00	0.66	0.03	278.	0.
1.000	0.00	0.66	0.02	278.	0.
0.000	0.00	0.66	0.00	278.	0.

TIME STEP # 2
* AB PROFILE 2 = 2nd segment of the hydrograph
COMPUTING FROM TIME= 0.0014 DAYS TO TIME= 0.0028 DAYS IN 1 COMPUTATION STEPS

TABLE SB-1: SEDIMENT LOAD PASSING THE BOUNDARIES OF STREAM SEGMENT # 1

SEDIMENT INFLOW at the Upstream Boundary:

GRAIN SIZE	LOAD (tons/day)	GRAIN SIZE	LOAD (tons/day)
VERY FINE GRAVEL..	1600.00		
		TOTAL =	1600.00

SEDIMENT OUTFLOW from the Downstream Boundary

GRAIN SIZE	LOAD (tons/day)	GRAIN SIZE	LOAD (tons/day)
VERY FINE GRAVEL..	54.65		
		TOTAL =	54.65

TABLE SB-2: STATUS OF THE BED PROFILE AT TIME = 0.003 DAYS

SECTION NUMBER	BED CHANGE (ft)	WS ELEV (ft)	THALWEG (ft)	Q (cfs)	TRANSPORT RATE (tons/day) SAND
18.000	-0.01	0.65	0.29	400.	2711.
17.000	0.00	0.60	0.28	400.	2836.
16.000	0.01	0.66	0.27	400.	2491.
15.000	0.02	0.67	0.27	400.	1705.
14.000	0.01	0.68	0.24	400.	1414.

13.000	0.01	0.68	0.22	400.	1181.
12.000	0.01	0.68	0.20	400.	993.
11.000	0.01	0.69	0.19	400.	838.
10.000	0.00	0.69	0.17	400.	710.
9.000	0.00	0.69	0.15	400.	602.
8.000	0.00	0.70	0.13	400.	512.
7.000	0.00	0.70	0.12	400.	434.
6.000	0.00	0.70	0.10	400.	368.
5.000	0.00	0.70	0.08	400.	312.
4.000	0.00	0.71	0.07	400.	263.
3.000	0.00	0.71	0.05	400.	221.
2.000	0.00	0.71	0.03	400.	160.
1.000	0.00	0.72	0.02	400.	106.
0.000	0.00	0.72	0.00	400.	55.

==

TIME STEP # 3
* AB PROFILE 3 = 3rd segment of the hydrograph
COMPUTING FROM TIME= 0.0028 DAYS TO TIME= 0.0042 DAYS IN 1 COMPUTATION STEPS

TABLE SB-1: SEDIMENT LOAD PASSING THE BOUNDARIES OF STREAM SEGMENT # 1

SEDIMENT INFLOW at the Upstream Boundary:

GRAIN SIZE	LOAD (tons/day)	GRAIN SIZE	LOAD (tons/day)
VERY FINE GRAVEL..	1600.00		
		TOTAL =	1600.00

SEDIMENT OUTFLOW from the Downstream Boundary

GRAIN SIZE	LOAD (tons/day)	GRAIN SIZE	LOAD (tons/day)
VERY FINE GRAVEL..	104.63		
		TOTAL =	104.63

TABLE SB-2: STATUS OF THE BED PROFILE AT TIME = 0.004 DAYS

SECTION NUMBER	BED CHANGE (ft)	WS ELEV (ft)	THALWEG (ft)	Q (cfs)	TRANSPORT RATE (tons/day) SAND
18.000	-0.06	0.69	0.23	479.	2631.
17.000	-0.03	0.70	0.25	479.	3578.
16.000	0.00	0.63	0.27	479.	3941.
15.000	0.03	0.64	0.28	479.	3565.
14.000	0.04	0.71	0.26	479.	2565.
13.000	0.03	0.72	0.24	479.	1702.
12.000	0.02	0.73	0.21	479.	1279.
11.000	0.01	0.76	0.19	479.	975.
10.000	0.01	0.76	0.17	479.	722.
9.000	0.01	0.77	0.15	479.	607.
8.000	0.01	0.77	0.14	479.	513.
7.000	0.00	0.77	0.12	479.	435.
6.000	0.00	0.78	0.10	479.	369.
5.000	0.00	0.78	0.09	479.	314.
4.000	0.00	0.78	0.07	479.	267.
3.000	0.00	0.78	0.05	479.	227.
2.000	0.00	0.78	0.04	479.	190.
1.000	0.00	0.79	0.02	479.	149.
0.000	0.00	0.79	0.00	479.	105.

==

TIME STEP # 4
* AB PROFILE 4 = 4th segment of the hydrograph
COMPUTING FROM TIME= 0.0042 DAYS TO TIME= 0.0056 DAYS IN 1 COMPUTATION STEPS

TABLE SB-1: SEDIMENT LOAD PASSING THE BOUNDARIES OF STREAM SEGMENT # 1

SEDIMENT INFLOW at the Upstream Boundary:

GRAIN SIZE	LOAD (tons/day)	GRAIN SIZE	LOAD (tons/day)
VERY FINE GRAVEL..	1600.00		
		TOTAL =	1600.00

SEDIMENT OUTFLOW from the Downstream Boundary

GRAIN SIZE	LOAD (tons/day)	GRAIN SIZE	LOAD (tons/day)
VERY FINE GRAVEL..	182.11		
		TOTAL =	182.11

TABLE SB-2: STATUS OF THE BED PROFILE AT TIME = 0.006 DAYS

SECTION NUMBER	BED CHANGE (ft)	WS ELEV (ft)	THALWEG (ft)	Q (cfs)	TRANSPORT RATE (tons/day) SAND
18.000	-0.03	0.89	0.26	559.	1029.
17.000	-0.03	0.85	0.24	559.	1356.
16.000	-0.02	0.73	0.24	559.	2192.
15.000	0.01	0.70	0.26	559.	3008.
14.000	0.03	0.73	0.26	559.	3062.
13.000	0.05	0.75	0.26	559.	2336.
12.000	0.03	0.77	0.23	559.	1764.
11.000	0.02	0.79	0.20	559.	1363.
10.000	0.02	0.80	0.18	559.	1080.
9.000	0.01	0.81	0.16	559.	918.
8.000	0.01	0.81	0.14	559.	787.
7.000	0.01	0.81	0.12	559.	683.
6.000	0.01	0.82	0.10	559.	596.
5.000	0.01	0.82	0.09	559.	521.
4.000	0.00	0.82	0.07	559.	456.
3.000	0.00	0.83	0.05	559.	400.
2.000	0.00	0.83	0.04	559.	351.
1.000	0.00	0.83	0.02	559.	273.
0.000	0.01	0.84	0.01	559.	182.

TIME STEP # 5
* AB PROFILE 5 = 5th segment of the hydrograph
COMPUTING FROM TIME= 0.0056 DAYS TO TIME= 0.0098 DAYS IN 3 COMPUTATION STEPS

TABLE SB-1: SEDIMENT LOAD PASSING THE BOUNDARIES OF STREAM SEGMENT # 1

SEDIMENT INFLOW at the Upstream Boundary:

GRAIN SIZE	LOAD (tons/day)	GRAIN SIZE	LOAD (tons/day)
VERY FINE GRAVEL..	1600.00		
		TOTAL =	1600.00

SEDIMENT OUTFLOW from the Downstream Boundary

GRAIN SIZE	LOAD (tons/day)	GRAIN SIZE	LOAD (tons/day)
VERY FINE GRAVEL..	126.36		
		TOTAL =	126.36

TABLE SB-2: STATUS OF THE BED PROFILE AT TIME = 0.010 DAYS

SECTION NUMBER	BED CHANGE (ft)	WS ELEV (ft)	THALWEG (ft)	Q (cfs)	TRANSPORT RATE (tons/day) SAND
18.000	0.08	0.74	0.38	501.	1016.
17.000	-0.04	0.81	0.23	501.	1135.
16.000	-0.02	0.80	0.24	501.	976.
15.000	-0.01	0.78	0.24	501.	1100.
14.000	0.02	0.76	0.25	501.	1325.
13.000	0.06	0.74	0.27	501.	1391.
12.000	0.05	0.76	0.25	501.	1269.
11.000	0.05	0.77	0.23	501.	913.
10.000	0.03	0.78	0.20	501.	693.
9.000	0.02	0.79	0.17	501.	547.
8.000	0.02	0.79	0.15	501.	445.
7.000	0.01	0.80	0.13	501.	375.
6.000	0.01	0.80	0.11	501.	318.
5.000	0.01	0.80	0.09	501.	270.
4.000	0.01	0.80	0.07	501.	230.
3.000	0.01	0.81	0.06	501.	196.
2.000	0.01	0.81	0.04	501.	167.
1.000	0.01	0.81	0.02	501.	144.
0.000	0.01	0.81	0.01	501.	126.

TIME STEP # 6
* AB PROFILE 6 = 6th segment of the hydrograph
COMPUTING FROM TIME= 0.0098 DAYS TO TIME= 0.0112 DAYS IN 1 COMPUTATION STEPS

TABLE SB-1: SEDIMENT LOAD PASSING THE BOUNDARIES OF STREAM SEGMENT # 1

SEDIMENT INFLOW at the Upstream Boundary:

GRAIN SIZE	LOAD (tons/day)	GRAIN SIZE	LOAD (tons/day)
VERY FINE GRAVEL..	1600.00		
		TOTAL =	1600.00

SEDIMENT OUTFLOW from the Downstream Boundary

GRAIN SIZE	LOAD (tons/day)	GRAIN SIZE	LOAD (tons/day)
VERY FINE GRAVEL..	77.61		
		TOTAL =	77.61

TABLE SB-2: STATUS OF THE BED PROFILE AT TIME = 0.011 DAYS

SECTION NUMBER	BED CHANGE (ft)	WS ELEV (ft)	THALWEG (ft)	Q (cfs)	TRANSPORT RATE (tons/day) SAND
18.000	-0.22	0.83	0.08	442.	7527.
17.000	-0.11	0.77	0.17	442.	10256.
16.000	0.22	0.76	0.49	442.	555.
15.000	-0.01	0.75	0.24	442.	619.
14.000	0.01	0.73	0.24	442.	768.
13.000	0.05	0.71	0.27	442.	849.
12.000	0.05	0.73	0.25	442.	857.
11.000	0.05	0.73	0.23	442.	613.
10.000	0.04	0.74	0.20	442.	451.

9.000	0.02	0.75	0.17	442.	333.
8.000	0.02	0.75	0.15	442.	256.
7.000	0.01	0.76	0.13	442.	207.
6.000	0.01	0.76	0.11	442.	167.
5.000	0.01	0.76	0.09	442.	135.
4.000	0.01	0.76	0.07	442.	109.
3.000	0.01	0.76	0.06	442.	87.
2.000	0.01	0.76	0.04	442.	68.
1.000	0.01	0.77	0.02	442.	69.
0.000	0.01	0.76	0.01	442.	78.

==

TIME STEP # 7

* AB PROFILE 7 = 7th segment of the hydrograph

COMPUTING FROM TIME= 0.0112 DAYS TO TIME= 0.0126 DAYS IN 1 COMPUTATION STEPS

TABLE SB-1: SEDIMENT LOAD PASSING THE BOUNDARIES OF STREAM SEGMENT # 1

SEDIMENT INFLOW at the Upstream Boundary:

GRAIN SIZE	LOAD (tons/day)	GRAIN SIZE	LOAD (tons/day)
VERY FINE GRAVEL..	1600.00		
		TOTAL =	1600.00

SEDIMENT OUTFLOW from the Downstream Boundary

GRAIN SIZE	LOAD (tons/day)	GRAIN SIZE	LOAD (tons/day)
VERY FINE GRAVEL..	0.98		
		TOTAL =	0.98

TABLE SB-2: STATUS OF THE BED PROFILE AT TIME = 0.013 DAYS

SECTION NUMBER	BED CHANGE (ft)	WS ELEV (ft)	THALWEG (ft)	Q (cfs)	TRANSPORT RATE (tons/day) SAND
18.000	-0.14	0.94	0.16	318.	0.
17.000	-0.11	0.93	0.16	318.	33.
16.000	-0.22	0.85	0.04	318.	17382.
15.000	-0.04	0.67	0.21	318.	18483.
14.000	0.48	0.67	0.71	318.	399.
13.000	0.05	0.66	0.27	318.	428.
12.000	0.05	0.65	0.25	318.	435.
11.000	0.06	0.66	0.24	318.	375.
10.000	0.04	0.66	0.20	318.	267.
9.000	0.03	0.67	0.17	318.	175.
8.000	0.02	0.67	0.15	318.	118.
7.000	0.01	0.68	0.13	318.	84.
6.000	0.01	0.68	0.11	318.	58.
5.000	0.01	0.68	0.09	318.	38.
4.000	0.01	0.68	0.07	318.	23.
3.000	0.01	0.68	0.06	318.	11.
2.000	0.01	0.68	0.04	318.	3.
1.000	0.01	0.68	0.02	318.	1.
0.000	0.01	0.68	0.01	318.	1.

$$END

```
       0    DATA ERRORS DETECTED.

TOTAL NO. OF TIME STEPS READ =           7
TOTAL NO. OF WS PROFILES =               9
ITERATIONS IN EXNER EQ =               171

COMPUTATIONS COMPLETED
RUN TIME =  0 HOURS,  0 MINUTES &  2.00 SECONDS
```